Thin Internal Wall Insulation (TIWI)

Measuring Energy Performance Improvements in Dwellings Using Thin Internal Wall Insulation

Annex B; TIWI Field Trials

Building Performance Evaluation (BPE)

BEIS Research Paper Number: 2021/016

LEEDS SUSTAINABILITY INSTITUTE

LEEDS BECKETT UNIVERSITY

Department for Business, Energy & Industrial Strategy

Contents

Researchers and authors

This research was undertaken by researchers at the Leeds Sustainability Institute (LSI) at Leeds Beckett University.

Dr David Glew
David Farmer
Dominic Miles-Shenton
Felix Thomas
Dr Martin Fletcher
Dr Adam Hardy
Professor Chris Gorse

Executive Summary

As part of a wide-ranging project, Leeds Becket University investigated the potential for internal wall insulation (IWI) and thin internal wall insulation (TIWI) to reduce space heating demand in solid wall homes. To do this the following tests were undertaken in three separate test houses (Test House A, B and C): coheating tests before and after retrofit; heat flux measurements and air tightness tests to measure the heat transfer coefficient (HTC); U-values measurements; and infiltration rates. In Test House A, the improvements achieved by three different products were evaluated; one IWI and two TIWI. These were installed sequentially, one after the other. Similarly, the same approach was taken in Test Houses B and C to measure the performance of four further TIWI - two in each home.

As summarised in Table 0-1, the coheating tests discovered that TIWI could reduce the heating demand of a home by between 10% to 17%, which is almost as much as IWI (18%). This was achieved even though U-value reductions were much greater for the IWI (86%) than the TIWI (64% to 38%). The savings were determined by both the surface area that was insulated (i.e. greater wall areas in House C resulted in proportionally higher savings) and reductions in U-value that the products achieved. Airtightness tests discovered that neither IWI nor TIWI reduced infiltration in these homes. Savings were therefore lower for less-well insulting products. However, due to the law of diminishing returns, even thinner TIWI achieved reasonable savings. The law of diminishing returns says that insulation provides less and less benefit as more and more is installed. For instance, more than doubling the insulation thickness from TIWI 1 to the conventional IWI only resulted in an additional 13% reduction in U-value and a 3% improvement in HTC.

Table 0-1, Changes in thermal performance resulting from TIWI retrofit

		Insulation Material	Insulation Thickness (mm)	Thermal Conductivity of insulation λ (W/mK)	Thermal Resistance of insulated wall R-value (m^2K/W)	Measured U-value of baseline wall (W/m^2K)	Measured U-value of insulated wall (W/m^2K)	U-value reduction	HTC reduction	Heat loss area that was Insulated
Test House A	IWI	Phenolic board	70	0.021	3.49	2.11	0.30	86%	18%	23%
	TIWI 1	PIR board	27	0.023	1.25	2.11	0.78	63%	15%	23%
	TIWI 2	Aerogel board	14	0.015	1.23	2.11	0.76	64%	13%	23%
Test House B	TIWI 3	EPS board	22	0.040	1.03	2.01	0.98	49%	15%	19%
	TIWI 4	Cork render	20*	0.037	0.93	2.01	1.36	32%	17%	19%
Test House C	TIWI 5	Latex rolls	10	0.052	0.68	2.10	1.30	38%	10%	32%
	TIWI 5 + 6	Thermo-paint on latex rolls	1Error! Bookmark not defined.	0.047	0.50	1.30	1.25	4%	7%	38%

The only insulation tested that did not yield improvements in HTC or U-values was TIWI 6 as the additional thermal resistance it added to walls was negligible.

The confidence in the coheating tests carried out for TIWI 3, 4 and 6 were affected by unseasonably warm conditions. Uncertainty in savings measured also arose for TIWI 4 as the application thickness of

* Due to application method, exact thickness was uncertain

the product could not be assured. Additionally, the depth of airspaces varied behind the TIWI 1, 2, 3 and 4 insulation boards.

It was not clear if thermal comfort was improved by the application of IWI or TIWI, despite an attempt to measure this. More prolonged testing over a greater range of external conditions would be needed to explore this more thoroughly. Similarly, to measure the impact of the insulation on household cooldown rates, which appeared to be only marginally affected by TIWI, would need more data to be collected over a longer period.

The success of IWI and TIWI in reducing the heat loss from dwellings when applied to walls led to an additional investigation into the application of IWI and TIWI in the room in roof (RiR) of solid walled homes. To do this a fourth solid wall Test House (D), with two RiR was secured. Into one RiR, IWI was installed, while in the other, a product similar in performance to TIWI 1 was installed. Before and after coheating tests, heat flux measurements and air tightness tests were performed. The results showed that retrofitting RiR can reduce whole house heat loss by more than IWI retrofits, meaning RiR retrofits could make a substantial contribution to reducing fuel bills for solid wall homes. The RiR retrofit was also observed to reduced infiltration rates, whereas solid wall insulation on walls did not, indicating that RiR may be a problematic area for infiltration.

The TIWI in the RiR was installed directly over the existing ceiling and walls as it was thinner, and this would not impact availability of space to the same degree as the thicker IWI. The conventional IWI had to be installed between the roof rafters. Removing the ceiling and walls to install the conventional IWI in the RiR was costly and caused more disruption than the TIWI, and also resulted in greater amounts of thermal bridging. Thus, TIWI over-boarding in RiR was simpler and cheaper to install, though installing the IWI between the rafters achieved marginally greater heat loss reductions.

1 Annex B; TIWI Field Trials

1.1 Research Project Overview

Thin internal wall insulation (TIWI) could play a role in UK energy policy, though the extent to which it can contribute to emissions targets, increase retrofit rates of solid wall homes, reduce fuel poverty, improve thermal comfort and mitigate unintended consequences is not fully understood.

On behalf of the Department for Business, Energy and Industrial Strategy (BEIS), Leeds Beckett University have investigated the potential of TIWI to achieve warmer homes and lower fuel bills with fewer unintended consequences than conventional internal wall insulation (IWI).

Five output reports describe the research and results from this project, these are:

1. Summary Report
2. Annex A, Introduction to TIWI: Literature, Household & Industry Reviews
3. Annex B, TIWI Field Trials: Building Performance Evaluation (BPE)
4. Annex C, Predicting TIWI Impact: Energy & Hygrothermal Simulations
5. Annex D, Moisture Risks of TIWI: Laboratory Investigations

1.2 TIWI Annex B Overview

This report presents the building performance evaluation (BPE) tests that were undertaken on 3 Test Houses to investigate the impact of 6 TIWI and 1 conventional IWI on overall aggregate heat loss (heat transfer coefficient), elemental heat loss (U-values), ventilation heat loss (infiltration) and thermal comfort. These tests established the improvements in technical performance that could be observed as well as identifying technical issues that might arise during retrofits.

This Annex is structured as follows:

- Section 2, The Impact of TIWI on Infiltration (Airtightness)
- Section 3, The Impact of TIWI on External Wall U-value
- Section 4, The Impact of TIWI on Whole House Heat Loss (HTC)
- Section 5, The Impact of TIWI on Thermal Comfort
- Section 6, The Impact of TIWI on Heat Up and Cooldown Times
- Section 7, The Impact of TIWI on Room in Roof Retrofits

2 The Impact of TIWI on Infiltration (Airtightness)

This section describes the process of measuring the infiltration rate in the Test Houses and the magnitude of the change that was caused by installing the IWI and TIWI. Previous research has shown that retrofits can substantially improve airtightness (Innovate UK, 2016). Specifically, research has shown that retrofits including IWI can reduce leakiness by between 8% and 61% depending on the amount of other work also being undertaken and if a whole house approach is adopted (Gorse et al., 2017).

The airtightness, or infiltration rate, is a measure of the uncontrolled ventilation for a dwelling. Together with purpose-provided ventilation, this establishes the total ventilation rate for the building fabric and affects how much heat is lost due to air exchange with the external environment. Heat loss through ventilation can have a major influence on energy efficiency; if the airtightness of a dwelling is not addressed during the refurbishment process the proportion of the dwelling's total heat loss attributable to ventilation can increase dramatically as other heat loss mechanisms are reduced[†].

Performing a blower door test is the approved method for ascertaining the airtightness of a dwelling in the Building Regulations 2010 Approved Document L1A for new-build dwellings. Approved Document L1B for existing dwellings does not specify an airtightness test methodology only stating that *"reasonable provision should be made to reduce unwanted air leakage through new envelope parts"* (NBS, 2010b, NBS, 2010c, NBS, 2010a). The tests undertaken in this project were done in compliance with the approved procedure for new-build dwellings provided by the Airtightness Testing and Measurement Association, Technical Standard L1A, Measuring Air Permeability of Building Envelopes (Dwellings) (ATTMA, 2010). Tests were conducted using an Energy Conservatory Minneapolis Series 3 blower door system, and the results reported (unless stated otherwise) are the mean value of both pressurisation and depressurisation tests. Where leakage detection was also performed to identify points of air leakage and infiltration pathways, this was carried out using handheld smoke puffers under dwelling pressurisation and by thermography under depressurisation. An induced pressure of ±50 Pa was used throughout this investigation when conducting leakage detection.

As described in the summary report, three Test Houses were investigated and six different TIWI plus a conventional IWI were installed in these homes to compare their performance. The materials retrofitted into each Test House are show in Table 2-1.

Table 2-1 IWI and TIWI investigated

Insulation	Product type	Thickness (mm)	Test House
IWI	Phenolic foam plasterboard laminate	70	A
TIWI 1	PIR plasterboard laminate	27	A
TIWI 2	Aerogel blankets	14	A
TIWI 3	EPS plasterboard laminate	22	B
TIWI 4	Cork Insulating render	20	B
TIWI 5	Latex foam rolls	10	C
TIWI 6	Thermo-reflective aerogel paint	1	C

† www.leedsbeckett.ac.uk/teaching/vsite/low_carbon_housing/airtightness/introduction/index.htm

2.1 Airtightness Test Results

The blower door tests showed no significant variation in infiltration rates as a result of the TIWI being installed, as shown in Figure 2-1. This is in direct contrast to the findings previously observed for IWI retrofits where infiltration was reduced. However, as mentioned, in most other field trials work in addition to the installation of IWI was being undertaken as part of the retrofit and it is possible that savings identified on other case studies may have been linked to these ancillary activities such as sealing around pipes, vents, loft hatches, windows and doors.

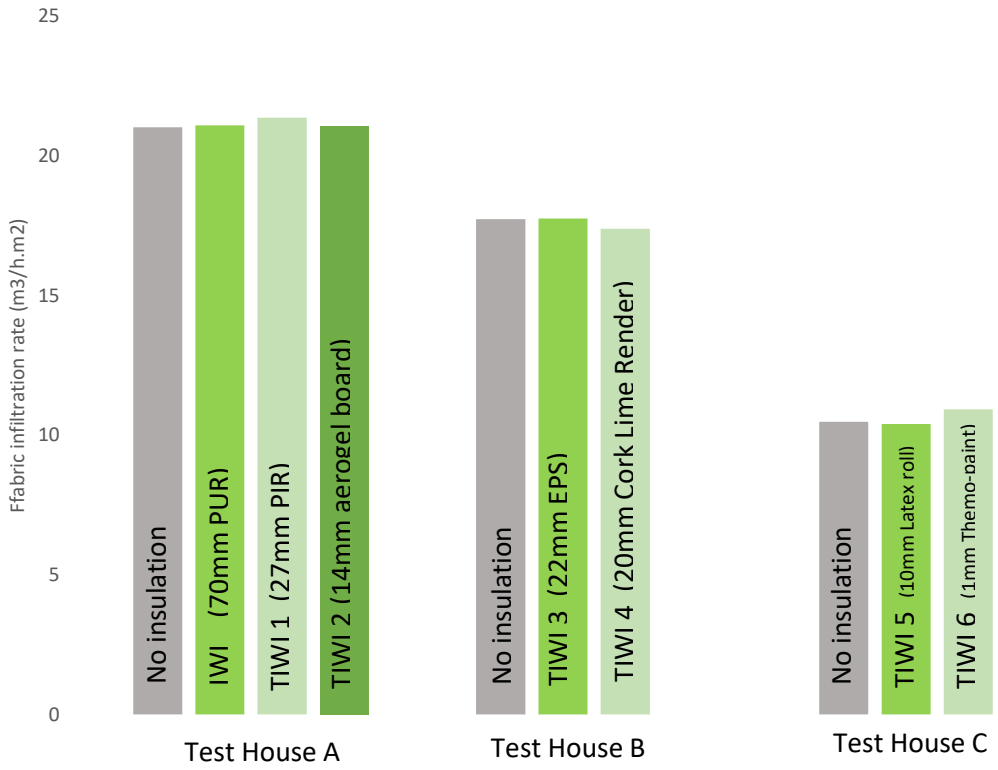

Figure 2-1 Impact of TIWI and IWI on dwelling airtightness

It was observed that the major infiltration routes were via the suspended timber ground floors and poorly sealed cellar and external doors and especially through service penetrations, boxed in pipe routes and plug sockets. Where laminate flooring was laid down, infiltration rates were reduced. Some evidence of air movement was also observed between neighbouring dwellings via intermediate floors.

2.2 Airtightness Test Summary

Blower door and CO_2 decay tests suggest that unregulated infiltration rates in Test Houses A and B were particularly poor; roughly double the infiltration rate of new build homes (21 and 18 $m^3/h.m^2$ respectively), while Test House C was roughly comparable with new build standards (11 $m^3/h.m^2$).

It was observed that cellar doors and suspended timber ground floors were responsible for most of the air leakage, which has implications for whole house retrofits. This highlights the importance of insulating floors in addition to walls in order to maximise savings as part of a whole house approach. Although TIWI appeared to have no impact on airtightness in any of the Test Houses, it is not clear if this will be the case for homes that are not already wet plastered.

3 The Impact of TIWI on External Wall U-value

The thermal transmittance of a building element (U-value) is defined in ISO 7345 (BSI, 2018) as the *"Heat flow rate in the steady-state divided by area and by the temperature difference between the surroundings on each side of a system"*. U-values are expressed in units of W/m^{2}K. The primary purpose of all the products tested (excluding TIWI 6) is to reduce the U-value of a thermal element, in this case, a solid brick external wall. To accurately quantify the reduction in U-value resulting from a fabric thermal retrofit, its U-value must be measured *in situ* both pre- and post-retrofit. This is due to the combined uncertainties relating to assumptions of pre- and post-retrofit thermal performance, brought about by phenomena known as the *prediction gap* and the *performance gap*:

- The prediction gap for uninsulated solid brick external walls is evidenced by a study in which the U-value of 85 walls was measured *in situ* (BRE, 2014). The sample mean was 1.57 W/m^{2}K, considerably lower than the RdSAP methodology assumption of a U-value of 2.10 W/m^{2}K at the time of the study. Importantly, the standard deviation of 0.32 W/m^{2}K highlighted a relatively large variation in U-values across the sample, thus no specific U-value is 'correct' in any given location. Therefore, pre-retrofit U-value assumptions do not provide a reliable baseline from which to calculate post-retrofit U-values. Nor do they provide an accurate benchmark from which to quantify the change in U-value post-retrofit.
- The performance gap describes the discrepancy between the calculated and measured change in thermal performance. Reasons for the performance gap include incorrect installation (e.g. workmanship, physical obstructions), susceptibility of retrofit measures to heat loss mechanisms such as wind washing, and differing product performance to that provided by manufacturers' datasheets (Gorse et al., 2017).

3.1 U-value Test method

In situ U-value and R-value measurements were undertaken in accordance with ISO 9869 (BSI, 2014). They were derived from measurements of heat flux density, using heat flux plates (HFPs) and the measured air temperature difference between the internal and external environments (ΔT). The thermograms in Figure 3-1, Figure 3-2, and Figure 3-3 show variation in surface temperature across the test wall of each house in their pre-retrofit (baseline) condition. This variation is not confined to areas affected by thermal bridging at junctions. The thermal inconsistency observed indicates a variation in the rate of heat loss across the plane element area of the wall, most likely caused by structural inhomogeneity (e.g. header bricks, variation in mortar fill, etc.). To account for this variation in heat loss, and therefore obtain an *in situ* U-value deemed representative of each test wall, *in situ* U-value measurements were undertaken at multiple locations using an array of HFPs positioned in a grid formation across the plane element area. The location of each HFP grid array was selected using thermography to avoid regions which were deemed to be affected by thermal bridging at nearby junctions (the additional heat loss at these locations is accounted for in thermal bridging calculations[‡]).

‡ HFPs were also positioned in proximity to junctions with other thermal elements (e.g. window reveals and intermediate floor) to assess the change in thermal bridging heat loss resulting from each retrofit measure at these locations.

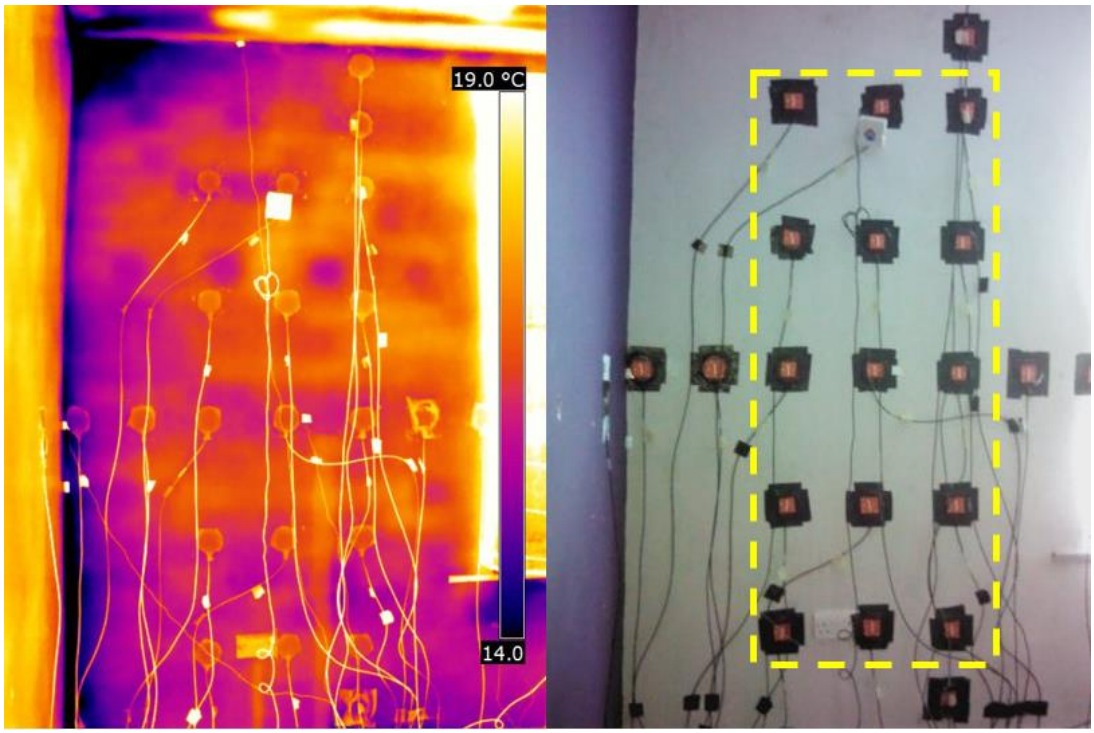

Figure 3-1 Thermogram showing surface temperature variation across the baseline external wall of Test House A (left) and the HFP grid array (within the yellow rectangle) used to derive the in situ U-value

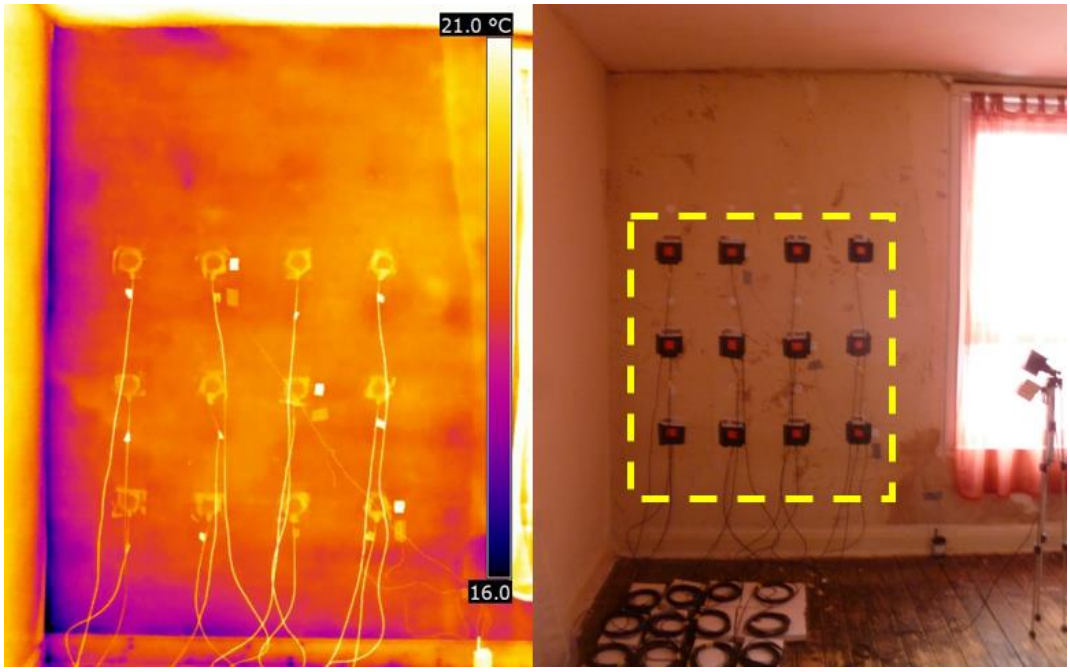

Figure 3-2 Thermogram showing surface temperature variation across the baseline external wall of Test House B (left) and the HFP grid array (within the yellow rectangle) used to derive the in situ U-value

The *in situ* U-value reported for each test wall is the arithmetic mean of the individual *in situ* U-values measured in each grid. The uncertainty reported for each *in situ* U-value is the standard error of the mean.

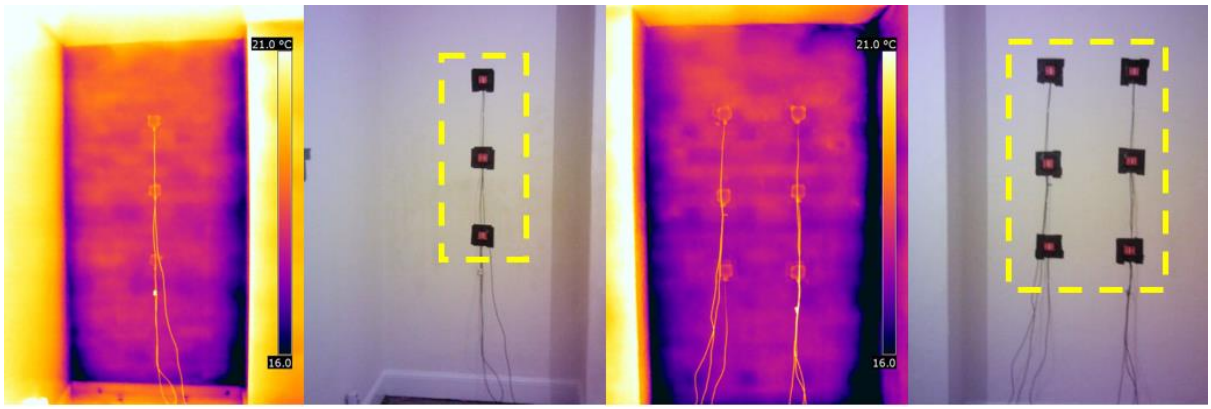

Figure 3-3 Thermogram showing surface temperature variation across the baseline external wall of Test House C (left) and the HFP grid arrays (within the yellow rectangles) used to derive the in situ U-value

For each test wall, the HFP array was placed in the same position across all test periods. This allowed a direct comparison to be made between the thermal performances of the wall pre- and post-retrofit. To reduce the uncertainty associated with solar irradiance, the north facing walls were selected for measurement in House A and House C. In the case of House B, where the only external walls were either east or west facing, the west facing wall was selected for measurement and plywood external shielding was mounted over the measurement location to prevent direct exposure to solar radiation on the surface of the wall, shown in Figure 3-4. The plywood shielding was offset from the wall surface to allow for air movement between the wall surface and the shielding.

Figure 3-4 External plywood shieling mounted on the west façade of House B to prevent direct solar radiation impinging of the wall surface at the location of the HFP grid array

3.2 Calculating retrofit target U-values

The retrofit target U-value for each product was calculated using Equation 1. The additional R-value provided by the retrofit materials was calculated in accordance with ISO 6946 (BSI, 2017) using values for λ and material thicknesses provided by the manufacturers' product datasheets.

Equation 1

$$U_t = \frac{1}{R_b + R_m}$$

Where: U_t = Retrofit target U-value

R_b = Baseline *in situ* R-value ($\frac{1}{U_{baseline}}$)

R_m = R-value of retrofit materials

An example of this calculation is provided in Table 3-1.

Table 3-1 Retrofit target U-value calculation for TIWI 4

Layer	λ (W/mK)	Depth (mm)	R-value (m^2K/W)	Source
Baseline wall			0.50	Measured *in situ*
Cork lime render	0.037	15	0.41	Datasheet
Finishing plaster	0.128	5	0.04	Datasheet
Total			0.94	
Retrofit target U-value = 1.06 W/m^2K				

3.2.1 House A U-value measurements (IWI, TIWI 1, & TIWI 2)

Figure 3-5 provides the mean *in situ* U-value and retrofit target U-value for the IWI (70mm Phenolic), TIWI 1 (27mm PIR) and TIWI2 (14mm Aerogel) installed on walls of House A.

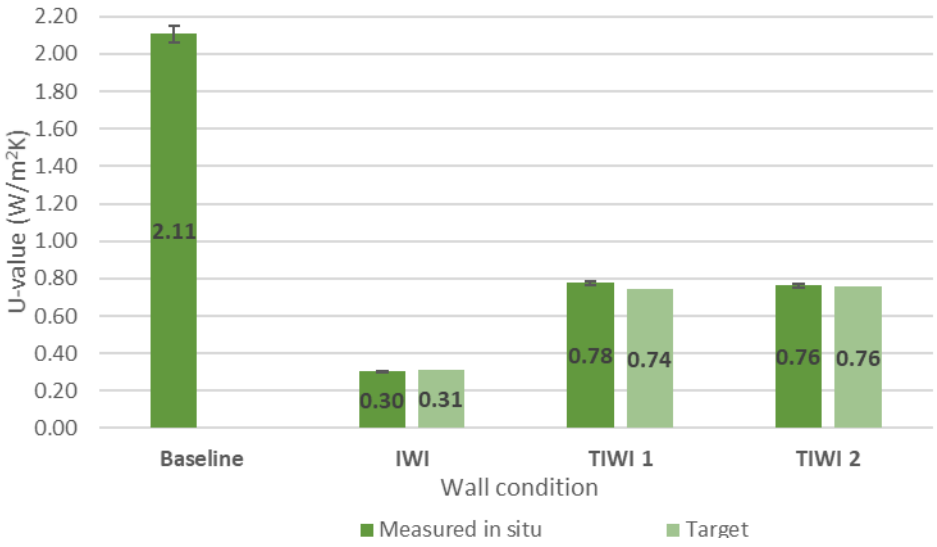

Figure 3-5 Mean in situ U-value and retrofit target U-values for the test wall of House A in each condition

A one-way ANOVA confirmed that there was a statistically significant difference between the mean U-value of the external wall in each condition, $F(3,56) = 1037$, $p = <0.001$.

A Games-Howell post-hoc test was used to compare differences between each external wall condition.

- The mean U-value ($\bar{x}$) of the external wall in its baseline condition ($\bar{x}$ = 2.11 ± 0.05) was significantly greater than when insulated with: IWI ($\bar{x}$ = 0.30 ± <0.01, p = <0.001), TIWI 1 ($\bar{x}$ = 0.78 ± 0.01, p = <0.001), and TIWI 2 ($\bar{x}$ = 0.76 ± 0.01, p = <0.001).
- The mean U-value of the external wall insulated with IWI was significantly lower than when insulated with ether TIWI 1 (p = <0.001) or TIWI 2 (p = <0.001).
- There was no statically significant difference between mean U-value of the TIWI 1 and TIWI 2 insulated external wall (p = <0.747), indicating that both retrofits resulted in a similar reduction in U-value. Though it must be noted that TIWI 2 achieved this reduction with an intervention of approximately two thirds the thickness of TIWI 1 (assuming a 15 mm airspace and 2 mm skim coat for both products), primarily due to its higher R-value.

It can be seen in Figure 3-5 that in essence all of the products tested achieved their target retrofit U-value. A 5% performance gap was measured for TIWI 1, however the underperformance is small and could be explained by the sensitivity of the retrofit target U-value to the thickness of the air layer between the insulation boards and original wall surface created by the dabs of adhesive; this is discussed further in Section 3.4.

3.2.2 House B U-value measurements (TIWI 3 & TIWI 4)

Figure 3-6 provides the mean *in situ* U-value and retrofit target U-value of TIWI 3 (22mm EPS) and TIWI 4 (20mm Cork lime render) for the test wall of House B.

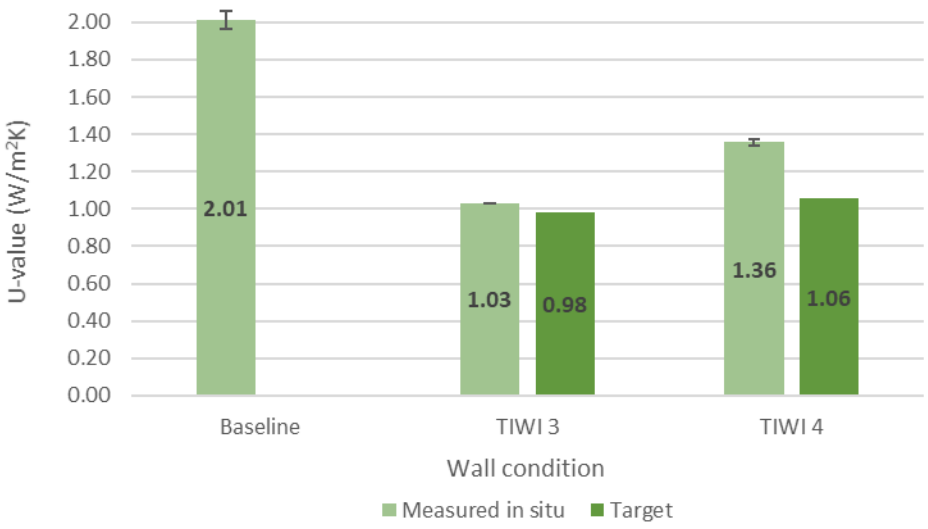

Figure 3-6 Mean in situ U-value and retrofit target U-values for the test wall of House B in each condition

A one-way ANOVA confirmed that there was a statistically significant difference between the mean U-value of the external wall in each condition, F (2,33) = 280, p = <0.001.

Again. a Games-Howell post-hoc test was used to compare differences pre- and post-retrofit:

- The mean U-value of the external wall in its baseline condition ($\bar{x}$ = 2.01 ± 0.05) was significantly greater than when insulated with TIWI 3 ($\bar{x}$ = 1.03 ± <0.02, p = <0.001) and TIWI 4 ($\bar{x}$ = 1.36 ± 0.02, p = <0.001).

- The difference between the mean U-value achieved with TIWI 3 and TIWI 4 was statistically significant (p = <0.001), which shows that TIWI 3 resulted in a greater reduction in U-value. It must be noted that the retrofit target U-value for TIWI 4 was 8% higher than TIWI 3, so a difference in mean U-value would have been expected had both products achieved their retrofit target U-values. However, it must be noted that TIWI 3 was almost twice as thick as TIWI 4, due to the presence of an approximate 15 mm airspace behind the EPS laminate boards and a 2 mm skim coat.

A performance gap of 5% was observed for TIWI 3. As with TIWI 1 the discrepancy could be due to assumptions regarding the depth of the air layer between the insulation and original wall surface (again, refer to Section 3.4). The 28% underperformance of TIWI 4 could be explained by the difficulty the installers faced with ensuring that the specified 15 mm depth of cork lime render was applied consistently across the entire surface area of the wall. If it is assumed that TIWI 4 performed as stated by the manufacturer's datasheet, the cork lime render was applied at an average depth of 7.5 mm. Protimeter readings indicated that the wall had dried out prior to measurement, which suggests that the underperformance was not caused by excess moisture.

3.2.3 House C U-value measurements (TIWI 5 & TIWI 5+6)

Figure 3-7 provides the mean *in situ* U-value and retrofit target U-value for TIWI 5 (10mm Latex rolls) and a combination of TIWI 5 and 6 (1mm thermo-reflective paint) installed on the test wall of House C.

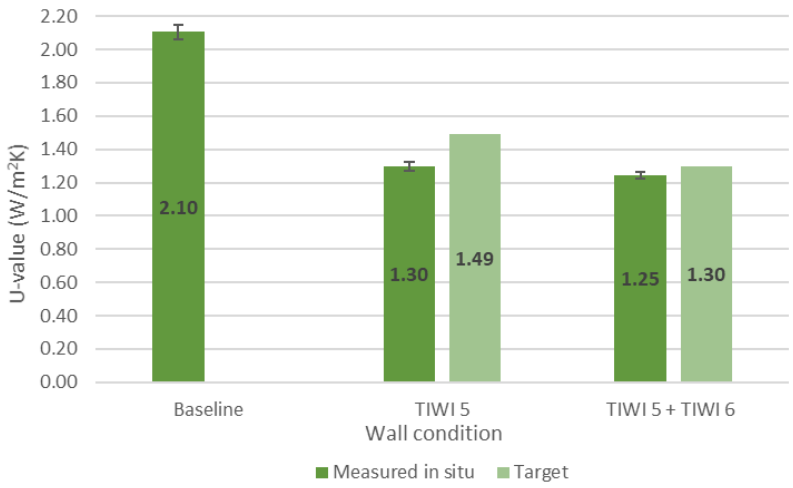

Figure 3-7 Mean in situ U-value and retrofit target U-values for the test wall of House C in each condition

A one-way ANOVA confirmed that there was a statistically significant difference between the mean U-value of the external wall pre- and post-retrofit, F (2,24) = 234, p = <0.001. A Games-Howell post-hoc test was again used to compare differences pre- and post-retrofit:

- The mean U-value of the external wall in its baseline condition ($\bar{x}$ = 2.10 ± 0.04) was significantly greater than when insulated with TIWI 5 ($\bar{x}$ = 1.30 ± <0.02, p = <0.001) and TIWI 5 + TIWI 6 ($\bar{x}$ = 1.25 ± 0.02, p = <0.001).
- There was no statistically significant difference between mean U-value of the TIWI 5 and TIWI 5 + TIWI 6 insulated external wall (p = <0.266), which suggests that the application of the thermo-reflective paint did not improve the U-value of the external wall (this may not be surprising as the manufacturer does not claim that the paint will reduce the U-value of a thermal element).

The reason for *in situ* U-value of the TIWI 5 retrofitted external wall being 13% lower than the retrofit target value has not been ascertained. The R-value of the latex roll applied to the walls was measured in the laboratory and was found to match that stated by the manufacturer's datasheet. It is possible that the moisture content of the baseline wall had reduced following the baseline test, however, this cannot be substantiated.

3.3 Diminishing returns of insulation

Figure 3-8 applies the measured increase in R-value from each product to external walls with different baseline U-values. It compares the reduction in U-value from the mean baseline external wall U-value of Houses A-C (2.07 W/m^{2}K) with the current RdSAP solid brick wall U-value of 1.70 W/m^{2}K (BRE, 2017).

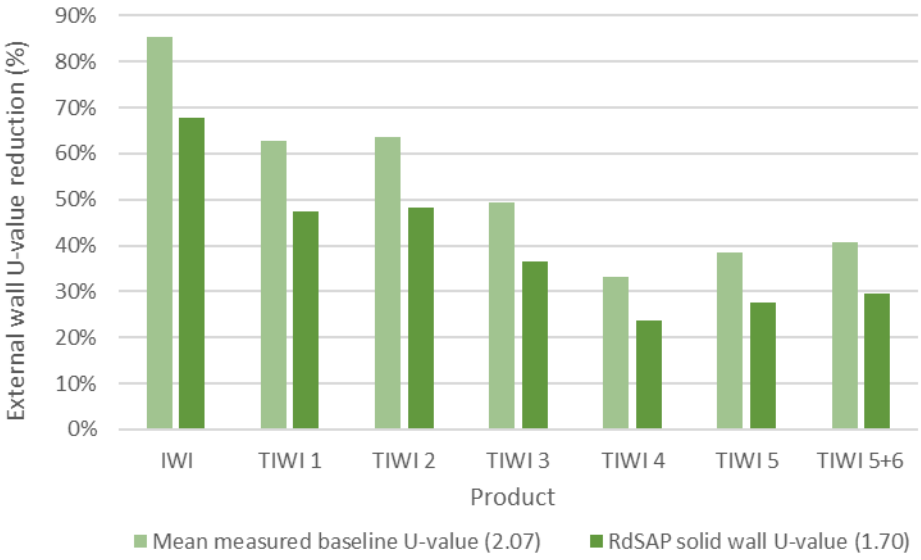

Figure 3-8 Percentage reduction in external wall U-value resulting from the application of each product to external walls with different baseline U-values

Figure 3-8 demonstrates the value of measuring the baseline U-value of a wall prior to retrofit. It can be seen in this case that the potential U-value reduction resulting from retrofit would have been underestimated if the RdSAP assumed a baseline U-value had been used. It is also interesting to note that the mean measured baseline *in situ* U-value of 2.07 W/m^{2}K is in good agreement with the previous RdSAP assumed U-value of 2.10 W/m^{2}K. This further underlines the limitations associated with using default values in models.

Thus, despite the insulating component of the conventional IWI being almost 4 times as thick as that of TIWI 1 and both having similar λ values (0.020 W/mK and 0.022 W/mK respectively), the conventional IWI only resulted in an additional 22% extra reduction in U-value. This is an example of the law of diminishing returns in regard to application of retrofit insulation, which is illustrated by the non-linear trend seen in Figure 3-9 and Figure 3-10.

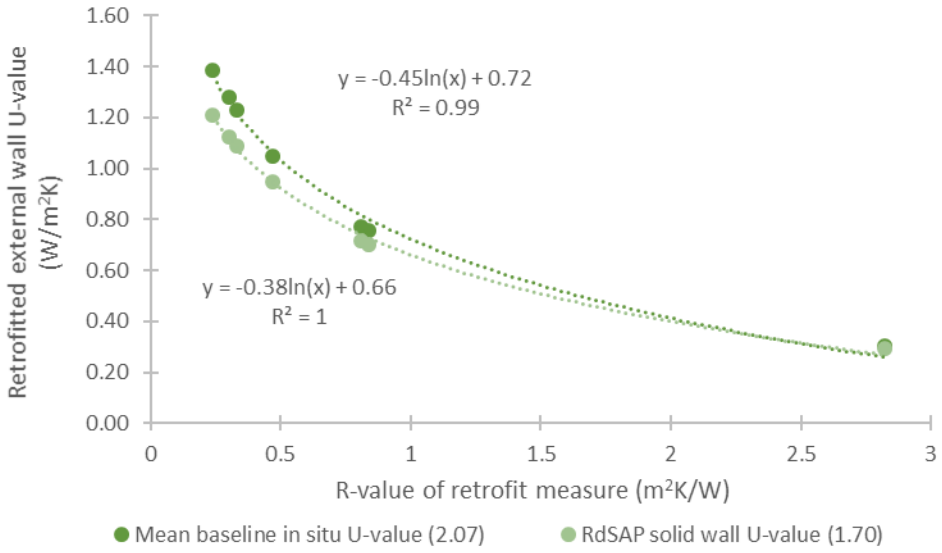

Figure 3-9 Measured R-value increase of insulation and measured external wall U-value applied to the mean measured baseline U-value of the three test walls and the RdSAP solid brick wall U-value

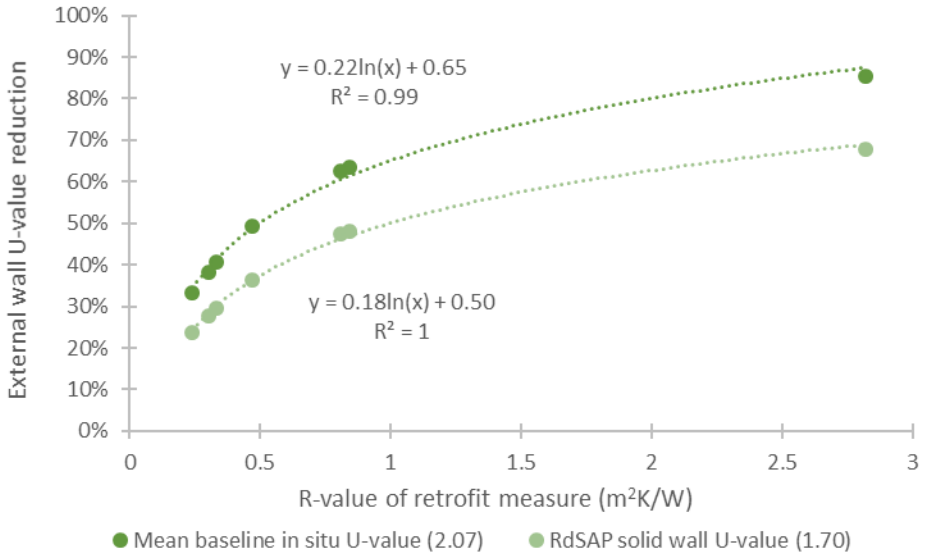

Figure 3-10 Measured R-value increase of insulation and measured reduction in external wall U-value applied to the mean measured baseline U-value of the three test walls and the RdSAP solid brick wall U-value

Figure 3-10 shows that, in the case of the external walls measured in this project, doubling the R-value of insulation applied to them only results in an additional approximate 15% reduction in U-value. This falls to approximately 12% if the RdSAP baseline is used. An initial increase in R-value to 0.5m²K/W was enough to reduce the *in situ* U-value by 50%.

3.4 R-value of airspace between an insulation board and inner wall surface

A source of uncertainty relating to the retrofit target U-values is the R-value attributable to the airspace behind the insulation boards of IWI and TIWI 1 – TIWI 3. Adhesive was used by the insulation installer to create a level finish due to undulation across the original wall surface which resulted in variation in the airspace behind the insulation. **Error! Reference source not found.** Figure 3-11 and Figure 3-12 provide images of the plasterboard adhesive applied to IWI and TIWI 1 and **Error! Reference source not found.** provides images of the foam adhesive applied to TIWI 2. The thickness of the adhesive corresponds to the thickness of the airspace behind the boards.

Figure 3-11 Plasterboard adhesive dabs applied to IWI and TIWI 1 indicating variation in the airspace thickness behind the insulation boards of between 5 mm to 25 mm

Figure 3-12 Foam adhesive dabs applied to TIWI 2 indicating variation in the airspace thickness behind the insulation boards of between 5 mm to 15 mm

BBA certificates for the insulation boards state that U-value calculations should be undertaken in accordance with ISO 6946 (BSI, 2017) and BRE Report BR 443 (BRE, 2006). BR 443 states that an adhesive dab thickness of 15 mm should be used in U-value calculations and the airspace should be assigned an R-value of 0.15 m^2K/W. Figure 3-13 shows that the airspaces observed could be assigned an R-value in the range of 0.11-0.18 m^2K/W.

Thickness of air layer	Thermal resistance $m^2 \cdot K/W$ Direction of heat flow		
mm	Upwards	Horizontal	Downwards
0	0,00	0,00	0,00
5	0,11	0,11	0,11
7	0,13	0,13	0,13
10	0,15	0,15	0,15
15	0,16	0,17	0,17
25	0,16	0,18	0,19
50	0,16	0,18	0,21
100	0,16	0,18	0,22
300	0,16	0,18	0,23
NOTE Intermediate values are obtained by linear interpolation.			

Figure 3-13 Table 8 of ISO 6946 providing the R-value of unventilated air layers at various thicknesses (ISO, 2017, p. 13)

Figure 3-14 shows the effect that differing airspace thickness can have on the retrofit target U-value.

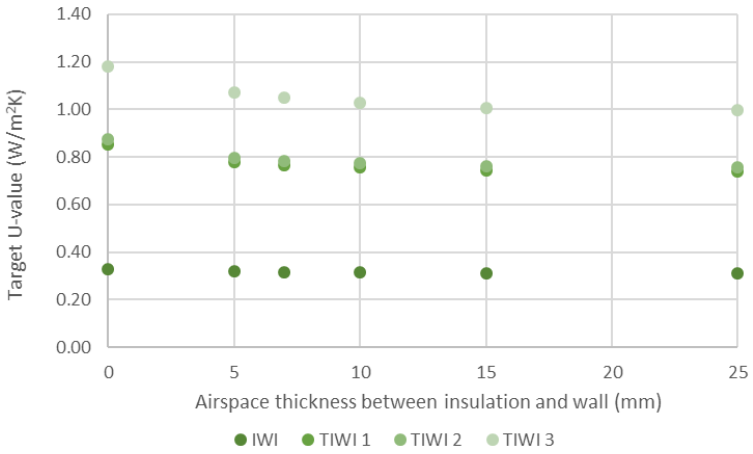

Figure 3-14 Effect of airspace thickness on the retrofit target U-value of the insulation boards. Values are derived from the baseline wall R-value, the R-value provided by manufacturers' datasheets, and R-values for an unventilated horizontal air layer stated in ISO 6946 (ISO, 2007)

In the case of TIWI 1, if the airspace behind the plasterboard was 5 mm, the target U-value would rise to 0.78 W/m^{2}K, which eliminates the performance gap measured. For TIWI 3, a reduction in the airspace from 15 mm to 10 mm would raise the retrofit target U-value to 1.03 W/m^{2}K, which would eliminate the performance gap.

Figure 3-14 also shows that the influence of the airspace thickness on the target U-value is more pronounced for products with a lower R-value. The R-value of the airspace can also contribute a significant amount to the overall increase in R-value of IWI, again the effect is more pronounced for products with a lower R-value. Figure 3-15 shows that one third of the total increase in R-value of TIWI 3 was attributable to the 15 mm airspace behind the insulation. This highlights the importance of including this airspace in retrofit calculations.

Figure 3-15 Contribution of a 15 mm airspace between the insulation and existing wall to the calculated total increase in R-value of SIWI and TIWI 1 – TIWI 3

3.5 U-value summary

Most of the products succeeded in achieving their retrofit target U-value. The only notable performance gap was for TIWI 4 (cork lime render) for which the insulation thickness was uncertain. Further, the cause of the underperformance is possibly due to the thickness of the primary insulation layer being less than specified.

The airspace between an insulation board and the original wall surface can result in uncertainty with regards to calculating target retrofit U-values. An airspace narrower than specified can result in underperformance. This is especially true of products with a low R-value.

The law of diminishing returns was observed which supports the theoretical position that the initial thin levels of insulation are proportionally the most effective and that increasing insulation thickness yields progressively smaller savings.

4 The Impact of TIWI on Whole House Heat Loss (HTC)

The heat transfer coefficient (HTC) is a metric of a building's thermal performance that quantifies the total rate of heat loss from the entire thermal envelope of a building in Watts per Kelvin of temperature differential (W/K) between the internal and external environments (ΔT). The HTC is an aggregate measure of the heat loss rates from plane elements, thermal bridges and air exchanges. The difference between the HTC of a building pre- and post-retrofit encompasses the combined change in the rate of heat loss from all these heat loss mechanisms caused by the retrofit.

4.1 HTC Measurement

HTC measurement techniques can be separated into two distinct categories: disaggregate and aggregate. To estimate the HTC of a building using disaggregate techniques, the *in situ* U-value of all thermal elements must be measured along with the background ventilation rate (using the $n_{50}/20$ Kronvall Persily rule) of the building and linear thermal bridging (Sherman, 1987). In this report, the disaggregated HTC value is referred to as HTB to differentiate it from the coheating test redrived HTC. However, such methods are impracticable and lead to high sources of uncertainty, this is because:

- of the high amount of apparatus required to measure the *in situ* U-value for each thermal element and potential uncertainties relating to the representative nature of spot *in situ* U-value measurements and bridging layers.
- of the uncertainty of the background ventilation rate derived from a blower door test.
- measuring linear thermal bridging is highly complex in a dynamic environment and thermal bridging heat loss models rely upon assumptions regarding the material and geometric composition of each junction.

Disaggregate techniques have been employed on House A to calibrate the dynamic simulation models detailed in Annex C. However, it was not practicable to perform them on each Test House. Instead, an aggregate method known as electric coheating was used to measure the HTC of each Test House.

The electric coheating test method (coheating test) has been shown to be reliable (Jack et al., 2018)and is a quasi-steady state test method which involves heating the internal environment of an unoccupied building to an elevated, homogenous, and constant temperature with electric resistance heaters and air circulation fans over a period of typically between 10 and 21 days in duration. The power input to the building as well as the internal and external environmental conditions are measured throughout the test. The HTC is derived from a multiple linear regression analysis of test data in which the dependent variable is the electric power input and the independent variables are the ΔT and solar irradiation. For an overview of the coheating test and data analysis refer to Bauwens and Roels (2014).

4.2 Coheating test method

In lieu of a recognised coheating test method (ISO), the coheating tests were undertaken according to the LBU's Whole House Heat Loss Test Method (Johnston et al., 2013) this is the method which most coheating tests undertaken in the UK during the last decade have followed (Jack et al., 2018).For each Test House a coheating test was performed in its baseline condition to ascertain the pre-retrofit HTC value.

The coheating test then measured following application of each IWI or TIWI product to derive the post-retrofit HTC. It is important to note that the HTC reduction is highly specific to each Test House and cross-comparison between the HTC reductions for products tested on other Test Houses is not advised.

The HTC of a house does not include heat exchange with adjoining dwellings, only heat loss to the external environment. Each Test House had two adjacent dwellings, therefore consideration had to be made to either minimise heat transfer between neighbours as this has been shown to reduce the accuracy of the coheating test (Bauwens and Roels, 2014).The thermostatic heater controllers were set to maintain an internal air temperature of 22 °C (lower than the 25°C set-point recommended in the LBU coheating test protocol) to minimise heat transfer across party walls. Heat flux plates (HFPs) were also installed on the party walls adjacent to each zone within a neighbour to ensure that any heat transfer between neighbouring houses was measured. The heat flux density measured by the HFPs was used to correct the measured electric heating power input during the coheating tests for heat transfer between adjoining dwellings. This correction effectively isolates each Test House from its neighbours, thus increasing the accuracy of the coheating test.

4.3 Coheating test results

4.3.1 House A HTC (IWI, TIWI 1 & TIWI 2)

Figure 4-1 provides the coheating test measured HTC for House A to compare the impact of IWI (70 mm PUR), TIWI 1 (27 mm PIR) and TIWI 2 (14 mm aerogel).

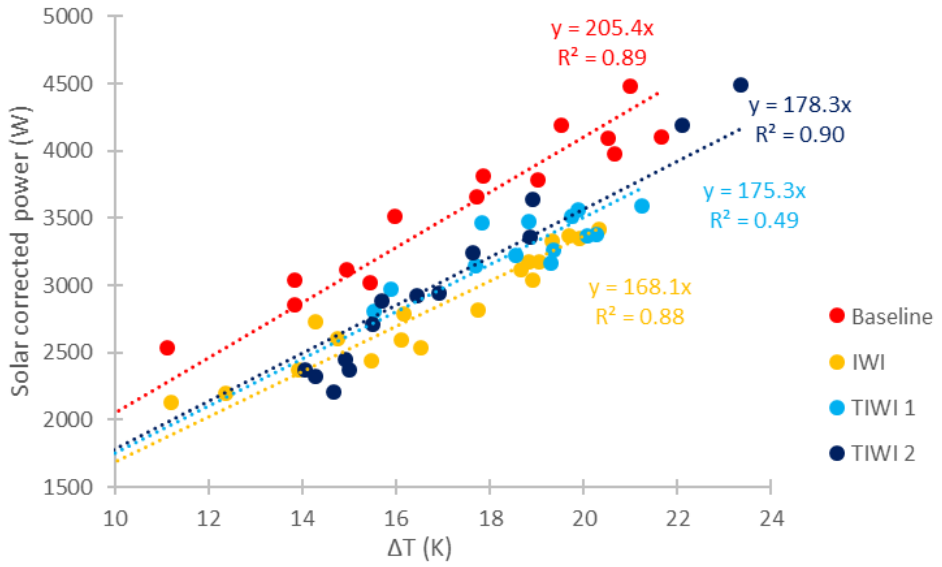

Figure 4-1 House A coheating test measured HTC for each external wall condition

Table 4-1 provides a summary of the multiple linear regression analysis statistics for each of the coheating tests performed on House A.

*Table 4-1 multiple linear regression analysis statistics for each of the coheating tests performed on House A (*denotes solar regression based upon heat flux density through glazing due to weather station malfunction)*

Test stage		Unstandardised Coefficients		Standardised Coefficients	t	Sig.	95.0% Confidence Interval for B		Collinearity Statistics	
		B	Std. Error	Beta			Lower Bound	Upper Bound	Tolerance	VIF
Baseline	ΔT	205.4	5.0	1.04	41.0	0.000	194.5	216.3	0.37	2.72
	Solar*	-16.7	7.5	-0.06	-2.2	0.046	-33.1	-0.3	0.37	2.72
IWI	ΔT	168.1	3.1	1.02	53.5	0.000	161.5	174.8	0.43	2.30
	Solar	-1.1	0.8	-0.02	-1.3	0.227	-2.8	0.7	0.43	2.30
TIWI 1	ΔT	175.3	4.0	1.03	44.1	0.000	166.6	184.0	0.42	2.37
	Solar	-1.8	0.9	-0.04	-1.9	0.083	-3.9	0.3	0.42	2.37
TIWI 2	ΔT	178.3	6.6	1.12	26.9	0.000	163.8	192.7	0.29	3.43
	Solar	-4.8	1.4	-0.15	-3.5	0.004	-7.8	-1.8	0.29	3.43

Figure 4-2 compares the percentage reduction in HTC and external wall U-value resulting from each external wall retrofit of House A.

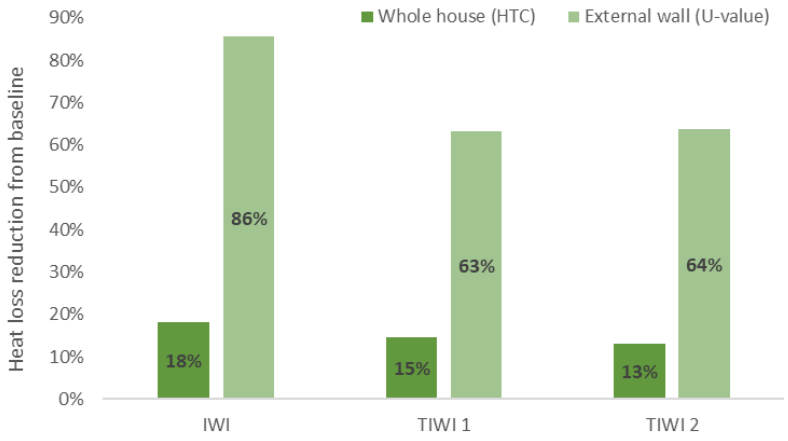

Figure 4-2 House A: Percentage reduction in HTC and external wall U-value resulting from each external wall retrofit measure

It can be seen in Figure 4-2 that the reduction in HTC was modest compared to the reduction in *in situ* U-values measured. The HTC reduced by an additional 3% when IWI was installed compared to TIWI 1, and an additional 5% compared to TIWI2. This is further demonstration of the law of diminishing returns applying to IWI retrofit (refer to Section 3.3). The reason for this is that only 23% of the heat loss area of House A was retrofitted.

Cross validation of the coheating test HTC reduction can be undertaken using the disaggregation techniques previously described. This involves summing the change in *in situ* U-value multiplied by the treated external wall area and the change in thermal bridging heat loss obtained from thermal modelling of the junctions which interface with the external wall. As the blower door tests did not result in a measurable change in airtightness, the change in background ventilation heat loss can be disregarded. Figure 4-3 compares the HTC reduction derived from coheating test measurements with the disaggregated approach.

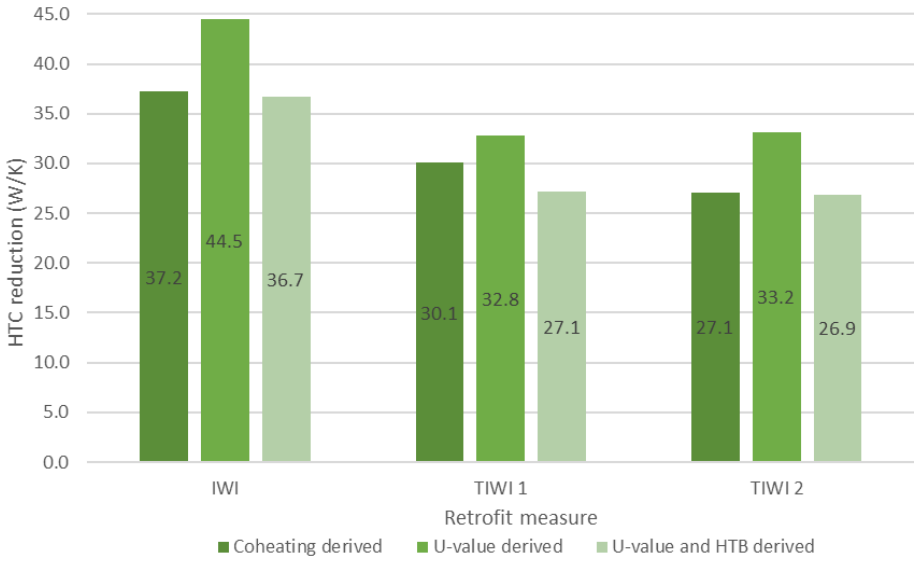

Figure 4-3 House A: Comparison of HTC reduction obtained by the coheating test and disaggregate techniques including in situ U-values and thermal bridging modelling (HTB)

Figure 4-3 shows that there is a high level of confidence with the reduction in HTCs derived from the coheating tests (especially for IWI and TIWI 2). It also demonstrates how the application of insulation to the external walls of a dwelling increases thermal bridging heat loss.

4.3.2 House B HTC (TIWI 3 & TIWI 4)

Figure 4-4 provides the coheating test measured HTC for House B to measure the impact of TIWI 3 (22 mm EPS) and TIWI 4 (20 mm Cork-lime render).

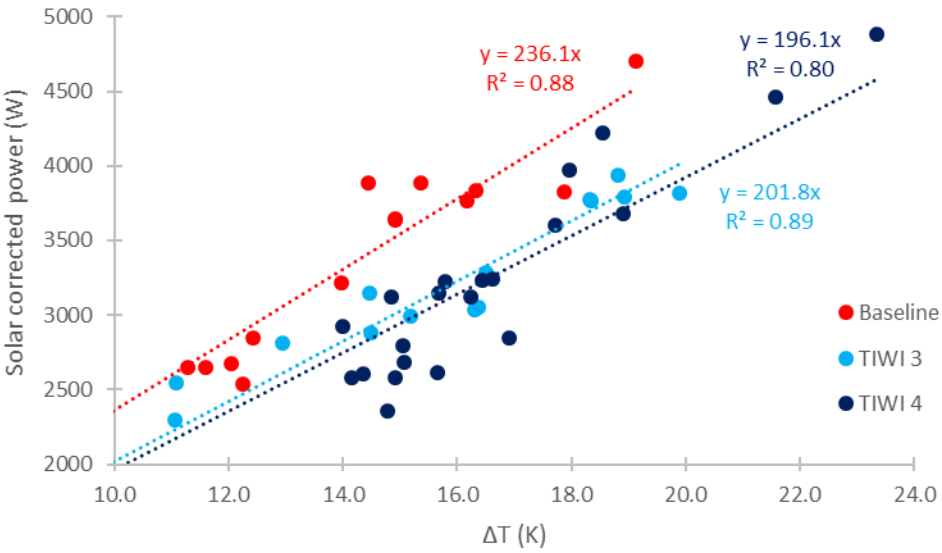

Figure 4-4 House B: Coheating test measured HTC for each external wall condition

Table 4-2 provides a summary of the multiple linear regression analysis statistics for each of the coheating tests performed on House B.

Table 4-2 multiple linear regression analysis statistics for each of the coheating tests performed on House B

Test stage		Unstandardised Coefficients		Standardised Coefficients	t	Sig.	95.0% Confidence Interval for B		Collinearity Statistics	
		B	Std. Error	Beta			Lower Bound	Upper Bound	Tolerance	VIF
Baseline	ΔT	236.1	5.8	1.02	40.4	0.000	223.3	248.8	0.56	1.79
	Solar	-3.6	2.6	-0.04	-1.4	0.188	-9.1	2.0	0.56	1.79
TIWI 3	ΔT	201.8	5.7	1.04	35.4	0.000	189.4	214.3	0.28	3.56
	Solar	-2.5	1.4	-0.05	-1.8	0.105	-5.6	0.6	0.28	3.56
TIWI 4	ΔT	196.1	7.4	1.04	26.7	0.000	180.7	211.5	0.30	3.29
	Solar	-2.2	1.5	-0.06	-1.4	0.171	-5.4	1.0	0.30	3.29

Figure 4-5 compares the percentage reduction in HTC and external wall U-value resulting from each external wall retrofit of House B.

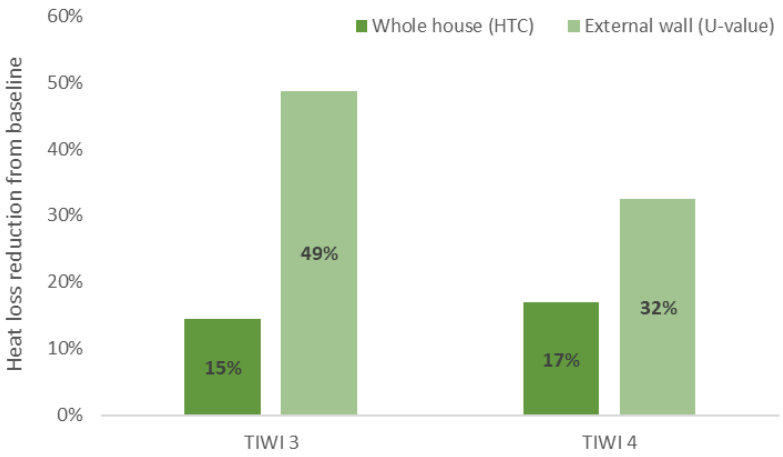

Figure 4-5 House B: Percentage reduction in HTC and external wall U-value resulting from each external wall retrofit measure

As with House A, the reduction in HTC was modest compared to the reduction in *in situ* U-values measured, again because only a small part of the heat loss area (19%) of House B was retrofitted with the TIWI. The HTC reduction resulting from TIWI 4 was greater than TIWI 3, which is contrary to the *in situ* U-value results. This could be explained by:

- Uncertainty associated with the coheating test results:
  - The solar coefficients for each coheating test were not statistically significant (p>0.05)
  - The difference between the HTC for TIWI 3 and TIWI 4 was not statistically significant (p=0.077). This is due to the uncertainty associated with the HTC for each test
  - The majority of datapoints for the TIWI4 coheating test were clustered within a 2K ΔT range which resulted in a relatively poor regression model.
- Uncertainty on the application thickness of the insulating render.
- The *in situ* U-value measurement location being unrepresentative of the entire wall area.
- A change in background ventilation heat loss not identified by the blower door tests.

Figure 4-6 compares the HTC reduction derived from coheating test measurements with the disaggregated approach.

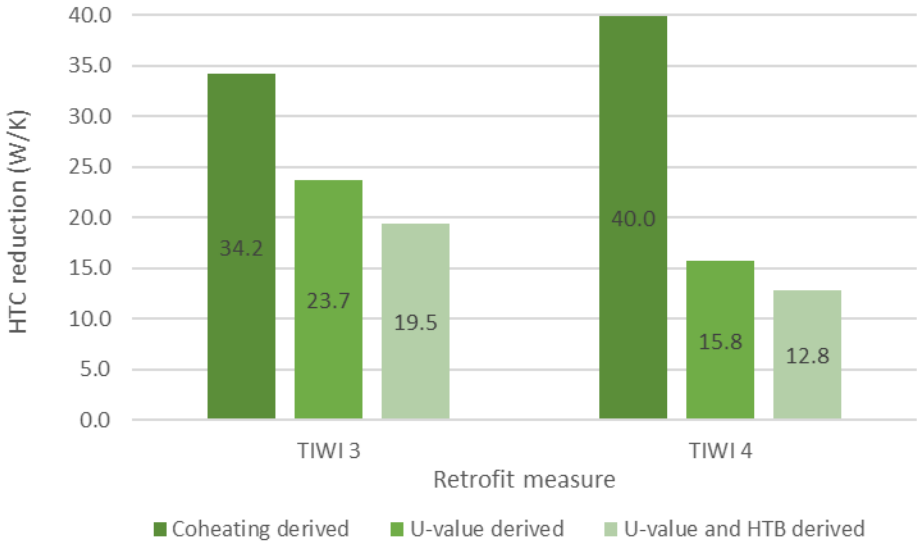

Figure 4-6 House B: Comparison of HTC reduction obtained by the coheating test and disaggregate techniques including in situ U-values and thermal bridging modelling (HTB)

Figure 4-6 confirms doubts about the reliability of the coheating test derived HTC reductions relating specifically to Test House B, especially in regard to TIWI 4. As only 19% of House B was insulated and the insulation materials had a modest R-value, it can be assumed that the U-value and HTB derived HTC change is a more robust assessment of the retrofit measures in this instance.

4.3.3 House C HTC (TIWI 5 & TIWI 5 & 6)

Figure 4-7 provides the coheating test measured HTC for House C to measure the impact of TIWI 5 (10 mm latex roll) and TIWI 6 (1 mm thermo reflective paint).

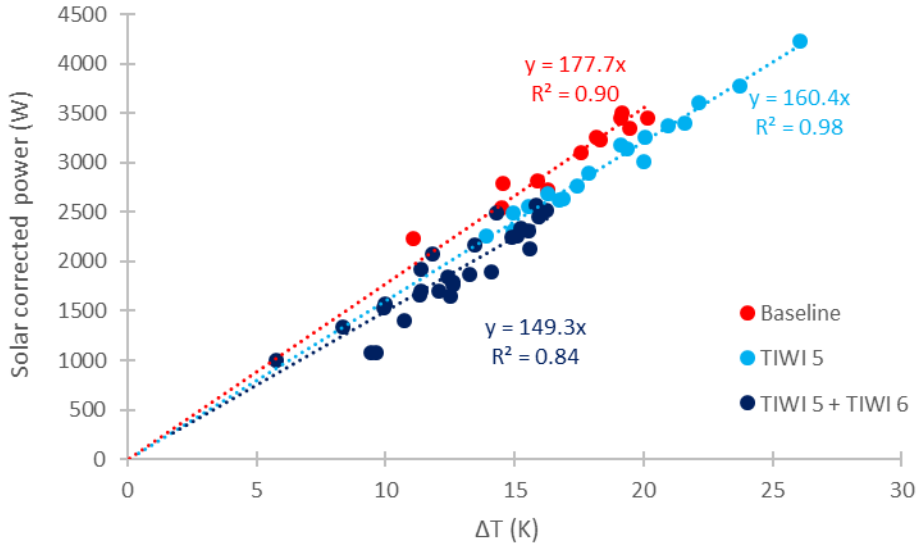

Figure 4-7 House C: Coheating test measured HTC for each external wall condition

Table 4-3 provides a summary of the multiple regression analysis statistics for each of the coheating tests performed on House C.

*Table 4-3 multiple regression analysis statistics for each of the coheating tests performed on House C (*denotes solar regression based upon heat flux density through glazing due to weather station location not providing representative solar data for the Test House*

Test stage		Unstandardised Coefficients		Standardised Coefficients	t	Sig.	95.0% Confidence Interval for B		Collinearity Statistics	
		B	Std. Error	Beta			Lower Bound	Upper Bound	Tolerance	VIF
Baseline	ΔT	177.7	2.2	1.00	81.8	0.000	172.9	182.5	1.00	1.00
	Solar	n/a	n/a	n/a	n/a	n/a	n/a	n/a	n/a	n/a
TIWI 5	ΔT	160.4	2.6	1.03	61.0	0.000	154.8	166.0	0.14	7.04
	Solar*	-13.6	6.2	-0.04	-2.2	0.044	-26.8	-0.4	0.14	7.04
TIWI 5 + TIWI 6	ΔT	149.3	4.3	1.08	34.5	0.000	140.4	158.2	0.38	2.61
	Solar*	-10.7	3.0	-0.11	-3.5	0.001	-16.9	-4.5	0.38	2.61

Figure 4-8 illustrates the percentage reduction in HTC and external wall U-value resulting from each external wall retrofit of House C. The baseline HTC measurement for TIWI 6 was the TIWI 5 HTC measurement.

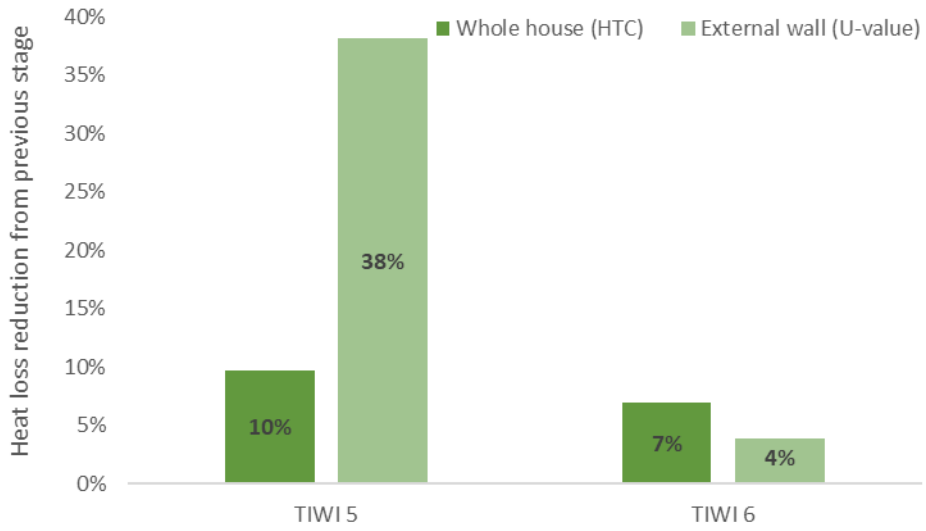

Figure 4-8 House C: Percentage reduction in HTC and external wall U-value resulting from each external wall retrofit measure

The 10% HTC reduction for TIWI 5 was similar in magnitude to the reductions measured for TIWI 1-4. However, this product was applied to 32% of the total heat loss area of House C, whereas the proportion of retrofitted area was lower for the products tested on House A (23%) and House B (19%).

The application of TIWI 6 resulted in a 7% further HTC reduction from that measured at the TIWI 5 test stage. The difference between the HTCs measured for TIWI 5 and TIWI 5+6 was statistically significant (P=0.01). However, the disaggregated HTB suggests there may be some issues with the coheating test for TIWI 6.

Figure 4-9 compares the HTC reduction derived from coheating test measurements with the disaggregated approach.

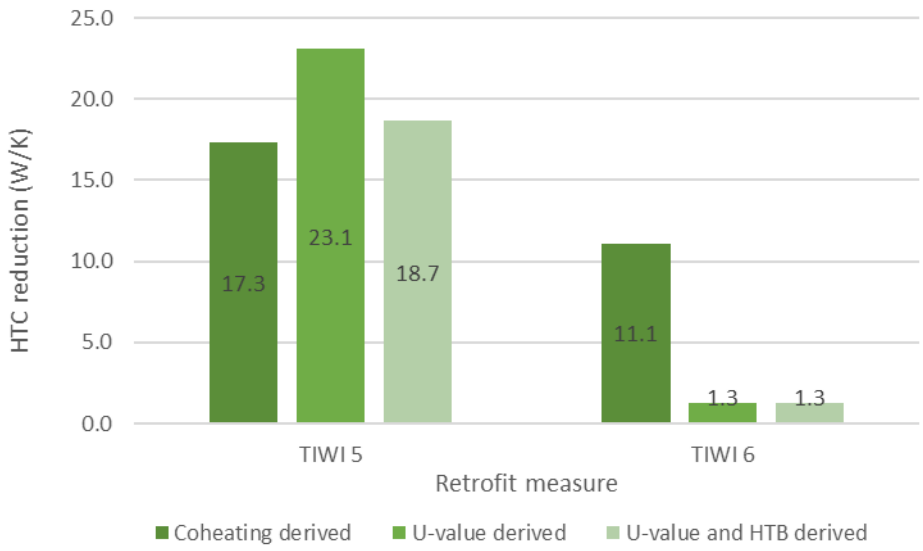

Figure 4-9 House C: Comparison of HTC reduction obtained by the coheating test and disaggregate techniques including in situ U-values and thermal bridging modelling (HTB)

The 8% difference between the coheating and disaggregate method derived HTC reduction for TIWI 5 provides confidence that the impact of TIWI 5 has been accurately measured. However, the discrepancy for TIWI 6 confirms doubts about the veracity of the coheating test for TIWI 6. The modest change in U-value (within measurement uncertainty) and the manufacturer's details that the thermo-reflective paint does not reduce the steady-state HTC of a house, means that it is very likely that TIWI 6 resulted in no HTC reduction.

4.4 Coheating test summary

Comparing the HTC reductions achieved between houses is not straightforward, as different areas of heat loss area were insulated in each home, i.e. 23%, 19% and 32% in Test Houses A, B and C, respectively. However, the HTC reductions within each Test House can be more easily compared since the heat loss area was insulated: in Test House A, IWI reduced the HTC by 18%, which is only marginally more than TIWI 1 and 2, which reduced the HTC by 15% and 13% respectively. This suggests that installing insulation with lower U-value would have a relatively small impact on fuel bill savings achieved by solid wall retrofits.

Uncertainty in the coheating test measurements were exacerbated by unseasonably warm weather during the testing of TIWI 3, 4 and 6, as well as variations in the thickness at which TIWI 4 was applied. However, using the U-value and HTB derived heat loss values provide more realistic performance indications in these instances.

5 The Impact of TIWI on Thermal Comfort

The built environment exists primarily to provide shelter from the external environment. The development of space conditioning systems has extended this role and internal environments are now expected to provide conditions that suit the preferences of the occupant. The fulfilment of thermal comfort therefore offers a key metric by which to judge an internal environment and, by extension, the building providing such conditions. Previous research undertaken by Leeds Beckett researchers has shown that occupants will take steps to achieve thermal comfort regardless of the impact on overall energy use or efficiency (Fylan et al., 2016, Johnston and Fletcher, 2015). It is therefore important to consider thermal comfort when designing measures to save energy.

Thermal comfort is influenced by two personal factors (metabolic rate and clothing insulation) and four environmental factors (air temperature, radiant temperature, air movement and humidity). Of the environmental factors, radiant temperature is particularly influential in thermal comfort sensation. This means excessively warm or cold surfaces have a significant impact on thermal comfort, for example, being near a single glazed window in winter.

IWI offers a potential solution to both cold air temperatures and cold internal surfaces that may otherwise cause a cooling effect on an occupant. Insulating internal walls slows the rate at which heat is lost through the building fabric, meaning the internal environment retains heat for longer. Further to this, IWI has the potential to raise the temperature of internal surfaces, reducing the negative influence of cold walls on thermal comfort. This is because the higher resistance insulating materials are in direct contact with the warm internal environment and retain heat for longer once they have become thermally charged. The potential for warmer internal surfaces is a key benefit of TIWI, as the resultant comfort improvement may compensate for a more modest improvement in thermal resistance when compared to thicker IWI products.

Studies evaluating the thermal properties of materials *in situ* introduce several considerations not present in laboratory-based experimentation. To establish the influence of TIWI on thermal comfort, it was necessary to develop a measurement methodology to permit the creation of robust datasets that are comparable between different properties and TIWI products, whilst also accommodating the additional limitations of *in situ* testing. Whilst guidance does exist for the field measurement of individual thermal quantities, the authors are not aware of a singular methodological approach that could be applied without modification to the current research project, hence the need to develop a bespoke method based on existing guidance.

5.1 Thermal Comfort Testing Protocol

Monitoring equipment must capture the environmental data required for the calculation of thermal comfort according to the protocols defined in both the deterministic (ISO 7730, 2005) and adaptive (ISO 15251, 2007) methods. This requires the measurement of internal air and mean radiant temperature in addition to humidity, air velocity and external conditions. The required accuracies for these quantities are given in Table 5-1, as per the guidance contained in ISO 7726 (2001).

Table 5-1 Measurement accuracies for thermal quantities (ISO 7726, 2001, p. 8-10)

Quantity	Measuring Range	Accuracy
Air Temperature	10°C - 40°C	Required: ± 0.5°C Desirable: ± 0.2°C
Mean Radiant Temperature	10°C - 40°C	Required: ± 2.0°C Desirable: ± 0.2°C
Air Velocity	0.05m/s – 1m/s	Required: 0.5 s Desirable: 0.2 s
Humidity	0.5kPa – 3.0kPa	± 0.15kPa
Surface Temperature	0°C - 50°C	Required: ± 1.0°C Desirable: ± 0.5°C

In addition to overall comfort calculation, there are also several additional environmental factors to consider relating to localised thermal discomfort. These include draughts, vertical temperature difference, warm and cool floors and radiant asymmetry. Equipment must therefore also supply data to satisfy any correction to overall thermal comfort with regard to local discomfort.

Thermal stratification is a key consideration when monitoring a thermally dynamic environment. Therefore, there is a need for multiple sensor heights to account for heterogeneous thermal quantities. Measurement heights for sensors are given by ISO 77726 (2001) and are shown in Figure 5-1 below with their required weighting coefficients.

Locations of the sensors	Weighting coefficients for measurements for calculation mean values				Recommended heights (for guidance only)	
	Homogeneous environment		Heterogeneous environment		Sitting	Standing
	Class C	Class S	Class C	Class S		
Head level			1	1	1,1 m	1,7 m
Abdomen level	1	1	1	2	0,6 m	1,1 m
Ankle level			1	1	0,1 m	0,1 m

Figure 5-1 Measuring heights for the physical quantities of an environment (ISO 7726, 2001, p. 11)

Internal air temperatures were monitored using Type-T thermocouples. These were chosen as they offer an accuracy of ± 0.3°C, in addition to having a fast reaction time. The sensors used for this research were cross-calibrated prior to testing by being placed together in a homogeneous environment. Variation between sensors was recorded as within the stated ± 0.3°C accuracy. Internal mean radiant temperatures were monitored using Type-T thermocouples placed within a 40mm diameter black sphere enclosure. This differs from the recommended sphere diameter of 150mm, however sphere diameter is not a strict limitation, as noted in ISO 7726 (2001). The guidance offered by CIBSE TM52 (2013) suggests the use of a 40mm sphere.

Relative humidity, as opposed to absolute humidity, was monitored due to greater ease of data collection. This can also be applied directly to the thermal comfort calculations. Sensors used have a stated accuracy of ±5%.

Surface temperatures were measured using Type-K Thermocouples with thermo-conductive paste applied to their bottom surface and held in place by adhesive silver foil over their upper surface. The sensors have a stated accuracy of ± 0.5°C. Up to 12 surface temperature measurements were taken in each room, with positioning and placement specific to the site under study. As a minimum, four surface temperature measurements were made near the staggered temperature array at heights of 850mm and 1400mm. Data from the weather station was also used to provide reference data for the thermal comfort tests.

Air velocity was measured as a single, spot measurement at each test building to confirm minimal internal air movement. Air velocity was then assumed to be 0.1m/s in all subsequent calculations. This is because instantaneous air velocity measurement requires high resolution data (one second intervals) to be meaningfully evaluated when considering rapid changes in air movement i.e. draughts. This was regarded as beyond the scope of this study as draught prevention is not within the performance remit of the TIWI products. However, despite not recording instantaneous air velocity, whole house air pressurisation tests were performed at each stage of the study indicating there was no change in dwelling airtightness resulting from different products.

The testing protocol includes heat provision from electrically powered oil radiators. The heating output of the oil radiator in a monitored space (set by using integrated settings on the radiator) was predetermined based on commercial sizing guidance for each room being studied and remained consistent in each testing phase. Electricity consumption was monitored to determine heat provision and radiators were controlled via thermostatic controllers to improve setpoint accuracy, with timer plugs for occupancy simulation.

In addition to heat provision from oil radiators, heat gain through party elements was recorded using heat flux plates. Sensors were Hukseflux HFP-01 with nominal stated sensitivity of 60 x 10^{-6} V/(W/m²). Solar heat gains were recorded via external weather station measurements as previously stated.

Since a novel approach to measuring thermal comfort was attempted the following section describes the experimental design and specifically the sensor positioning in detail.

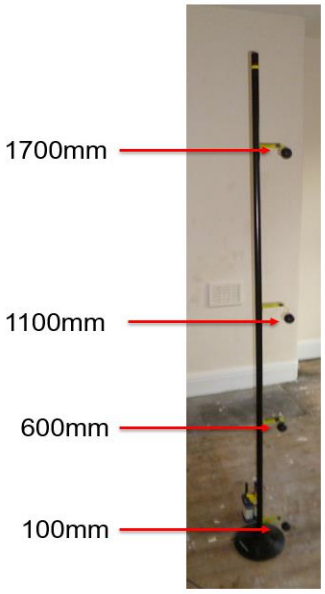

Figure 5-2 Temperature monitoring stand room centre

Each room under investigation was equipped with 5 temperature stands, with each stand measuring air temperature and Mean Radiant Temperature (MRT) at heights of 100mm, 600mm, 1100mm and 1700mm. One temperature stand is positioned at the centre of the room (Figure 5-2), with the remaining four stands positioned in a staggered array with sensors at distances of 50mm, 150mm, 250mm and 350mm from the inner surface of the external wall (Figure 5-3and Figure 5-4). Staggered arrays are positioned 500mm from the junction with the adjacent wall to minimise influence of thermal bridging effects.

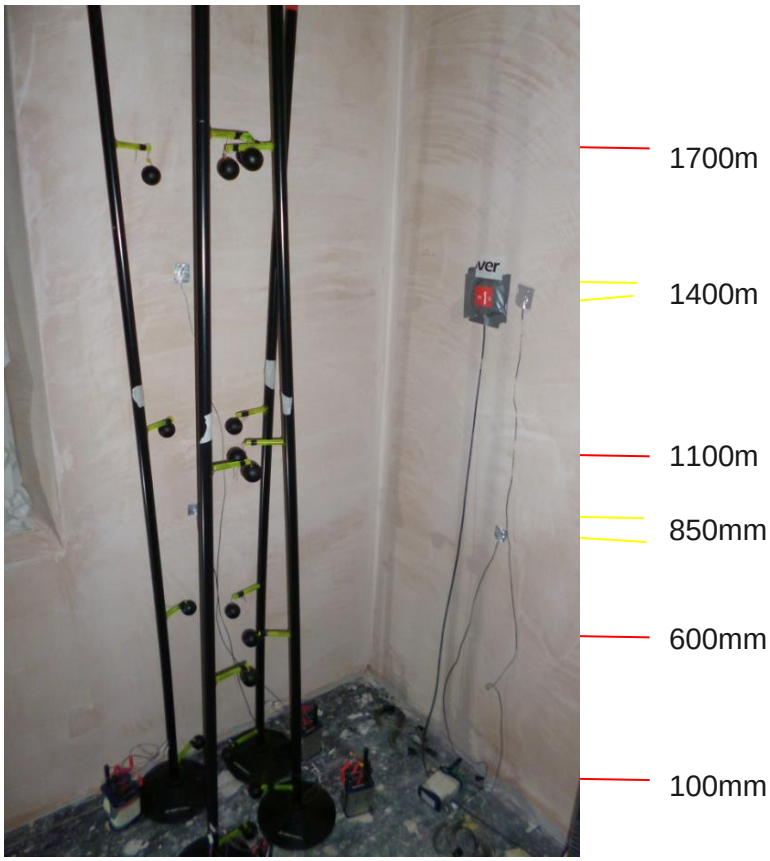

Figure 5-3 Staggered temperature monitoring with local surface temperatures

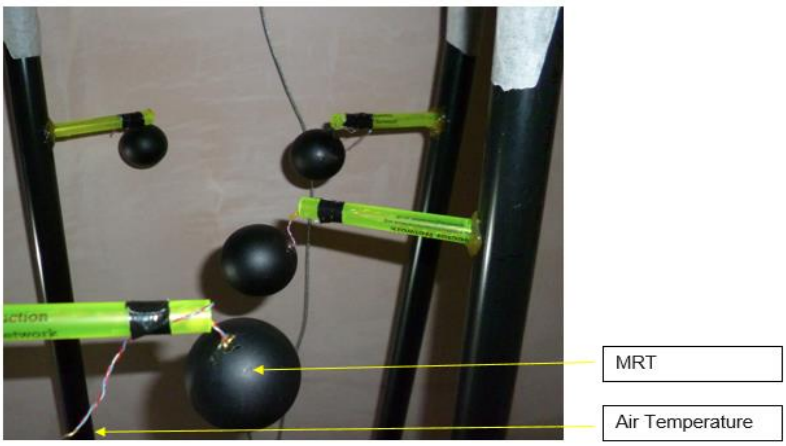

Figure 5-4 Staggered temperature monitoring

Placement of surface temperature sensors is dependent on the layout of the room under study. As a general rule, however, sensors should as a minimum be on every major surface (including ceiling and floor), plus any hot or cold surfaces (i.e. radiator, window, etc.). Major in this context means a significant proportion of the total internal envelope surface area. The number of measurements should be determined based on practical limitations; in the present study twelve surface temperature measurements were taken.

Whilst surface temperature positioning is highly dependent on room geometry, four sensors should be placed on the walls framing the staggered temperature array at heights of 850mm and 1400mm i.e. midpoints between measurement heights as per ISO 7726. Standard height for surface temperature measurement is 1400mm, as this offers a midway point between seated and standing head height as per ISO 7726. Surface temperature measurement should be positioned a minimum of 500mm away from any thermal bridge, if not possible this should be noted e.g. in the case of a bay window. Sensor positioning should be informed by thermography to ensure sensors are not positioned on thermal anomalies that are not visible to the naked eye, such as point thermal bridges, concealed heat sources or fabric discontinuities.

Relative humidity measurement should be taken at the geometric centre of the room, or as close as is reasonably possible. In the event of high ceilings, a height of 1400mm is recommended, approximating the average head height of an occupied space. Heat flux plates should be located on external and party elements so that heat gains may be accounted for. Again, sensor positioning should be informed by thermography to ensure sensors are not positioned on thermal anomalies that are not visible to the naked eye, such as point thermal bridges, concealed heat sources or fabric discontinuities. Care should be taken to assess all unaccounted heat sources to ensure they are acknowledged in subsequent analysis. Heat provision is to be supplied by electrically powered oil filled radiators. These should be positioned in front of existing radiators so as to best reflect a real heating scenario. The thermostatic controller should be positioned at the geometric centre of the room. An example test set up is illustrated in Figure 5-5.

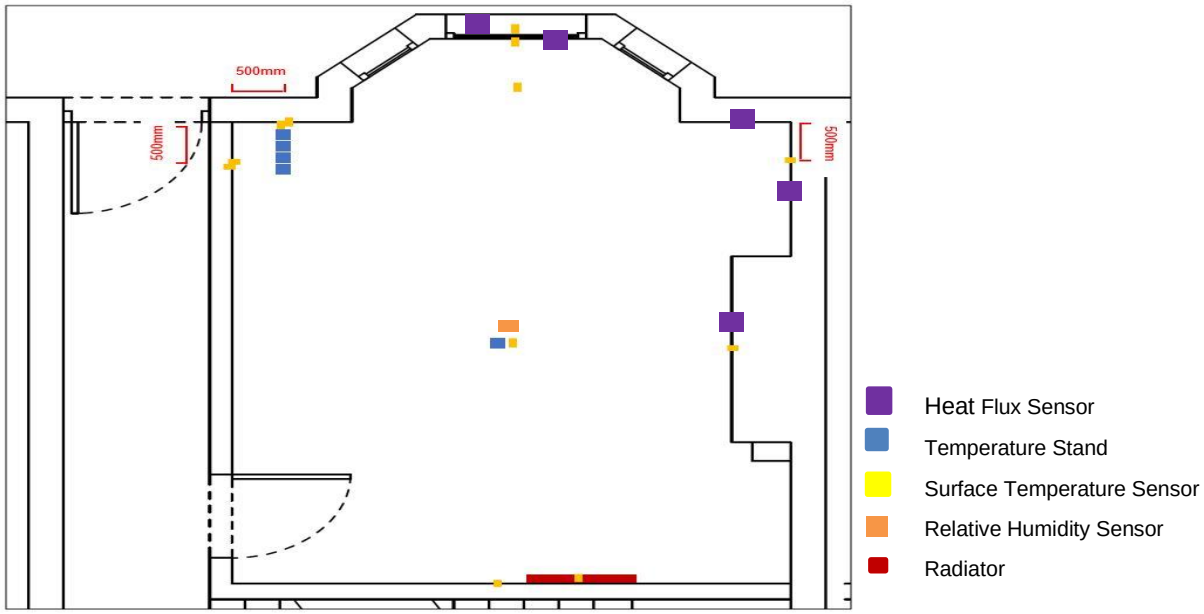

Figure 5-5 Floorplan showing example measurement setup

The experimental protocol followed has been designed to reflect a realistic occupancy schedule. As such, testing is dynamic, with intermittent periods of heat supply. Heating set points and supply times for each room type are given in Table 5-2. During testing, the building should be undisturbed.

Table 5-2 Heating profile and setpoints

Room Type	Heating Schedule	Setpoint (°C)
Living Room	07:00 – 09:00 15:00 – 22:00	21°C
Kitchen	07:00 – 09:00 15:00 – 22:00	21°C
Bedroom	07:00 – 09:00 15:00 – 22:00	18°C
Bathroom	07:00 – 09:00 15:00 – 22:00	18°C
Basement	Unheated	N/A

Before testing commences, the following points should be noted:

- Equipment should be left untouched for an hour prior to the measurement beginning so that sensors can acclimatise.
- Measurement resolution is dictated by practical considerations; a logging interval of 1 minute is recommended.
- Sensor equipment to be positioned as per the above guidance.
- If the radiator being used has multiple settings for heat output, these should be representative of the radiator sizing used under real conditions. This is a function of room volume.
- Experiment begins at 06:00.
- Experiment to run undisturbed, with data logged ideally at one-minute intervals.
- Experiment should run for a minimum of three days, giving 6 heat-up and cool-down curves; a longer period is preferred.
- Experiment Ends at 06:00.
- If testing multiple materials, sensor position must be identical at each test stage.

The following section describes the changes to the thermal comfort that were measured following the retrofit of each TIWI in the Test Houses.

- Cat III Max Upper temperature limit to fulfil Category 3 Adaptive comfort requirement
- Cat III Min Lower temperature limit to fulfil Category 3 Adaptive comfort requirement
- ExT External Air Temperature
- FF First Floor
- GF Ground Floor
- OpT Operative Temperature
- PMV Predicted Mean Vote
- SF Second Floor

Although an inherently subjective phenomenon, extensive research has led to the formulation of metrics to evaluate thermal comfort based on environmental and personal parameters relevant to the thermoregulatory balance. Two metrics are foremost in this regard:

1) The first, developed by P O Fanger (Fanger, 1970), utilises the thermo-physical balance of heat generation and heat loss in the human body in a deterministic model to derive theoretical comfort under steady state conditions. The model regards the person as a passive recipient of thermal stimuli and assumes maximum thermal comfort to be achieved at the point of thermal balance i.e. heat production and loss are equal. This model was developed into international standard ISO 7730 (BSI, 2006). The output of this approach is a Predicted Mean Vote (PMV) of thermal comfort, which is presented on a symmetrical numerical scale and ranges from Cold (-3) to Hot (+3) with Neutral (0) at its centre, representing the optimum state of thermal balance.

2) The second commonly used thermal comfort evaluation metric is Adaptive comfort. This method regards the person as an active agent, incorporating physiological, psychological and behavioural adaptations to achieve thermal comfort. Adaptive comfort presents an acceptable temperature range based on external environmental conditions, suggesting that comfort may be achieved within this range as a result of adaptive opportunities such as modifying clothing. This model was developed into international standard ISO 15251 (BSI, 2008).

Both of these thermal comfort evaluation methods were applied to a synthetic occupancy dataset collected following the installation of each TIWI product, in addition to the pre-insulation dwelling baseline based on the method described. Further details of the synthetic occupancy testing protocol are outlined in the preceding section.

Operative temperature is used during adaptive analysis as it incorporates both air and radiant effects. This is important to note, as one of the key perceived benefits of TIWI is an increase in the surface temperature which will be reflected in operative temperature but may not be noticeable in an air temperature measurement. For deterministic comfort evaluation both air and mean radiant temperature are included as separate variables, so any radiant effects will also be incorporated.

It is relevant to note that the condition of the dwellings in this study does not necessarily reflect the condition in which they would be inhabited. For example, the dwellings were largely without carpets, curtains and soft furnishings, which all have an impact on the thermal qualities of a space by reducing thermal gradients and the influence of cold surfaces. As such, this analysis is as a ‘worst case’ scenario, however, still serves to illustrate the likelihood of both comfort and set points being achieved under the various TIWI scenarios.

5.2 Adaptive Comfort Test Results

5.2.1 Test House A, adaptive comfort

This section describes the internal temperature of the ground floor living room and first floor bedroom together with external temperature during synthetic occupancy. The adaptive comfort method as outlined in ISO 15251 (BSI, 2008) uses external temperature to define upper and lower threshold temperatures. Red (upper or warmer) and blue (lower or cooler) lines show these, where comfort would be described as any position within these two lines.

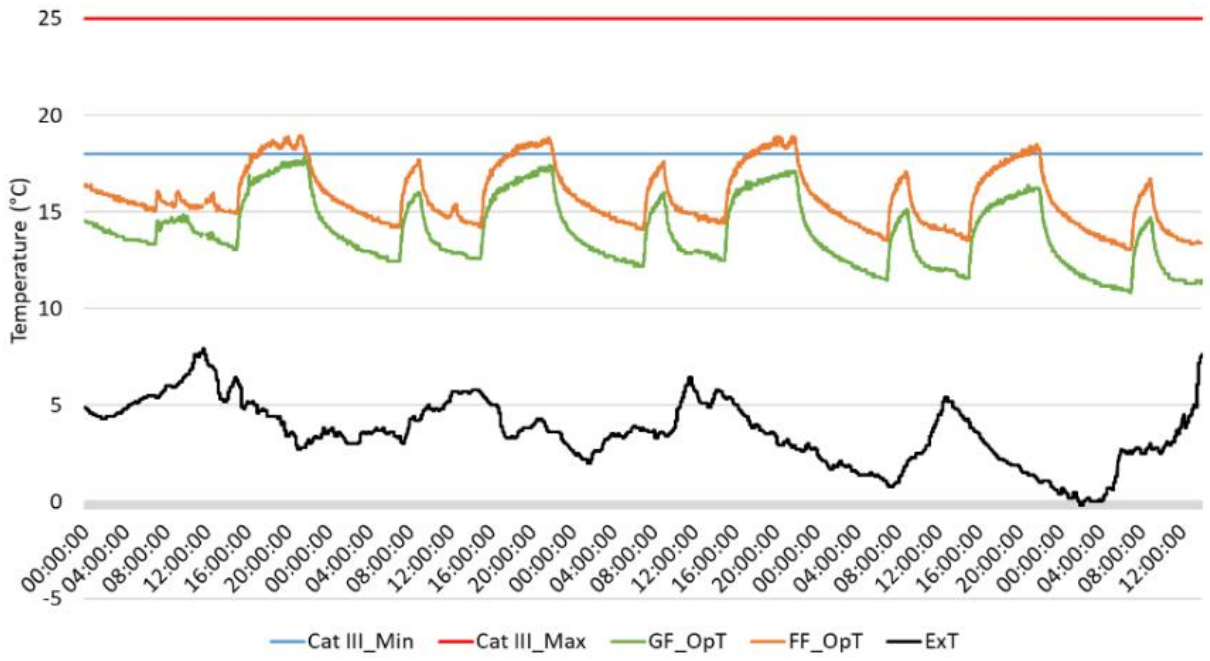

Figure 5-6 House A Adaptive Comfort Baseline

It is apparent from Figure 5-6 that under baseline conditions both internal spaces struggled to reach the minimum comfort temperature within the heating period. The first-floor bedroom did achieve the minimum thermal comfort requirement towards the end of the longer heating period (15:00 – 22:00) but was unable to during the shorter morning heating period. Ground floor temperatures did not achieve the minimum temperature required for thermal comfort.

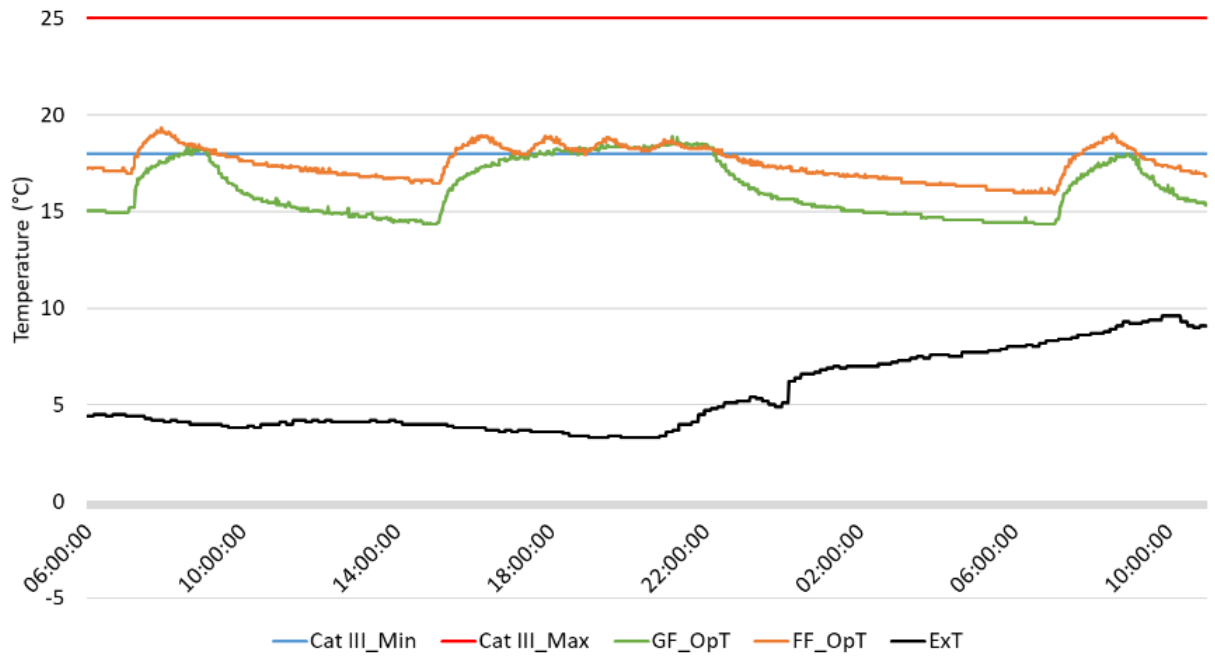

Figure 5-7 House A Adaptive Comfort IWI

During the evaluation of IWI (Figure 5-7), TIWI 1 (Figure 5-8) and TIWI 2 (Figure 5-9) it is apparent that the temperature requirement for thermal comfort was achieved in the bedroom for both morning and evening heating periods. During the evening heating period this was reached earlier than during baseline tests and subsequently sustained, as shown by oscillation around the 18°C bedroom set point.

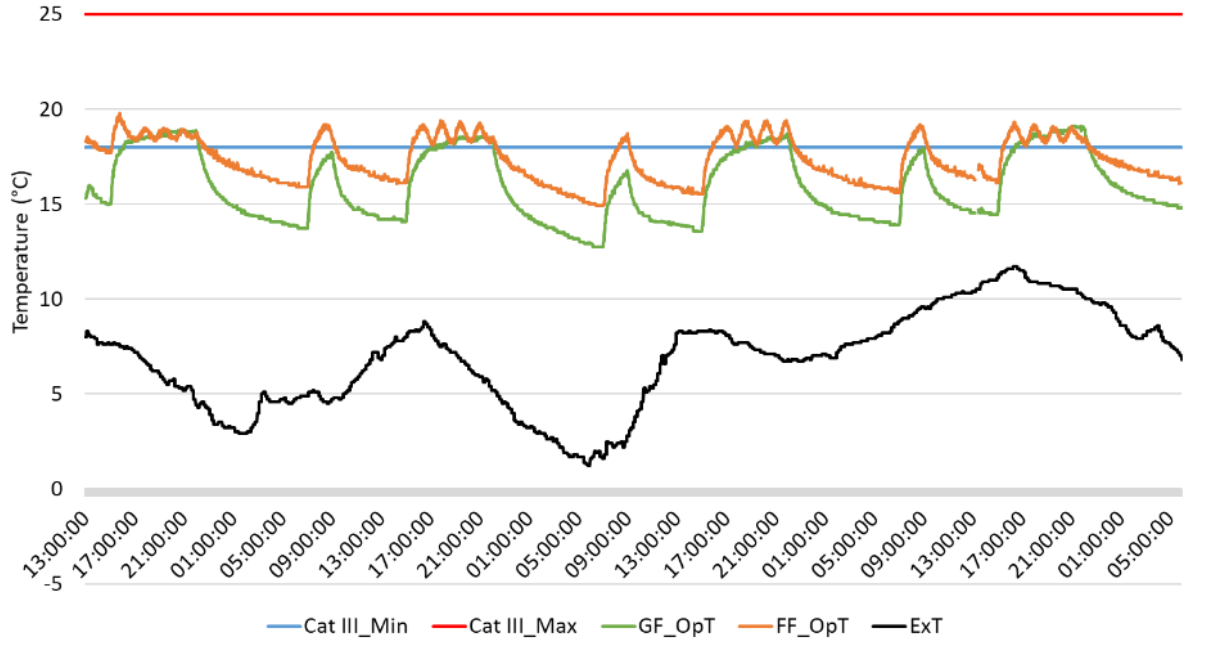

Figure 5-8 House A Adaptive Comfort TIWI 1

The living room set point of 21°C was not reached during any test phase, with the rate of temperature increase beyond 18°C appearing to decrease in all scenarios. The minimum comfort threshold was achieved on the ground floor for all test phases at points, however this was only ever consistently possible during the longer evening heating period, with heat supply ending before the acceptable temperature could be attained during the shorter morning heating.

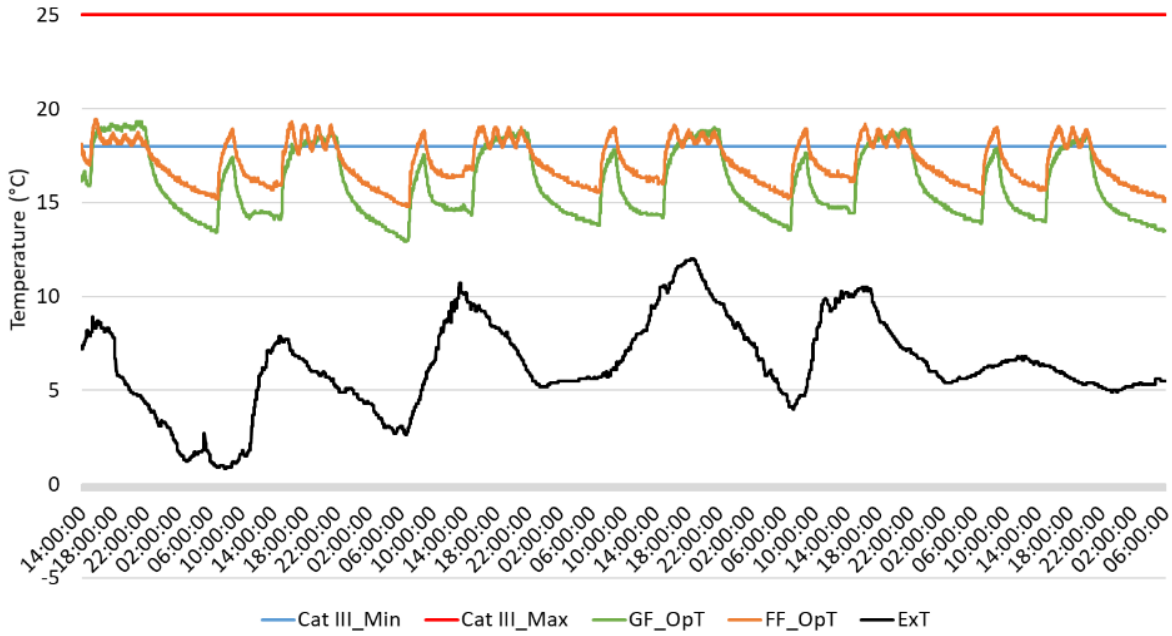

Figure 5-9 House A Adaptive Comfort TIWI 2

Poor baseline performance may be partially explained by cooler external temperatures compared to subsequent insulation phases; however, it would not be expected to fully account for the discrepancy in performance. Starting temperature (before heating began) was typically 1-2°C cooler during the baseline scenario. In the bedroom it took 5-7 hours to achieve the 18°C set point, whereas during all insulation test phases this was achieved within 1 hour. This quicker heat up than the base cases may also be an indication of faster response times, but the colder external conditions make this difficult to verify. This oscillation of temperature around the set point requires less energy as radiators are not drawing power during the cooldown phase; this contrasts with the baseline scenario where energy use was sustained for a much longer duration. When considering the insulation products, the test phases for TIWI 1 and 2 had similar external conditions and internal temperature data appear to show similar behaviour, suggesting a similar level of insulative performance.

5.2.2 Test House A, deterministic comfort

Figure 5-10 displays the average PMV during each 1-minute interval of all test phases in House A together with the corresponding external air temperature to provide environmental context. It is noteworthy that all PMV values are below the optimum value of 0, and in fact are rarely above -1 which is regarded as the minimum acceptable value for comfort. This corresponds with the temperature value for minimum comfort in the adaptive comfort analysis.

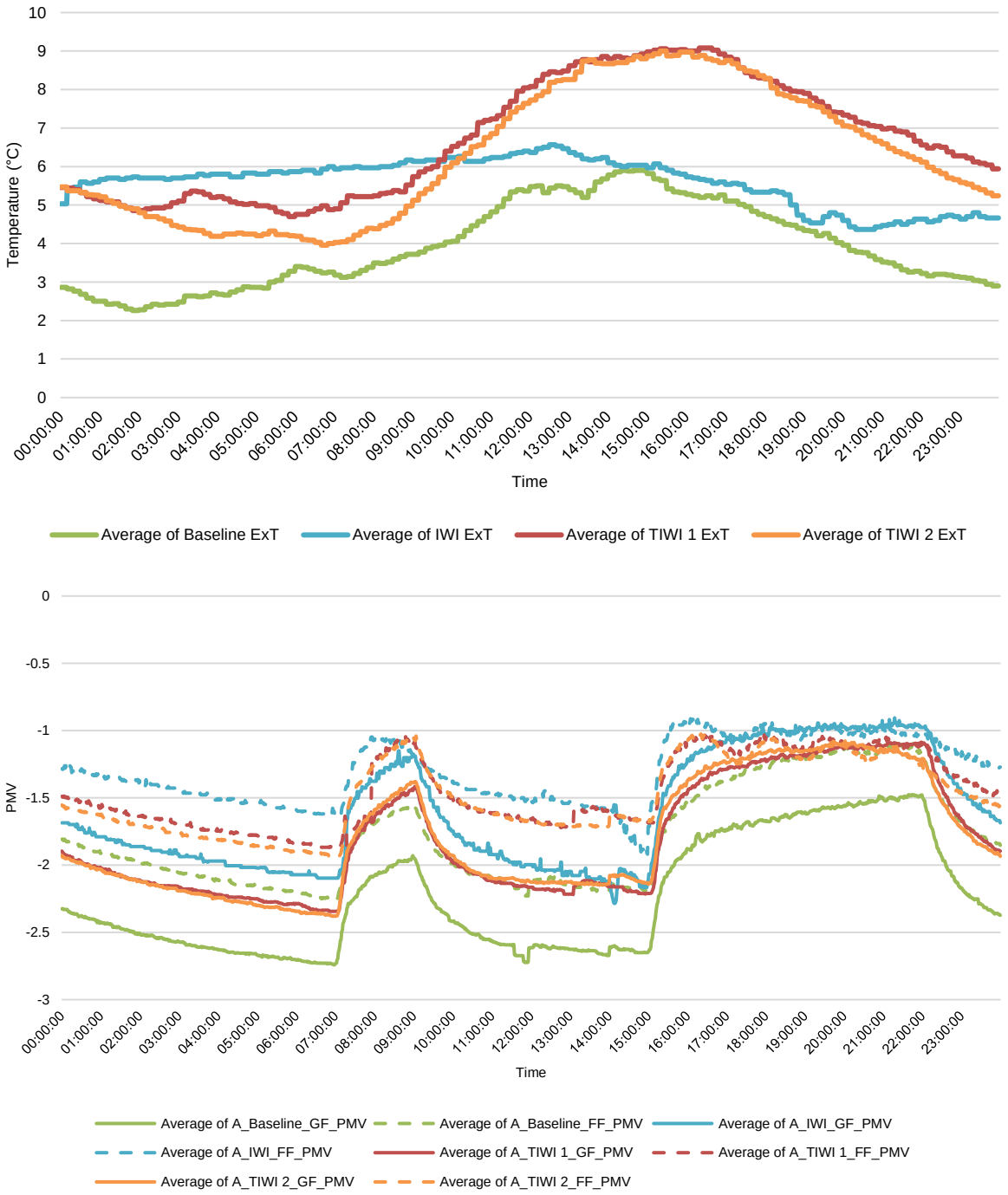

Figure 5-10 House A average Predicted Mean Vote daily profile (bottom) with average external temperature during synthetic occupancy (top) on ground floor (GF), first floor (FF)

The oscillation around the 18°C set point in the bedroom is significant as it corresponds with the -1 PMV value, i.e. the acceptable minimum level of comfort. If the set point were set at a higher temperature, the data suggest that greater comfort could be achieved as there was available heating capacity. In other words, the chosen set point restricted achievable comfort to a maximum PMV value of -1. This approach prioritises energy saving, assuming that an occupant would maximise energy saving by targeting minimum acceptable comfort conditions.

It may be that the occupant chooses to use the same energy as in the baseline scenario (with constant heat input) to heat the space to a higher temperature, thus increasing the PMV value closer to 0. This is known as comfort taking, whereby energy saving is nominal, but gains are made in occupant satisfaction.

Comfort conditions are consistently highest on both the ground and first floor for the IWI, which is a traditional internal insulation with greater thickness, despite conditions being cooler than other test periods. The IWI also appears to be the only product that enabled the ground floor to achieve a comparable PMV value during the shorter morning heating period suggesting that it is performing the most effectively. The testing phases for TIWI 1 and 2 were very similar, facilitating a good direct comparison. As can be seen, the two products perform almost identically, heating and cooling at a similar rate and enabling a PMV value of -1 on the first floor during both heating periods and on the ground floor during the longer evening period.

5.2.3 Test House B, adaptive comfort

Figure 5-11, Figure 5-12, and Figure 5-13 display the internal temperature of the ground floor living room and first floor bedroom together with external temperature during synthetic occupancy for the base case, TIWI 3 retrofit and TIWI 4 retrofit that took place in Test House B. It should be noted that an equipment failure led to the second heating period of the baseline test, shown in Figure 5-11, being different from that used in all other test periods. Despite this issue, the data are presented for further illustration of heat-up and cooldown behaviour.

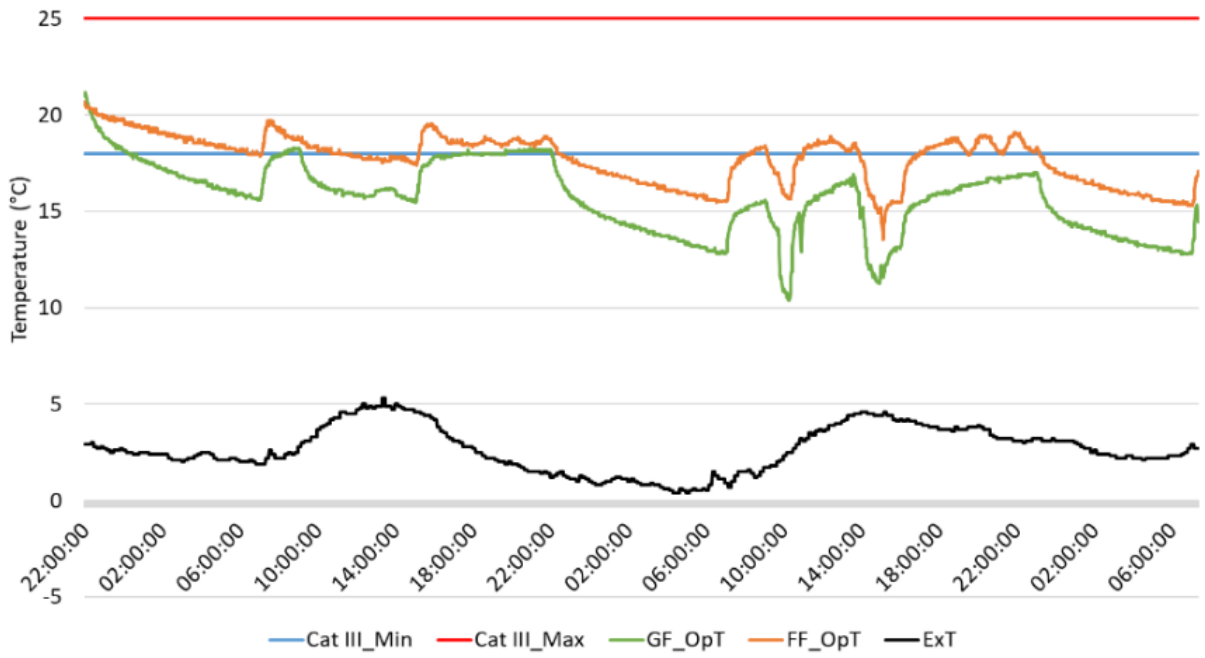

Figure 5-11 Test House B, adaptive comfort baseline

Under test conditions, it appears that the minimum temperature for thermal comfort in both monitored spaces is achieved for both the baseline and TIWI 3 under similar environmental conditions. It is notable that for the ground floor, TIWI 3 causes a greater temperature uplift during the heating periods with the baseline scenario struggling to maintain the minimum acceptable temperature.

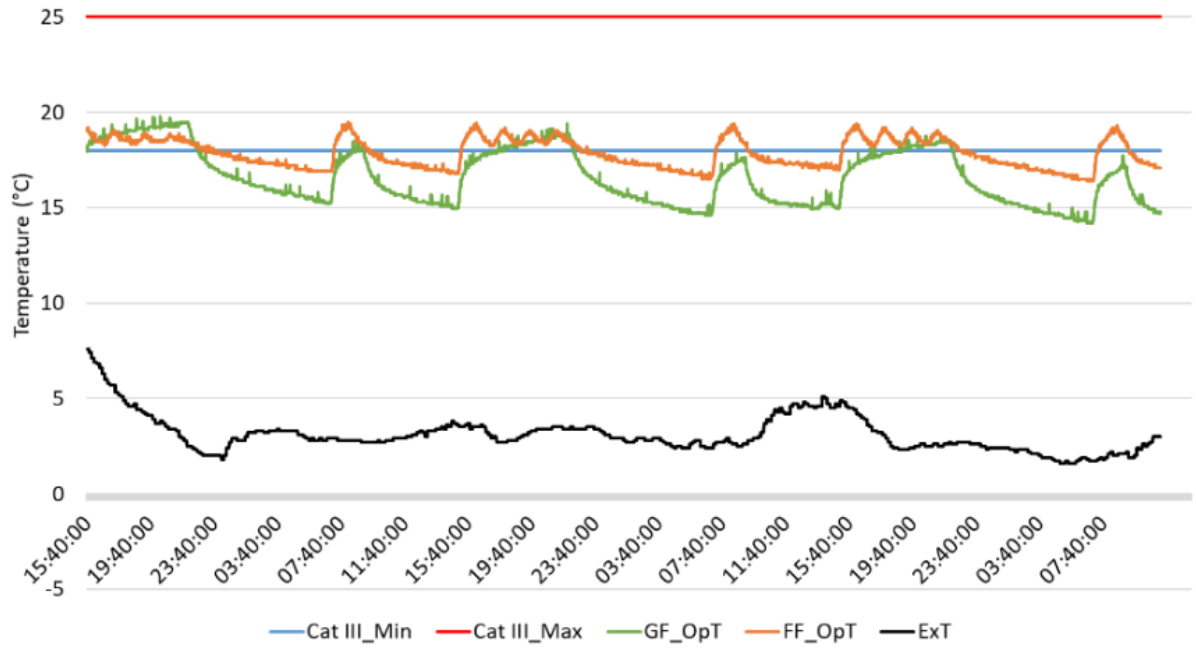

Figure 5-12 House B adaptive comfort TIWI 3

External temperatures during the baseline test and the TIWI 3 testing regime were very similar, however, cooldown appears markedly different, with internal temperatures in both the lounge and bedroom dropping 2-3°C further between the heating turning off at 22:00 and turning back on at 07:00. This suggests that the insulating benefit of TIWI 3 means the dwelling has a greater capacity to retain heat within the structure, slowing the rate of cooldown.

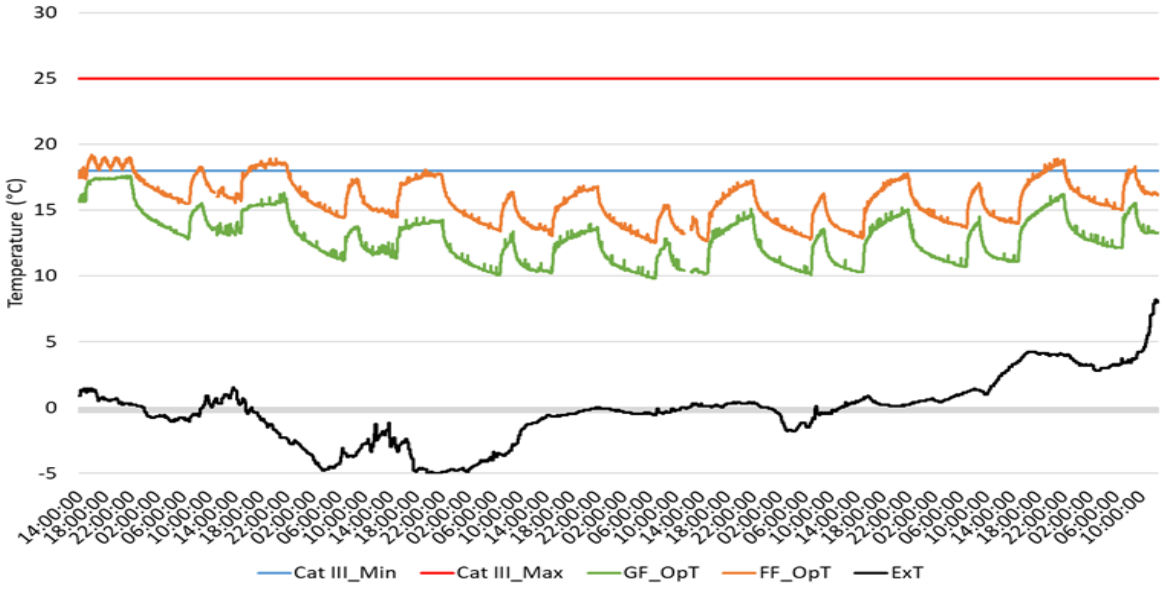

Figure 5-13 House B adaptive comfort TIWI 4

The testing period for TIWI 4 was substantially colder than both the baseline study and that of TIWI 3, and this is reflected in the data. The colder external temperature appears to be significant enough that the experimental heating schedule is not able to achieve the minimum comfortable temperature.

5.2.4 Test House B, deterministic comfort

Figure 5-14 displays the average PMV during each 1-minute interval of all test phases in House B together with the corresponding external air temperature to provide environmental context. It is noteworthy that all PMV values are below the optimum value of 0, and in fact are rarely above -1 which is regarded as the minimum acceptable value for comfort. This corresponds with the temperature value for minimum comfort in the adaptive comfort analysis. External temperature during testing for the baseline and TIWI 3 were similar, yet baseline conditions appears to perform slightly better than with TIWI 3. However, this may be a function of fabric still having residual heat from a preceding test phase since there appears to be an improvement provided by TIWI 3 that is evident in the evening heating period, with ground floor comfort exceeding that of the baseline. The substantially cooler external temperatures during testing for TIWI 4 limits a direct comfort comparison, however it is notable that a PMV increase of 0.8 - 0.95 was possible. The data suggest that during very cold periods the current heating schedule combined with TIWI 4 would be insufficient to provide comfort in either monitored space, and that additional heating energy would therefore be required.

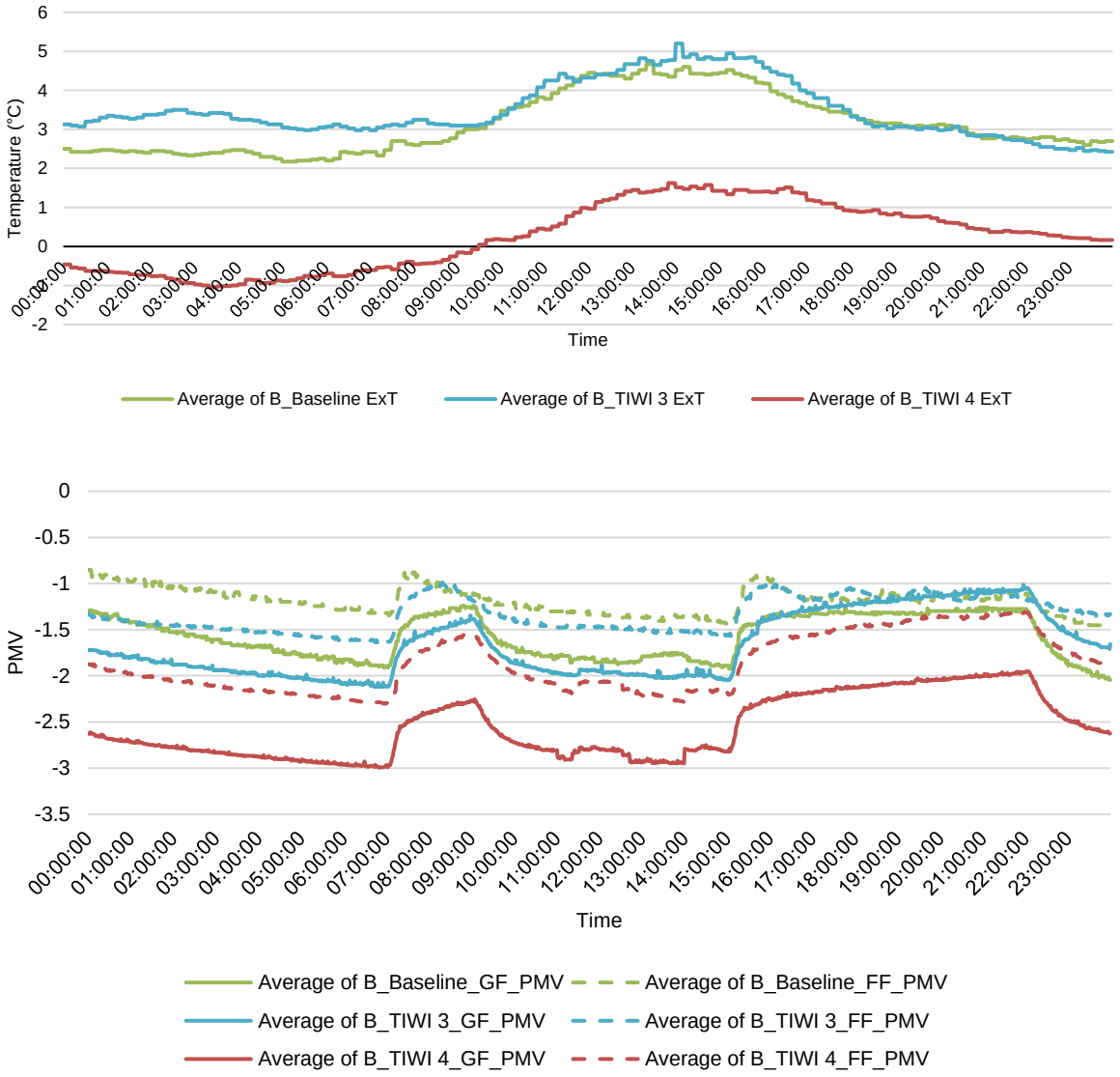

Figure 5-14 House B average Predicted Mean Vote daily profile (bottom) with average external temperature during synthetic occupancy (top).

5.2.5 Test House C, adaptive comfort

Figure 5-15, Figure 5-16, Figure 5-17, and Figure 5-18 display the internal temperature of the ground floor living room and first floor bedroom together with external temperature during synthetic occupancy for Test House C before and after the installation of TIWI 5 and TIWI 6. It is noteworthy that thermal comfort testing for this property included the second-floor loft space in addition to the ground and first floor. TIWI 5 was evaluated on both ground and first floor, consistent with other product testing, with TIWI 6 evaluated in isolation in the room in roof only since TIWI 5 could not be removed from the walls.

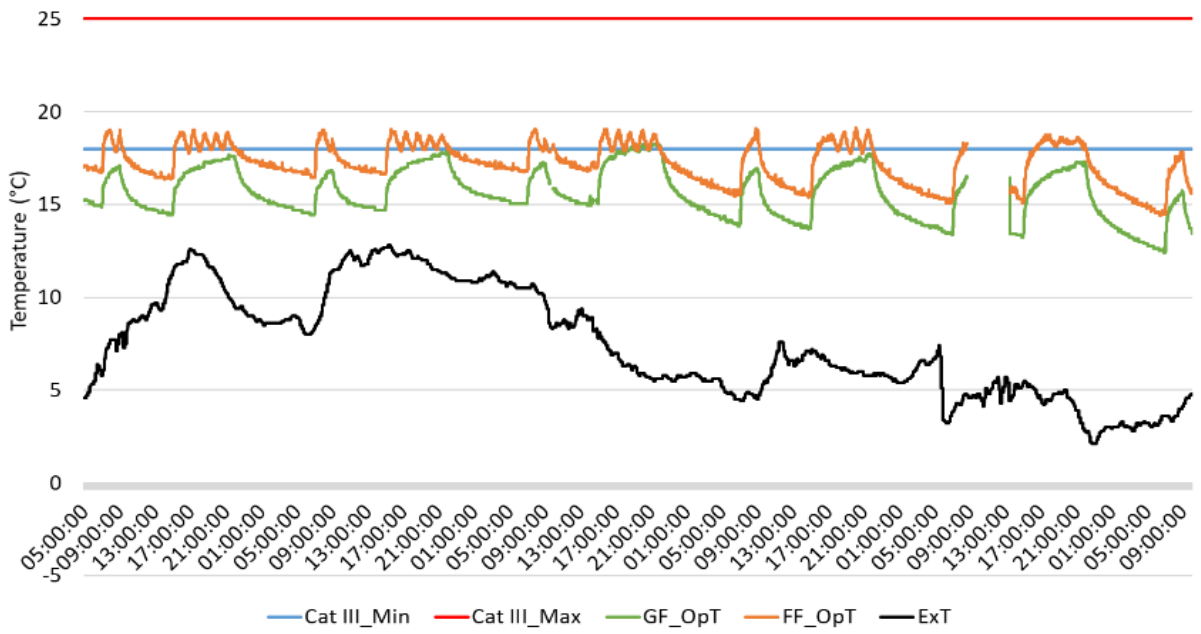

Figure 5-15 House C Adaptive Comfort Baseline (Ground and First Floor)

The external conditions were notably warmer during the baseline testing period, with up to a 10°C difference between daytime temperatures in comparison to the testing period of TIWI 5. This is evident during the heating periods, where the adaptive comfort minimum temperature is reached quickly in the bedroom such that it was possible to reach the point of oscillating around the set point during the shorter morning heating period. It is revealing, however, that even with the warmer external conditions the minimum comfort temperature is rarely achieved on the ground floor even during the longer evening heating period.

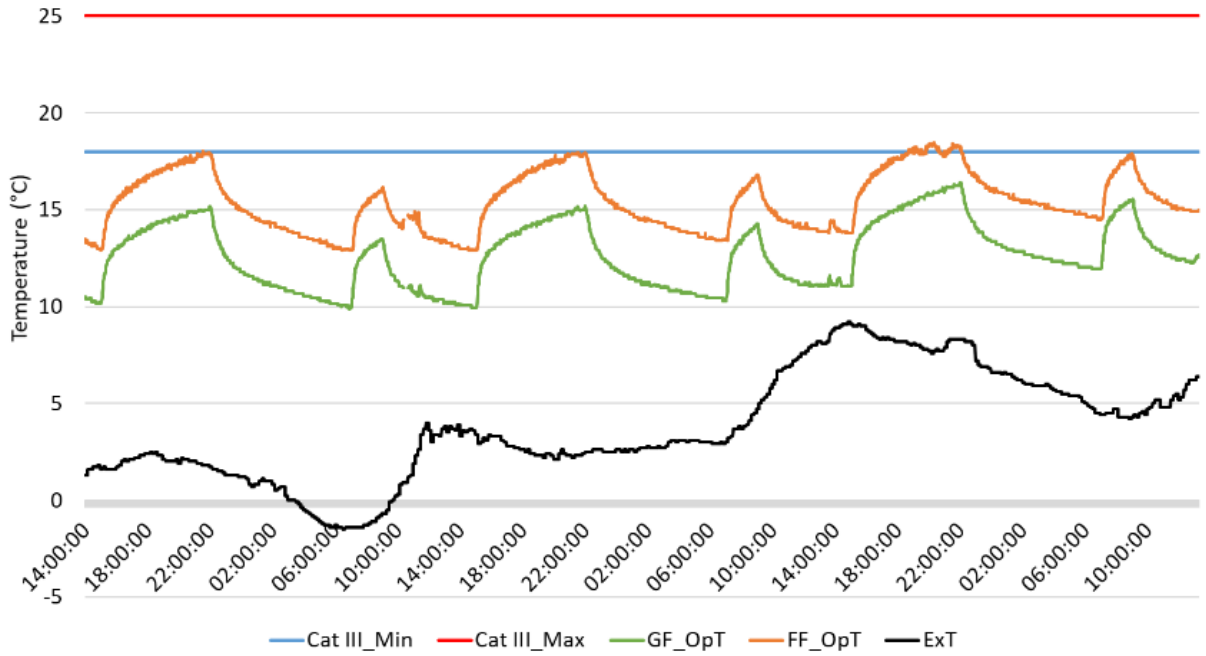

Figure 5-16 House C Adaptive Comfort TIWI 5

During warmer external temperature periods, it is apparent that a comfortable temperature was achieved readily in the bedroom during both baseline and TIWI 5 tests. It is notable that during periods of similar external conditions the baseline appears to achieve and maintain the temperature set point in the bedroom earlier and for longer than with TIWI 5. This may be related to the thermal performance of TIWI 5 or may be a function of the preceding warmer external conditions and resultant residual heat still contained in the thermal mass. Neither the comfort temperature nor the set point temperature were achieved on the ground floor, suggesting that additional heating (either duration or output) would be required to achieve comfort on the ground floor.

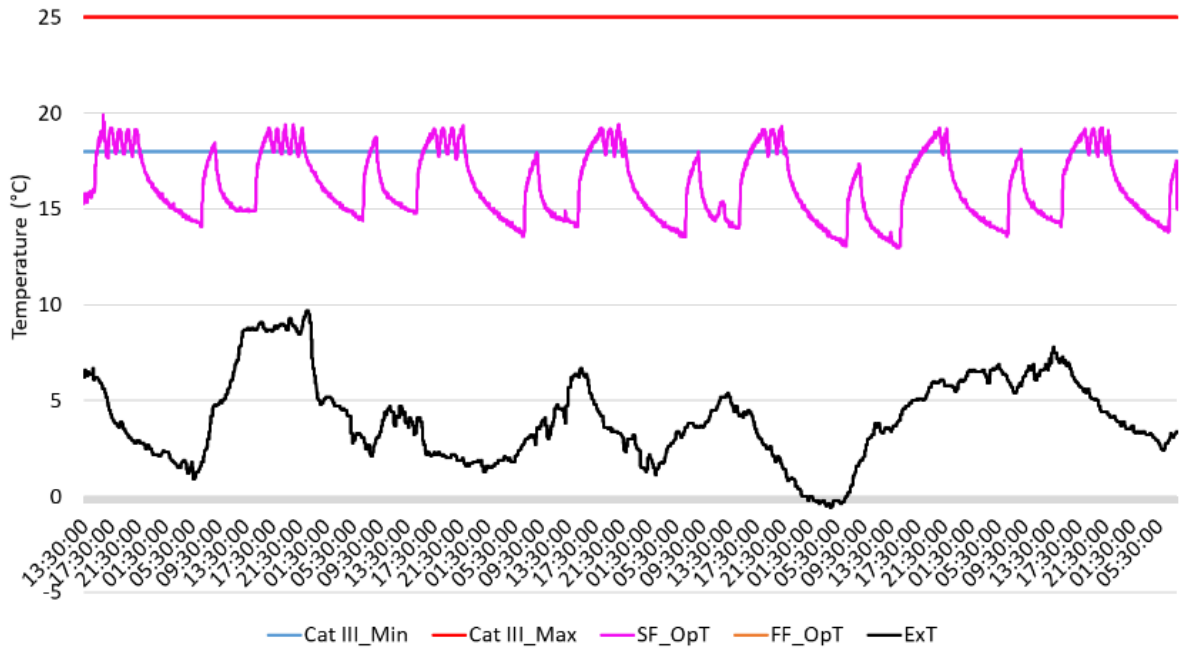

Figure 5-17 House C Adaptive Comfort Baseline (Second Floor)

During both baseline and TIWI 6 testing, it is apparent that the comfort temperature is achievable in the loft space during the longer evening heating period, with external temperature determining whether the comfort temperature is achievable during the short morning heating period. Temperature oscillation around the set point indicates that comfortable temperatures are sustained when heating is occurring. Comparison of similar periods of external conditions suggests that there is little difference in performance between the baseline scenario and when TIWI 6 is applied with regard to the duration of comfortable conditions.

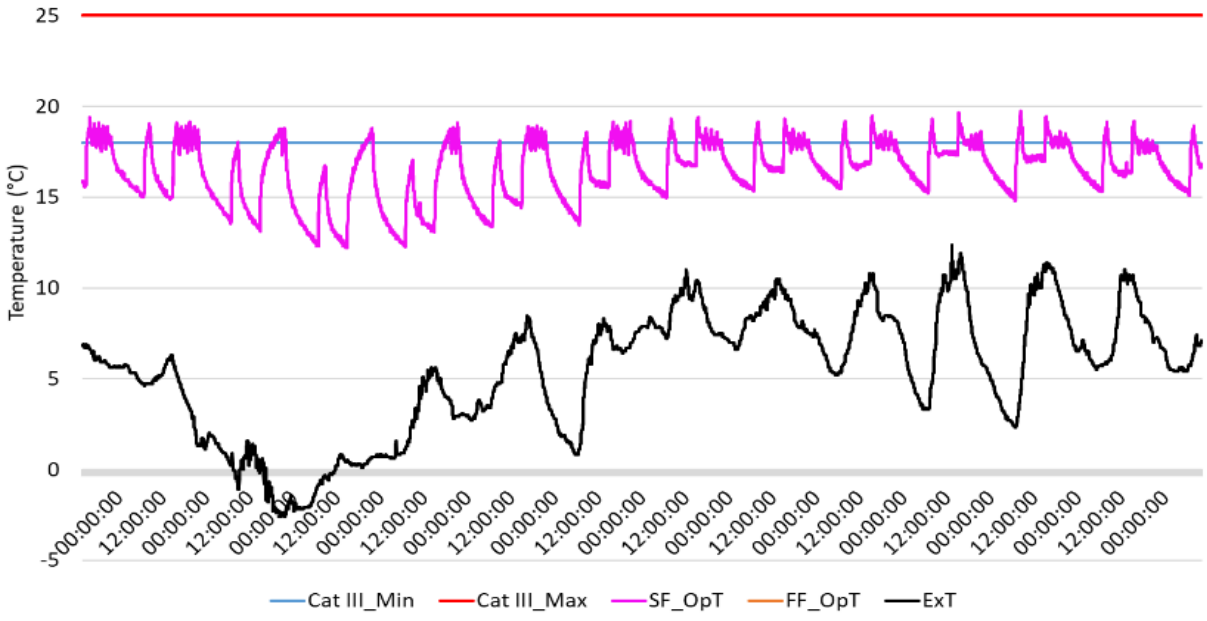

Figure 5-18 House C Adaptive Comfort TIWI 6

5.2.6 Test House C, deterministic comfort

The results shown in Figure 5-19, suggest that comfort was greatest during the baseline scenario; this is likely a function of the warmer external conditions influencing the aggregated average values as opposed to any effects specific to the insulation products. Even with warmer conditions, the ground floor baseline scenario was unable to attain the minimum acceptable PMV value of -1.

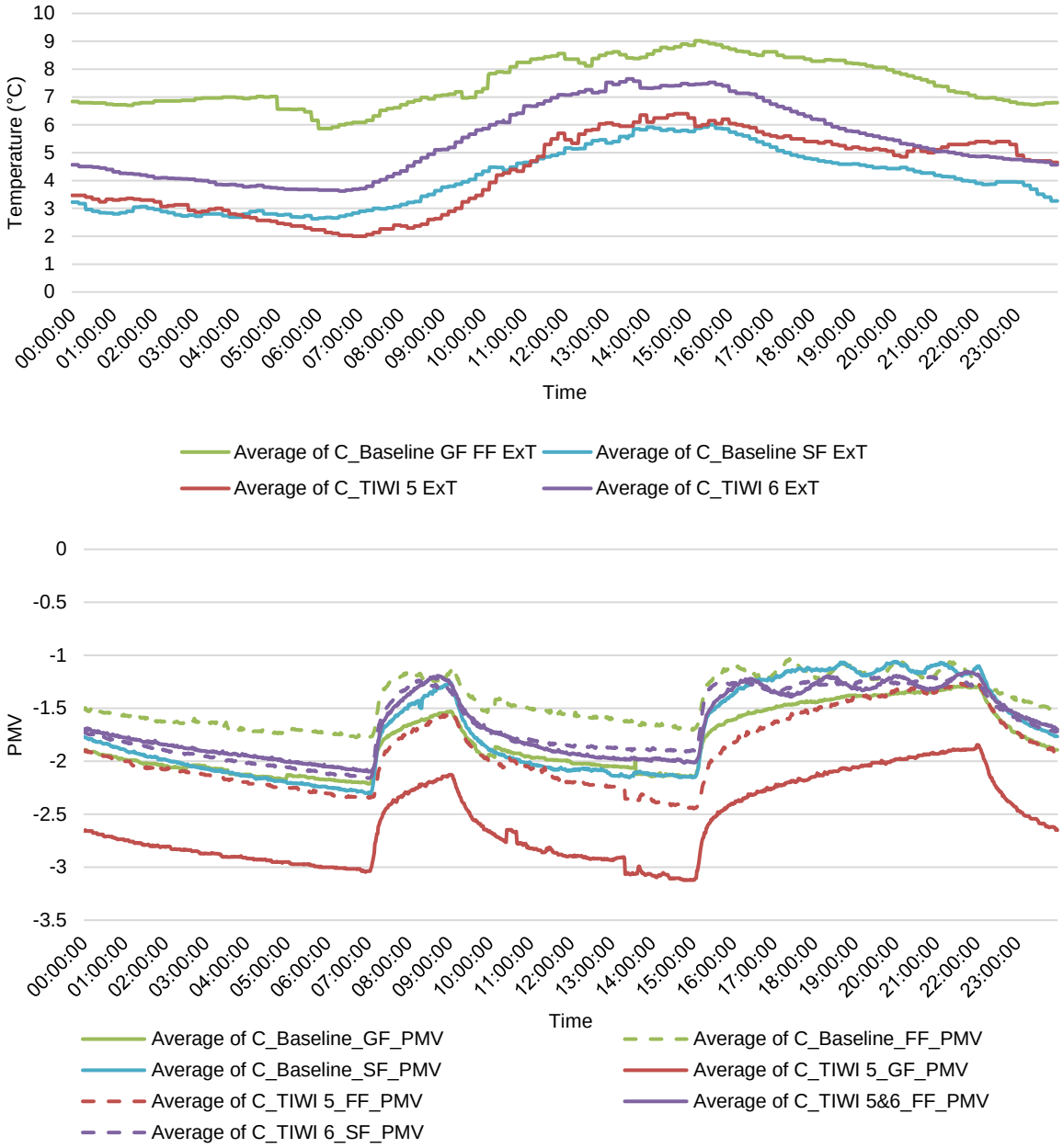

Figure 5-19 House C average Predicted Mean Vote daily profile (bottom) with average external temperature during synthetic occupancy (top).

Thermal comfort is readily attainable on both the first and second floors when applying the deterministic methodology, a finding consistent with the adaptive analysis. Comfort on the ground floor does not approach the minimum acceptable PMV value of -1 and appears highly influenced by the colder external conditions.

Higher PMV values were evident for TIWI 6 when compared to the baseline for the second floor, with this sustained throughout the cooldown phase between heating periods (09:00 – 15:00) despite similar starting points and comparable external conditions. This suggests that TIWI 6 is having a positive impact on the rate of cooldown. This effect appears to be evident also when TIWI 6 was applied to TIWI 5; the difference in PMV value between the before and after scenarios of TIWI 6 application grows progressively larger during cooldown. This may be partially explained by slightly warmer (~1°C) external temperatures, but the sustained difference may also be indicative of an improvement in performance.

5.3 Thermal comfort summary

The analysis of the thermal comfort under standardised synthetic occupancy has identified several findings consistent with all properties and product types:

- Ground floor temperatures were never able to achieve the heating set point of 21°C, and only with specific products achieved a greater than minimum level of comfort according to both adaptive and deterministic analysis methods. This suggests that all test versions would require additional heat supply or additional efficiency measures to achieve the set point and any resulting comfort improvement.
- First floor temperatures were often within an acceptable comfort range. There are two key reasons for this: firstly, the heated ground floor provides an additional source of heat to the first floor; secondly the ground floor acts as a buffer between the unheated basement such that incoming air drawn in from the lower floor is preheated. These effects are further shown in the monitored data from the second floor in house C, which displayed the greatest level of comfort.
- In many cases, first floor temperature oscillates around the 18°C set point. This set point corresponds with minimum comfort according to both evaluation metrics. The chosen set point therefore acts as a functional 'upper limit' on attainable comfort in this space. The implication of this is that greater comfort is attainable in the bedroom if the set point were to be increased.

The dynamic nature of the test protocol together with variation in external conditions and test duration all contribute to greater complexity in the comparison of insulation products. Internal temperatures are significantly impacted by the external temperature, and a larger internal-external difference has the potential to obscure any potential improvement arising from the insulation product. As such, this analysis serves to act as a descriptive illustration of the predicted level of comfort attainable under a specific synthetic occupancy schedule. For direct comparison, each product should be tested under identical environmental conditions, either in a controlled laboratory or during periods of stable external conditions and compared to a common baseline; this presents an opportunity for further research. In conclusion:

- A novel attempt to measure thermal comfort has been made.
- External conditions dominated thermal comfort measurements.
- IWI appears to improve thermal comfort, and for TIWI, despite marginal improvements, homes often remained uncomfortably cool, especially in ground floor rooms.
- Uninsulated solid wall homes are not achieving set point temperatures using recommended heating power supply, particularly during shorter morning heating periods.
- More data is needed to validate the impacts that IWI and TIWI have on thermal comfort, specifically considering comfort in furnished houses with carpets etc.

6 The Impact of TIWI on Heat up and Cooldown Times

As mentioned, a possible advantage for IWI and TIWI products is that post retrofit, homes may heat up quicker and cooldown more slowly, thus improving comfort for the occupant. To evaluate this further, data from the simulated occupancy trials conducted in the test dwellings were analysed. During simulated occupancy, the heating system was active during the day and inactive between 22:00 and 07:00, as described in the previous section on Thermal Comfort. Analysis showed no significant difference to heat up behaviour, though some interesting observations were made for cooldown behaviour. Figure 6-1 shows a typical air temperature during this cooldown period. The air temperature during this cooldown can be approximated by Equation 2:

Equation 2

$$T(t) = T_{Ext} + (T_0 - T_{Ext})e^{-kt}$$

where T is the air temperature, t is time, T_{Ext} is external temperature, T_0 is the temperature at time t=0 and k is constant which determines how rapidly the surface dissipates heat. Equation 2 was not enough to explain the air temperature in isolation, as the air temperature displayed behaviour suggestive of a rapid decay component and a slower, long-term component (see Figure 6-1). Two versions of Equation 2 were therefore used to model the air temperature decay; one which explained the decay in the first 3 hours, and a second which explained the decay between 01:00 and 07:00. This was done to account for the 2 phases of cooldown rate; faster cooldown initially and followed by a slower cooldown rate. A linear least squares method was used to find the values of k for both components.

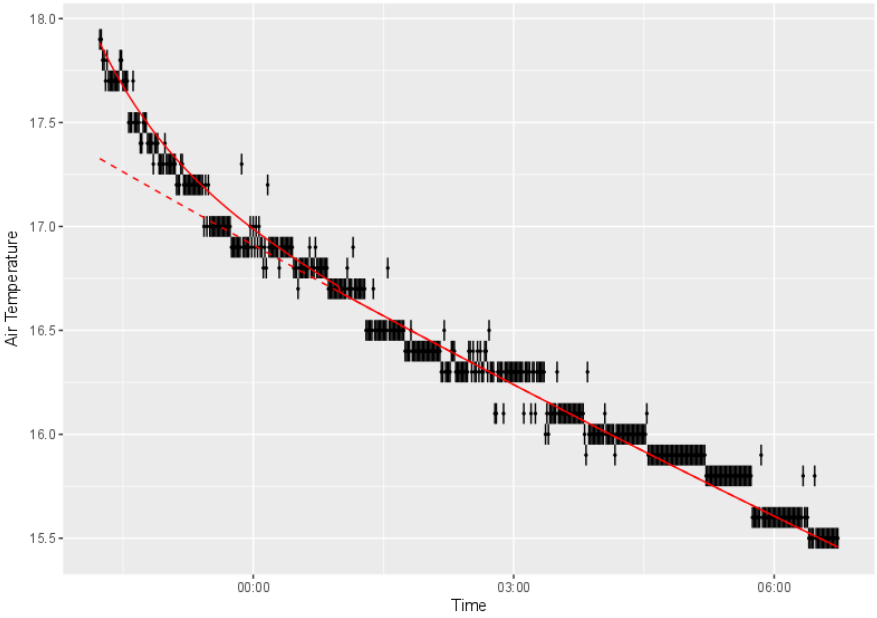

Figure 6-1 Example of air temperature decay. Black points show the observed data. The solid red line shows the model fit to the data. This model is the sum of a slow decay component (shown by the dashed red line), and a rapid decay component which is most apparent at the start of the cooldown period

Each cooldown period was modelled by Equation 2 and values of k were obtained. These values of k were used to calculate how the air would react if the initial temperature were 18 degrees, and the external temperature were consistent at 0 degrees. Using these consistent temperature conditions, each cooldown period could then be compared.

6.1 Test House A cooldown

In Test House A, 70mm phenolic foam, a 27 mm PIR, and 14mm Aerogel board were tested. The modelled cooldown curves for these are displayed in Figure 6-2, Figure 6-3, and Figure 6-4. The baseline cooldown in these graphs is displayed as the grey line, and the IWI cooldown the green line and the shaded regions show the 95% confidence interval on the mean.

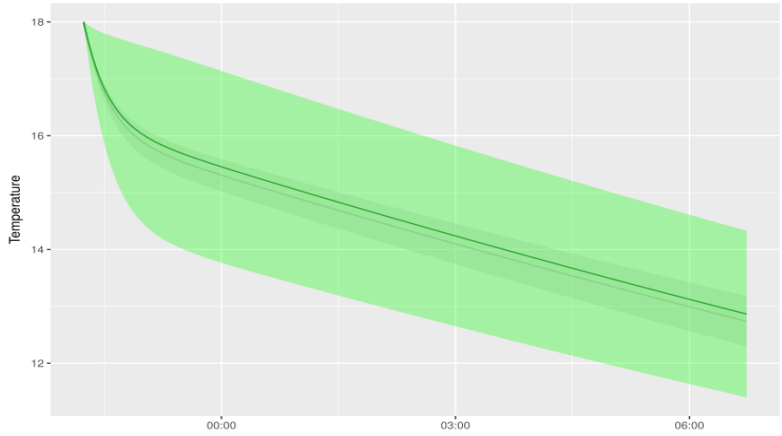

Figure 6-2 Effect of Conventional Phenolic IWI on cooldown behaviour

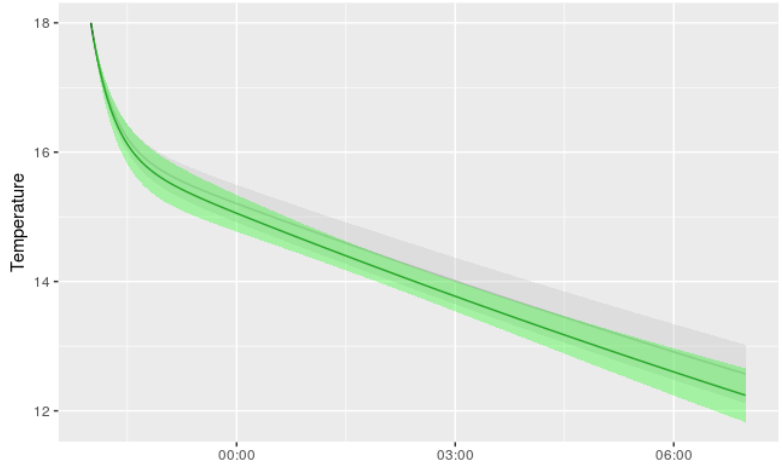

Figure 6-3 Effect of PIR TIWI on cooldown behaviour

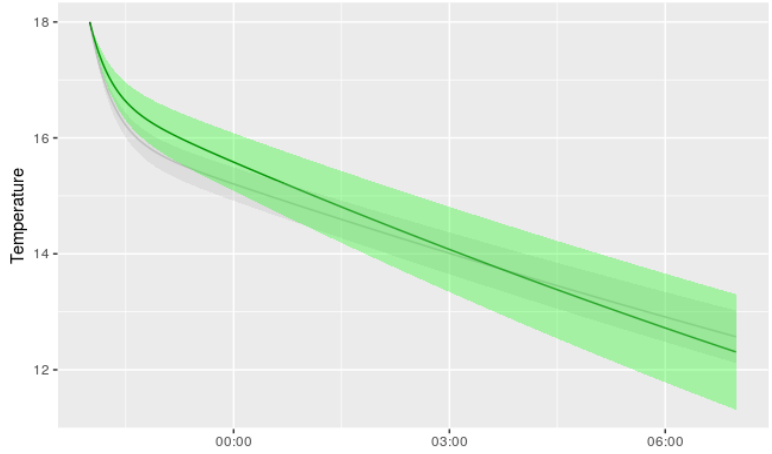

Figure 6-4 Effect of Aerogel laminate TIWI on cooldown behaviour

A good metric for the success of an insulation product is the temperature of the room after the cooldown period (in this case at 07:00). A successful product would have a higher room temperature at 07:00 than for a non-insulated room, i.e. the green line would be substantially above the grey line in these graphs. For all the products tested in Test House A, no significant difference between insulated and non-insulated room temperatures was found at 07:00. However, only 3 nights of cooldown data were obtained for each product in Test House A, and these small numbers mean that finding a significant difference is challenging.

This is particularly clear in Figure 6-4, in which, the short duration of data collection cause the cooldown to have a particularly large uncertainty. For this product, only 2 nights of data were available due to equipment malfunction. If the IWI is influencing the internal temperature, monitoring an increased number of cooldown periods may reveal this effect.

6.2 Test House B cooldown

In Test House B, two TIWI products were tested. These were a 22mm EPS wall board and a 20 mm cork render. The modelled average cooldown curves for these products is displayed in Figure 6-5 and Figure 6-6. Again, there were only a small amount of data available for the analysis in this house. For the both TIWI, the average temperature appears to be greater because of the IWI, but statistical tests (a Wilcoxon rank sum test) applied to this cooldown suggest there is no significant difference at the 95% confidence interval. Insulated render on the other hand does show a significant difference at 07:00. EPS had a marginally greater effect with an average room temperature which is 0.71 degrees greater than the baseline case.

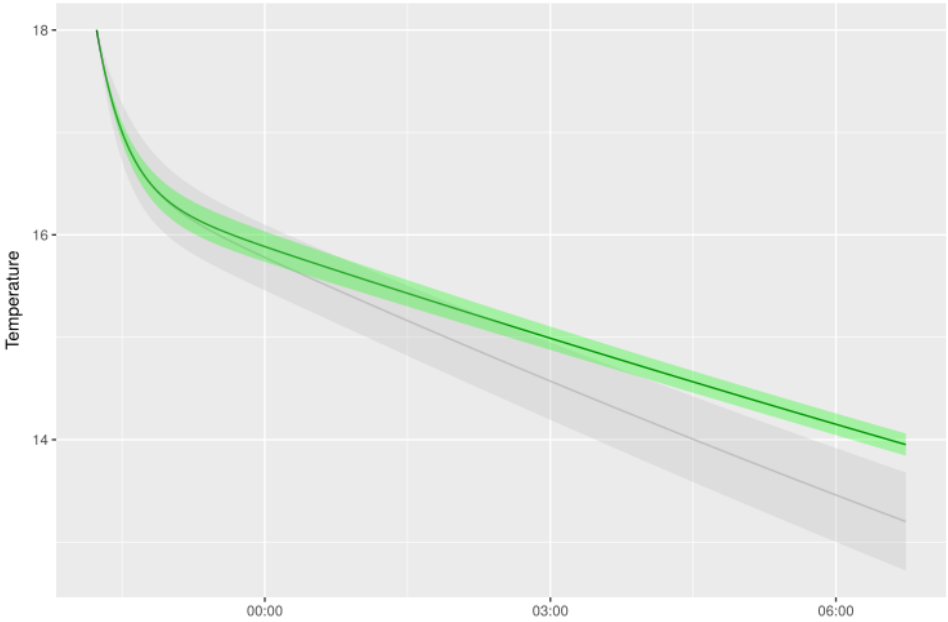

Figure 6-5 Effect of EPS laminate TIWI on cooldown behaviour

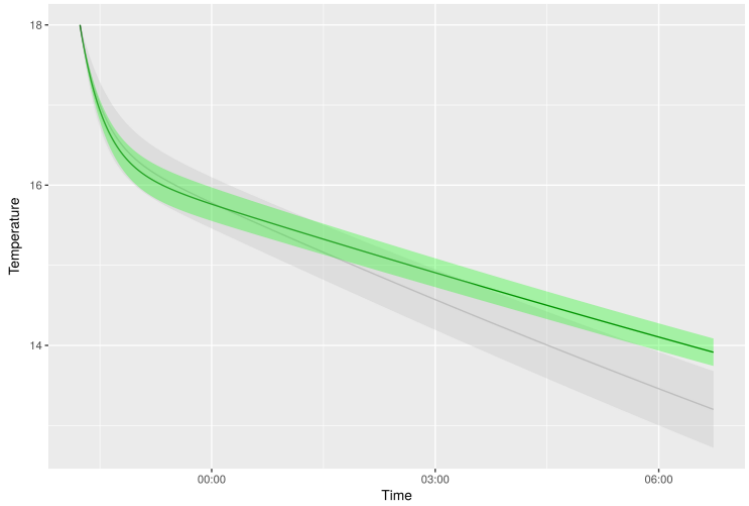

Figure 6-6 Effect of Cork render TIWI on cooldown behaviour

6.3 Test House C cooldown

In Test House C, two unique TIWI products were tested, Latex rolls and thermo-reflective paint. In addition, these products were combined for a final test of these two TIWI with the paint being applied on top of the latex rolls. Cooldown analysis for these are shown in Figure 6-7 and Figure 6-8.

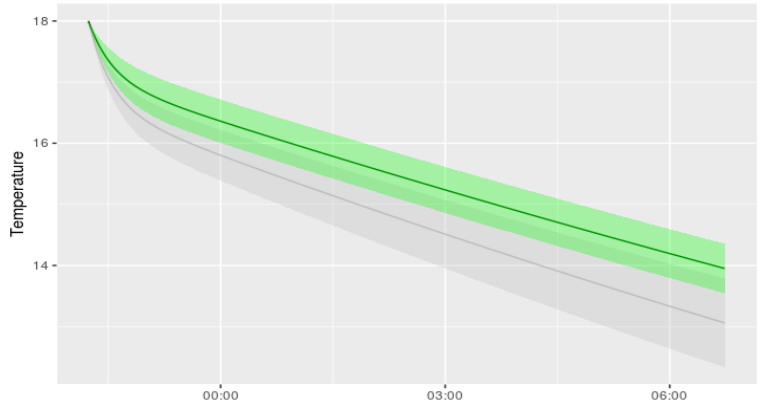

Figure 6-7 Cooldown of Thermo-reflective paint compared to a baseline.

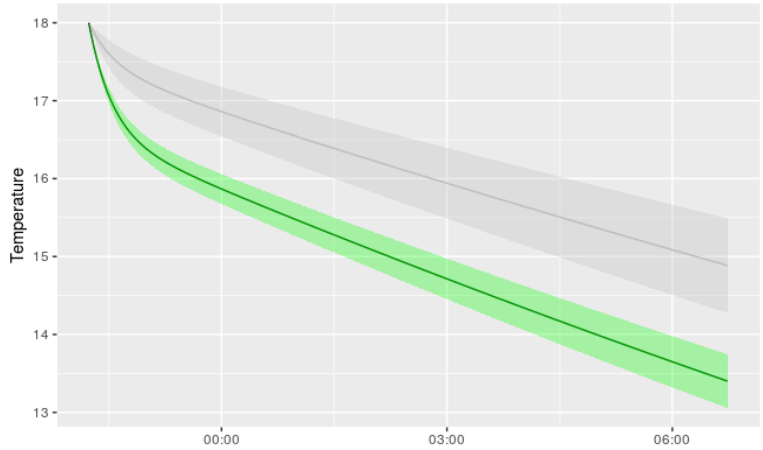

Figure 6-8 Cooldown of latex rolls compared to a baseline.

Figure 6-7 displays the mean cooldown periods of a wall with and without thermo-reflective paint indicating the thermo-reflective paint does display a significant difference in internal temperature at 07:00, with an internal temperature 0.9 degrees higher because of the TIWI. Figure 6-8 suggests the latex rolls appear to have caused the internal temperature to be lower during the cooldown, and this difference is significant at the 95% confidence level.

This may be the result of the latex rolls insulating out the benefit of the thermal mass of the wall: the brick wall both receives and gives heat energy to the room. With no TIWI, the wall is heated easily, and will discharge some of this heat into the room when the heating is switched off. With the latex rolls installed, the increased thermal resistance may mean that the wall is not receiving as much thermal energy. Likewise, when the heating is off, it cannot discharge as much heat into the room, thus causing the room temperature to be lower. Alternatively, a bout of particularly windy weather may have caused the pattern seen in the latex rolls data. However, the weather data obtained did not suggest that the latex rolls was tested under windy conditions. Furthermore, the brick wall temperatures of the room suggest the wall is indeed colder because of the latex rolls. This is expected to be the case for all the TIWI though the measurement periods do not appear to be sufficient to observe this trend with certainty. In Figure 6-9 the solid line shows a typical wall surface temperature with no TIWI. The dashed line shows a typical wall surface temperature after latex rolls were installed. It is apparent from this graph that the wall surface under the latex rolls is noticeably colder. In either case, this is an interesting phenomenon that could be explored further in tests with IWI.

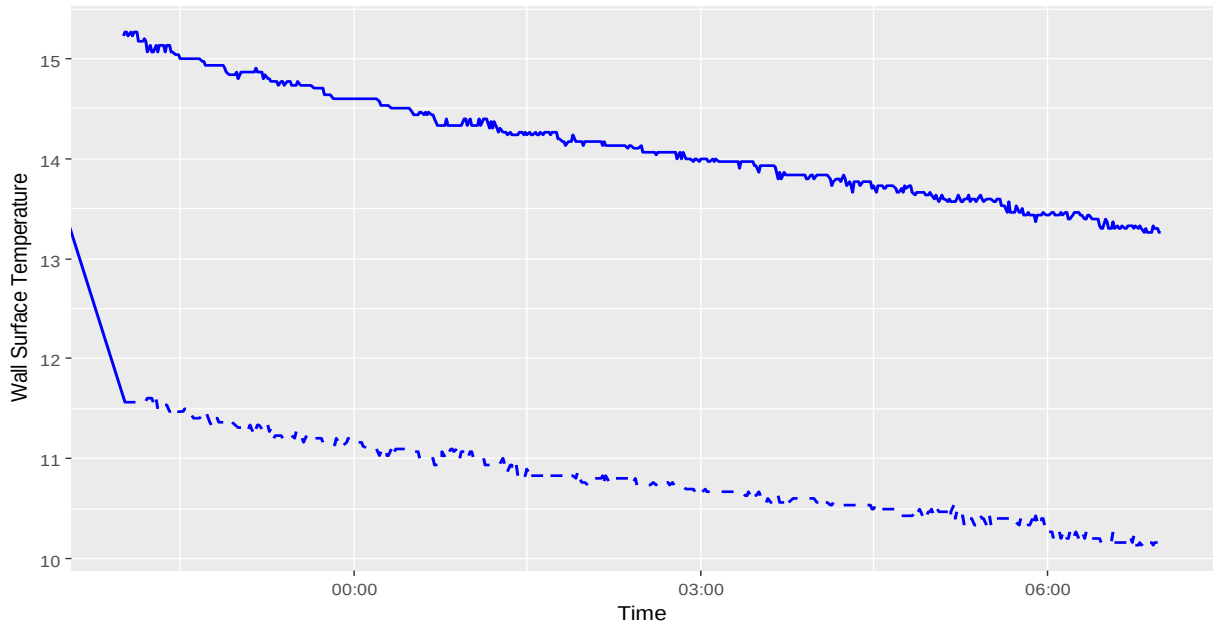

Figure 6-9 Wall surface temperatures before and after TIWI. The solid line shows the surface temperature before TIWI. The dashed line shows the wall surface temperature (under the TIWI), following the latex rolls install. The latex rolls cause the wall surface temperature to reduce.

Following the latex rolls install, thermo-reflective paint was applied in one of the rooms to create a TIWI which combined the two products. Figure 6-10 displays the mean cooldown periods of a wall with and without latex rolls and thermo-reflective paint. Again, a significant difference is found at the 95% confidence level, though the internal temperature in this case is again lower because of the TIWI.

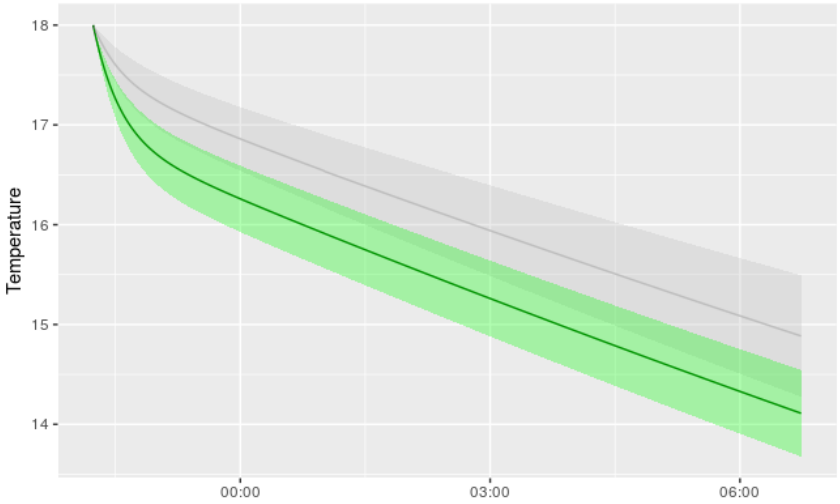

Figure 6-10 Effect of latex rolls and thermo-reflective paint on cooldown behaviour

6.4 Heat up and cooldown summary

In conclusion, neither IWI nor TIWI showed a statistically significant improvement in heat up rates.

TIWI may influence improving cooldown rates, however, the effect is not substantial and appears to not be linked to the insulation's ability to reduce heat loss. Latex rolls reduced the cooldown rate compared to the base case, and when thermo-reflective paint was added this appears to have the greatest impact, reducing temperature drops by 0.9°C over a single evening cooldown. However, uncertainty is very high and some TIWI were found to accelerate cooldown rates or have no effect at all. More data collection over a longer duration and different house types is needed to validate the cooldown modelled predictions for each TIWI.

7 The Impact of TIWI on Room in Roof Retrofits

7.1 Rationale for room in roof TIWI retrofit evaluation

The proposal for the room-in-roof (RiR) experimental work originated from the solid wall TIWI findings. Houses A-C each contained an apparently poorly insulated or uninsulated RiR that constituted a large proportion of the total heat loss area. All the solid wall TIWI products tested (excluding TIWI 4 cork lime render which may need testing for its adhesion at thicker depths) are suitable for application on the elements that comprise a RiR. RiR is a different retrofit solution in ECO to IWI, requiring installers to have different qualifications to be able to offer this under the regulations, even though they could be using the same products. This research attempts to measure the improvement in thermal performance resulting from a RiR-only retrofit, as this may be an appropriate retrofit for solid wall homes. The work also intends to highlight the potential advantages and disadvantages of retrofitting a RiR with IWI compared to a TIWI.

7.2 Experimental design

Building performance evaluation (BPE) work was undertaken during the baseline (pre-retrofit) and post-retrofit stages. The BPE methods used in the RiR work are the same as the solid wall TIWI work:

- HTC measurements derived from electric coheating
- *In situ* U-value measurements in accordance with ISO 9869-1
- Blower door tests to measure air permeability and air leakage rate in accordance with ATTMA TS L1
- Thermographic surveys to identify areas of good/poor thermal performance and to identify points of air infiltration under building depressurisation

The LBU research team was present throughout the retrofit process to make observations, take photographs, and gain feedback from the installers. The experiment was designed to compare a TIWI RiR retrofit with the conventional RiR retrofit method. The two methods can be summarised as:

- Conventional; removal of existing RiR surfaces and placement of insulation between structural timbers (e.g. joists, rafters, studs). Application of a new surface over the RiR structural timber.
- TIWI overboarding; application of TIWI boards straight onto the existing surface of a RiR. However, as PAS 2030 requires the base of residual loft space above the habitable room below to be insulated, it may be necessary to create an access hatch if not already present.

It was decided that the TIWI board selected should be widely available and familiar to the construction trade. Thus, a material resembling TIWI 1 was selected; a 27 mm laminated plasterboard comprising 9.5 mm plasterboard and 17.5 mm XPS board, with an R-value of 0.54 m2K/W.

PIR insulation board (λ 0.022 W/mK) was selected for the conventional retrofit as loft retrofits often use an insulation material with low thermal conductivity between structural timbers to meet the requirements of Part L1b of the Building Regulations. The thickness of the insulation could not be specified until the RiR surface had been removed and the structural timber measured as the sloping ceiling, ridge roof, and dormer roof all require a 50 mm ventilation path between the insulation and roof covering.

7.3 Room in Roof TIWI Test House

It was not possible to regain access to Houses A-C to perform the RiR work as they had been occupied after the solid wall work ceased. The Test House used for the RiR TIWI test (Test House D) was made available to the research team by a housing charity who offered the home for study in exchange for the retrofit, and located on the parallel and adjacent street to House B and is of similar age, form, and construction. House D is shown in Figure 7-1 and the pre retrofit condition of the room in roof is shown in Figure 7-2.

Figure 7-1 Room in Roof Test House D

House D has a roof structure that is of similar form and construction on both elevations (i.e. both sides of the roof contain similar sized dormer windows, sloping ceilings, and dwarf walls). This enabled the comparison of retrofit methods to be taken on the same house. The RiR on the east elevation was selected for the TIWI overboarding retrofit and has an external heat loss area of 22.3 m^2. The RiR on the west elevation was selected for the conventional and has an external heat loss area of 22.2 m^2.

Renovation work by the housing charity delayed handover of House D until mid-April which had repercussions for the *in situ* U-value measurements (see Section 7.6). Renovation work had already started on the RiR and some of the surfaces had been removed. The housing charity recommended that they finished removing the surfaces and then re-cover with plasterboard before the experimental work commenced. The research team visited House D during the renovation work and found that much of the original surface was insulated with an EPS plasterboard. Figure 7-2 shows this being removed from the dormer ceiling. When House D was handed over, the research team had been told that all of the insulation had been removed from the RiR and that there was nothing behind the plasterboard. However, when the plasterboard was removed during the conventional retrofit, many of the elements were found to contain mineral wool insulation (Figure 7-2).

Figure 7-2 Pre-existing EPS plasterboard being removed from the ceilings of House D prior to handover (left). Mineral wool found in dormer of conventional retrofit RiR following baseline tests

It was initially thought that only the conventional retrofit side of the RiR contained pre-existing insulation during the baseline measurement stage. However later analysis of thermography and U-value measurements strongly suggested that the dormer cheeks of the TIWI retrofit RiR contained insulation. Figure 7-3 reveals that the dormer cheek of the TIWI over-boarded RiR was insulated during the baseline test as the studwork is colder than the rest of the element. This means that the overall reduction of HTC from both the TIWI and IWI RiR retrofits may be conservative estimates.

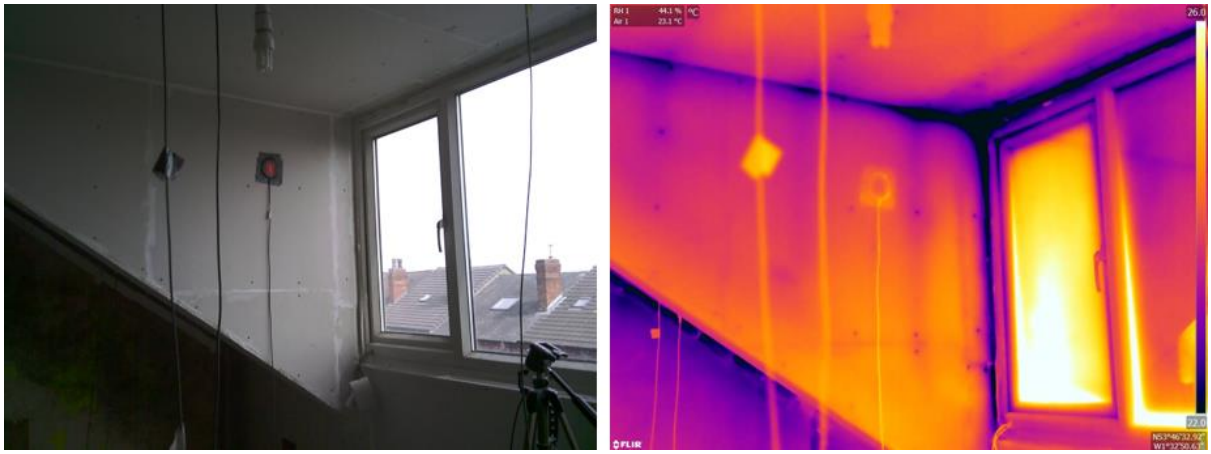

Figure 7-3 thermogram of TIWI over-boarded RiR dormer cheek that revealed the presence of insulation within the structure at the baseline test stage

7.4 Retrofit observations

Researchers visited House D during and after the retrofit process to make observations and obtain feedback from the installers. The main findings were that the TIWI overboarding RiR retrofit was completed three times faster than the conventional RiR retrofit. In addition, it was easier to specify, since the insulation for the conventional retrofit could not be ordered until the pre-existing surfaces had been removed as the depth of structural timber work needed to be measured. This was important for specifying insulation between ceiling joists as a ventilation gap (≥ 50 mm) needed to be maintained between the insulation and roof covering. Furthermore, the TIWI overboarding RiR retrofit actually maintained the pre-existing 100 mm ventilation gap between the original plaster and roof covering, whereas, the conventional RiR retrofit reduced the ventilation gap to 50 mm, meaning more air movement may be achieved in the TIWI retrofit, further reducing the risk of damp behind the boards.

A practical benefit for the installers for the TIWI product was that there was substantially less material for disposal when using the TIWI overboarding method. For example, the knee wall was the only part of the pre-existing RiR structure that was removed during the TIWI overboarding retrofit to allow for the residual loft space to be insulated (Figure 7-4). The conventional retrofit resulted in the creation of substantially more dust due to the removal of the entire RiR surface area and the need to cut more insulation.

Although the retrofit work was generally undertaken to a high standard, the cutting of insulation boards inevitably resulted in gaps (typically 2-3 mm) between and around insulation boards for both retrofits, specifically:

- As the TIWI overboarding required less cutting, the proportion of gaps between TIWI boards across the surface of the RiR was less than the conventional retrofit. Gaps were filled with a flexible sealant (Figure 7-4).
- Gaps were present around the edges of many of the insulation boards used in the conventional RiR retrofit (Figure 7-5). Larger gaps were sealed with polyurethane (PU) expanding foam prior to taping. The most time-consuming task during the conventional RiR retrofit involved cutting the insulation boards to the correct size to fit between structural timbers.

There were also more workarounds needed with the conventional retrofit that relied on expandable PU foam spray to fill awkward gaps between the party walls and rafters, and the dormer beams and ceiling joist (Figure 7-6), whereas these areas could be more simply over-boarded with TIWI. It was observed that some insulation boards fitted during the conventional RiR retrofit were not always flush with the edge of the structural timbers (Figure 7-5). This air gap creates a space for potential wind washing of the insulation if any air path is present to the cold side of the insulation.

Figure 7-4 TIWI over-boarded RiR retrofit work. Insulation being installed in the residual loft space behind the knee wall (left). Small gaps evident between TIWI boards (right)

Figure 7-5 Conventional RiR retrofit work. Gaps evident around edges of insulation boards prior filling to taping between upper dormer beam and adjacent dormer ceiling joist (left) and recessed insulation boards on dormer ceiling (right)

Figure 7-6 Upper dormer beam and dormer trimmer rafter for each RiR. TIWI was used to overboard these timbers (left) whereas timbers were left untreated in conventional RiR retrofit (right). Channel between the upper-dormer beam and adjacent dormer ceiling joist (right)

Further assessment was undertaken using infra-red thermography. Figure 7-7 shows that locations of structural timber within the over-boarded TIWI RiR do not create a thermal bridge, whereas they do in the conventional retrofit as the timber work remained uninsulated.

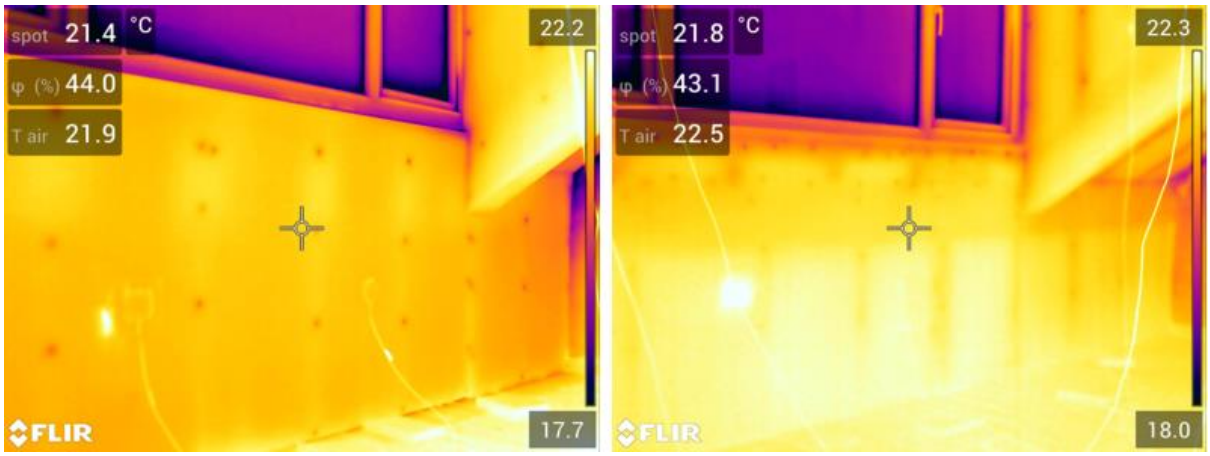

Figure 7-7 Thermograms of knee wall of TIWI over-boarded RiR (left) and conventionally retrofitted RiR (right)

Figure 7-7 also shows a greater level of thermal consistency across areas of the knee wall (excluding timber stud locations) for the TIWI, whereas a horizontal band of lower thermal performance was observed across the top of the conventionally retrofitted knee wall. Figure 7-8 shows that this area of lower performance corresponds with the lower dormer beam which prevented insulation placement.

Figure 7-8 Image of conventionally retrofitted RiR showing lack of insulation at location of the lower dormer beam (left) and thermogram highlighting reduced thermal performance at this location.

Figure 7-9 shows greater thermal consistency across the roof in the TIWI over-boarded RiR. Though some regions of additional heat loss can be seen at joints between insulation boards, notably where TIWI boards had to be cut to meet a sloping section of ceiling. Point thermal bridges through metal fixing screws are also prominent. The liberal use of fixing screws in some locations was due to the occasional difficulty installers had at locating structural timber to affix the TIWI boards. The insulation boards for the conventional retrofit were accurately cut to size at most locations. However, there were notable gaps between the ridge level ceiling joists and insulation boards that required expanding foam. Figure 7-9 shows that excessive heat loss was observed at these locations.

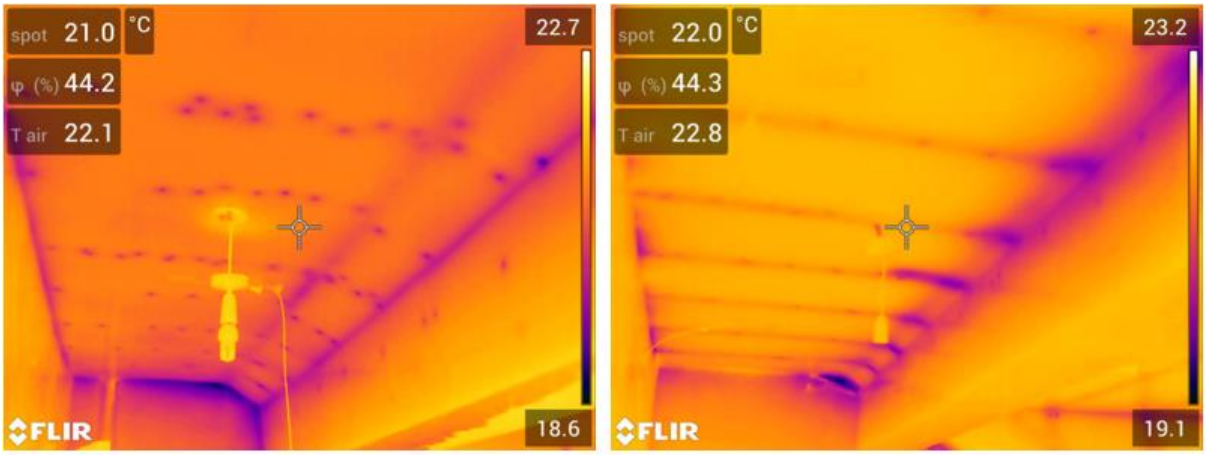

Figure 7-9 Thermograms showing roof below ridge and upper dormer beam for; TIWI over-boarded RiR (left) and conventionally retrofitted RiR (right)

Figure 7-10 reveals excessive thermal bridging along the dormer windowsill following the TIWI retrofit. This behaviour is not evident for the conventionally retrofitted dormer windowsill. It was later established that the installer had used a metal edge bead at this location to create a defined corner which has resulted in a significant thermal bridge. The conventional retrofit sill was treated with a section of TIWI.

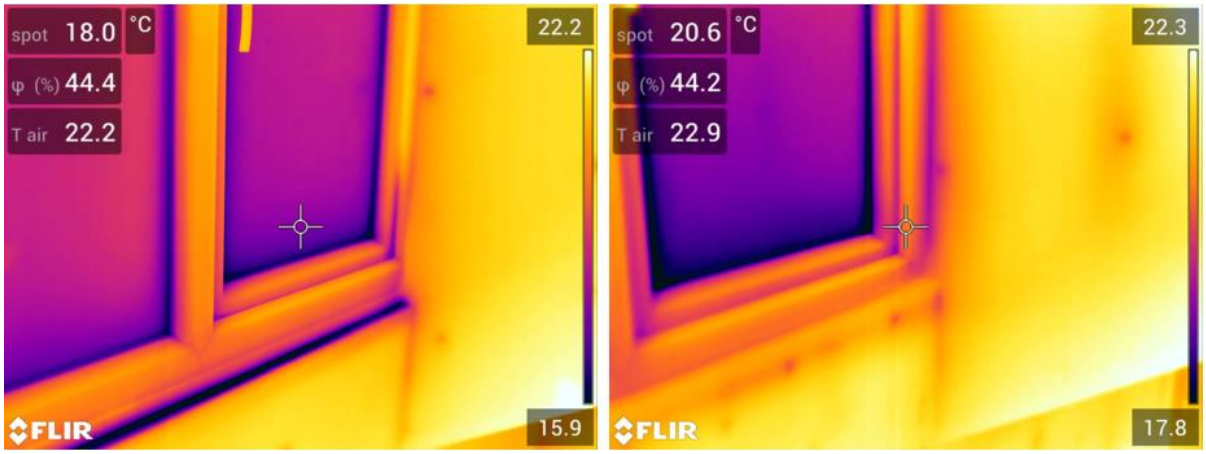

Figure 7-10 Thermograms showing dormer windowsill detail for TIWI over-boarded RiR (left) and conventionally retrofitted RiR (right)

7.5 RiR Retrofit and Airtightness

Figure 7-11 provides the results of the baseline and post-retrofit blower door tests.

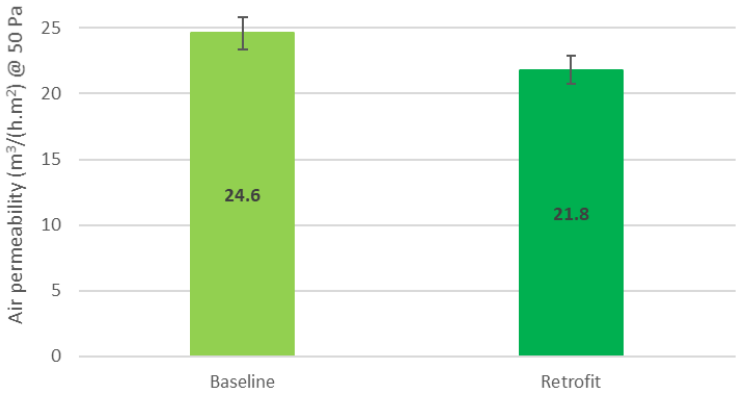

Figure 7-11 Blower door test results for House D in its baseline and retrofit conditions

The RiR retrofit resulted in an 11% reduction in air permeability of House D. A reduction in ventilation heat loss of 12.2 W/K was derived from the blower door test results, again using the n_{50}/20 Kronvall Persily rule. This is a substantial reduction, indicating lofts may be useful location for airtightness improvements. The dwelling appeared to have a high infiltration rate, and despite the reduction, post retrofit it was still twice the maximum allowed under Part L1A of the building regulations for new builds.

The warm weather conditions on the day of the retrofit blower door test meant that conditions for infrared air infiltration investigatory work were not ideal. Air infiltration was observed at the intermediate floor and knee wall junction for both types of retrofit method. Air infiltration at this location should be significantly reduced once skirting boards and carpet are installed.

The conventionally retrofitted RiR appeared to be susceptible to wind washing as air movement was observed between the insulation layer and plasterboard. Figure 7-12 shows examples of air movement behind the plasterboard, highlighting airpaths, which enable warm air to circumvent the insulation layer. It is suspected these paths are caused by gaps in the tape between the rigid insulation boards and structural timber. The TIWI over-boarded RiR was not susceptible to wind washing of the insulation layer as no gap is present between the plasterboard and insulation layer.

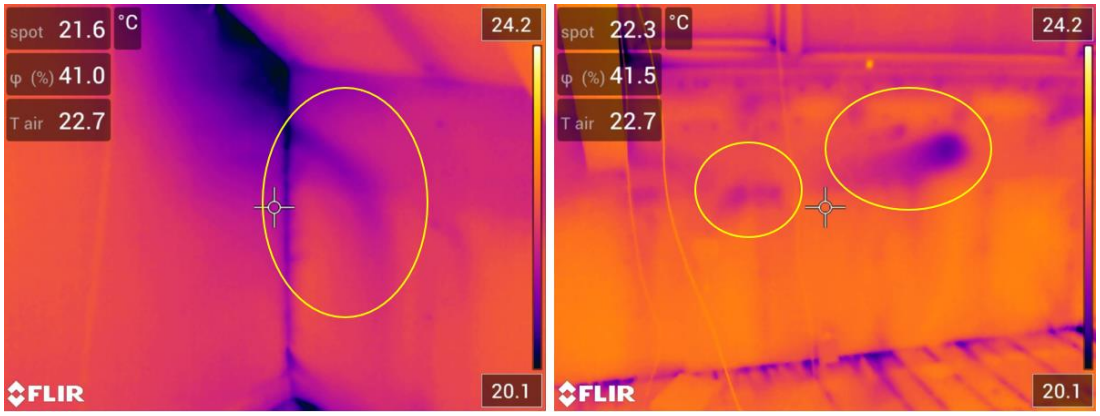

Figure 7-12 Air movement between the plasterboard and insulation boards (circled) in the conventionally retrofitted RiR. Air infiltration at the intermediate floor/knee wall junction

7.6 RiR Retrofit *In situ* U-values

The *in situ* U-value measurements were undertaken concurrently with the coheating tests. Heat flux plates (HFPs) were installed on each of the RiR thermal elements at the same locations both pre- and post-retrofit to measure heat flux density. Figure 7-13 and Figure 7-14 show the HFPs, RTD temperature sensors, and coheating equipment within each RiR post-retrofit.

Figure 7-13 Experimental set-up in the TIWI over-boarded RiR (red disks are the HFPs)

Figure 7-14 Experimental set-up in the conventionally retrofitted RiR (red disks are the HFPs)

The delay in handover of House D resulted in the experimental work being undertaken from mid-April until mid-May. This period is outside the optimum period for measuring *in situ* fabric thermal performance in the UK when a positive ΔT between internal and external environments can be expected (mid-October to mid-March). Additionally, the experimental period for the baseline stage coincided with unseasonably warm and sunny weather. Figure 7-15 and Figure 7-16 illustrate the internal and environmental conditions experienced during the baseline and post-retrofit test periods.

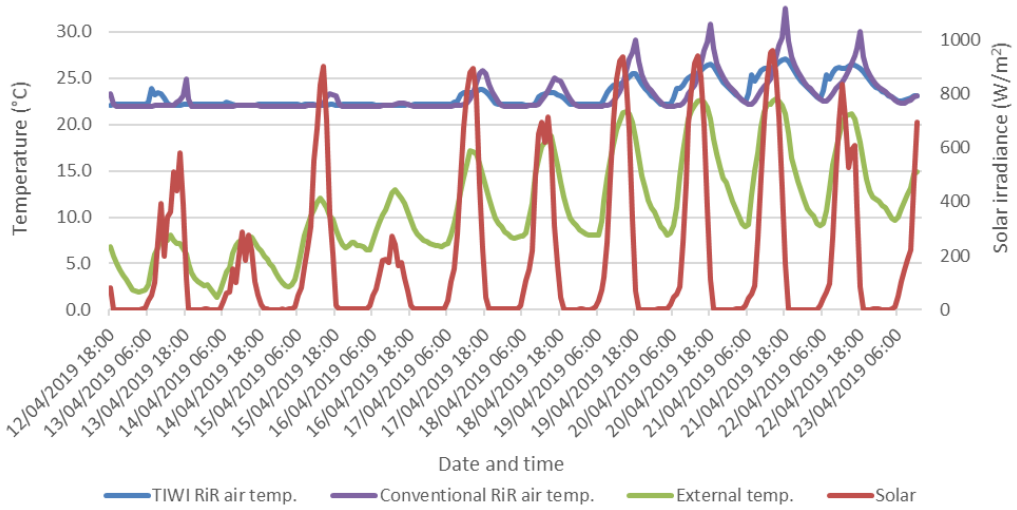

Figure 7-15 internal and environmental conditions experienced during the baseline test period

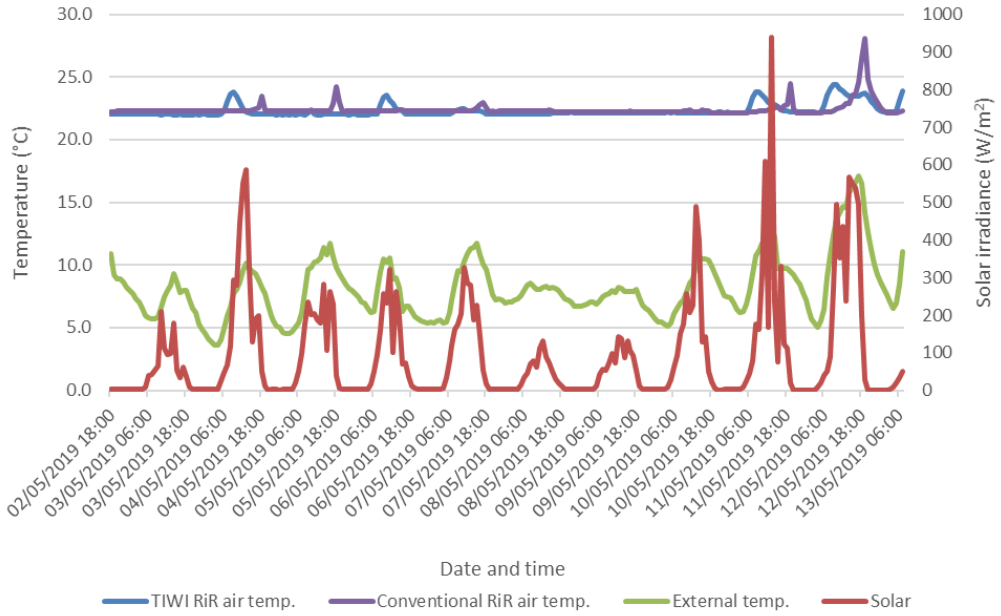

Figure 7-16 internal and environmental conditions experienced during the post-retrofit test period

It can be seen in Figure 7-15 that during the baseline test period a combination of high external air temperatures and high solar irradiance caused the internal air temperature of each RiR to rise above the internal set-point temperature of 22°C on numerous occasions. Figure 7-16 shows that test conditions were more favourable post-retrofit.

The RiR subject to the conventional retrofit on the west elevation of House D demonstrated the greatest tendency to overheat both pre- and post-retrofit. Figure 7-17, Figure 7-18, Figure 7-19, and Figure 7-20 demonstrate the effect that a negative ΔT and high solar irradiance had upon the heat flux density measurements which are used to calculate *in situ* U-values, i.e. negative heat flow was occasionally observed pre-retrofit, though rarely post-retrofit from the external to internal environment. The location and identifier of each HFP is provided in Table 7-1.

Table 7-1 Location and identifier of each RiR HFP

Element	TIWI RiR	Conventional RiR
Knee wall	V1, V2, V3	W1, W2, W3
Sloping ceiling	V4, V5, V6	W4, W5, W6
Dormer cheek	V7, V8	W7, W8
Dormer roof	V9, V10	W9, W10
Ridge roof	V11, V12	V16, V17

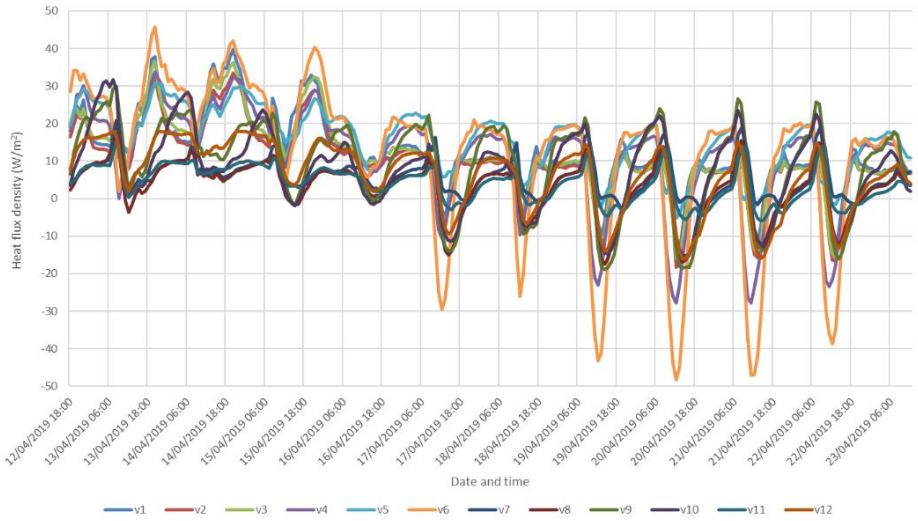

Figure 7-17 Heat flux density measured by each HFP on the TIWI over-boarded RiR at the baseline stage when uninsulated

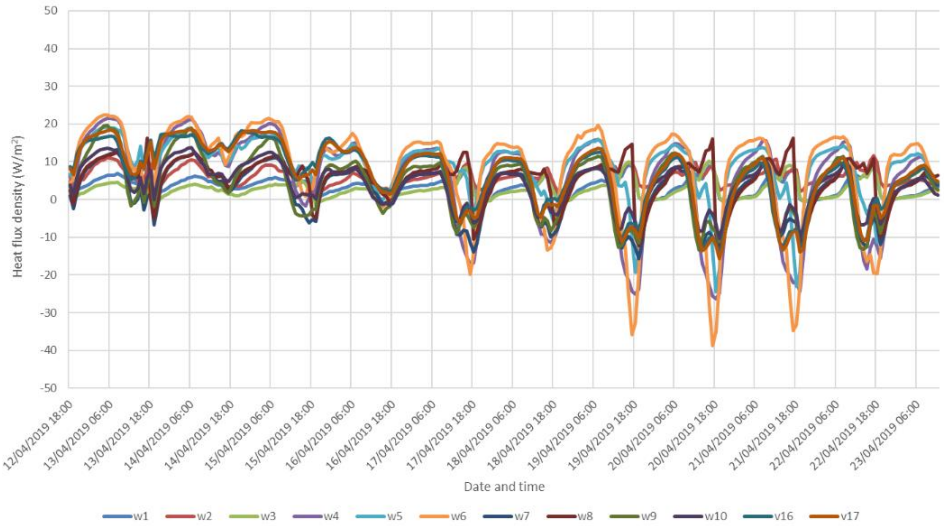

Figure 7-18 Heat flux density measured by each HFP on the conventional RiR at the baseline stage when the pre-existing insulation was in place

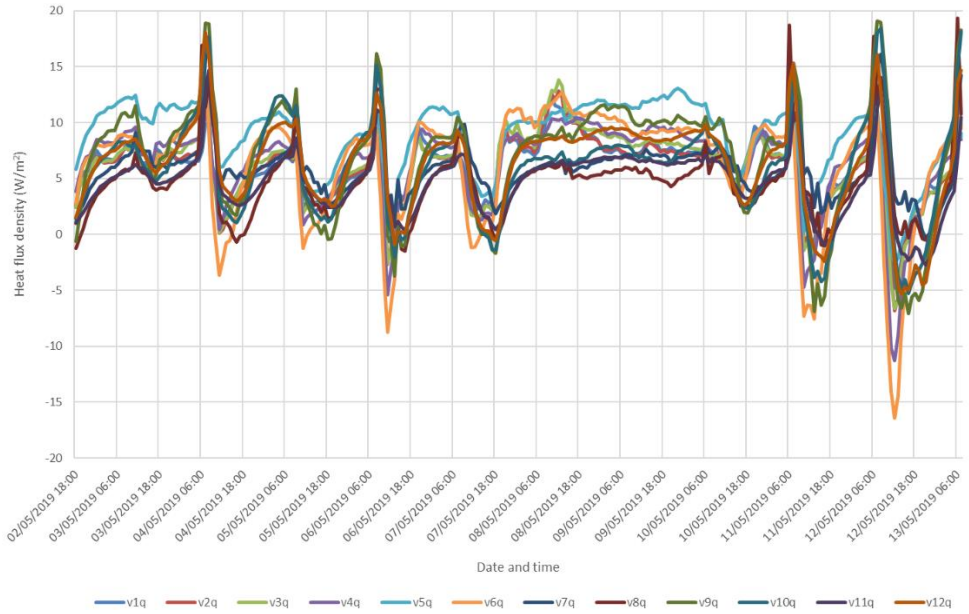

Figure 7-19 Heat flux density measured by each HFP on the TIWI over-boarded RiR post-retrofit

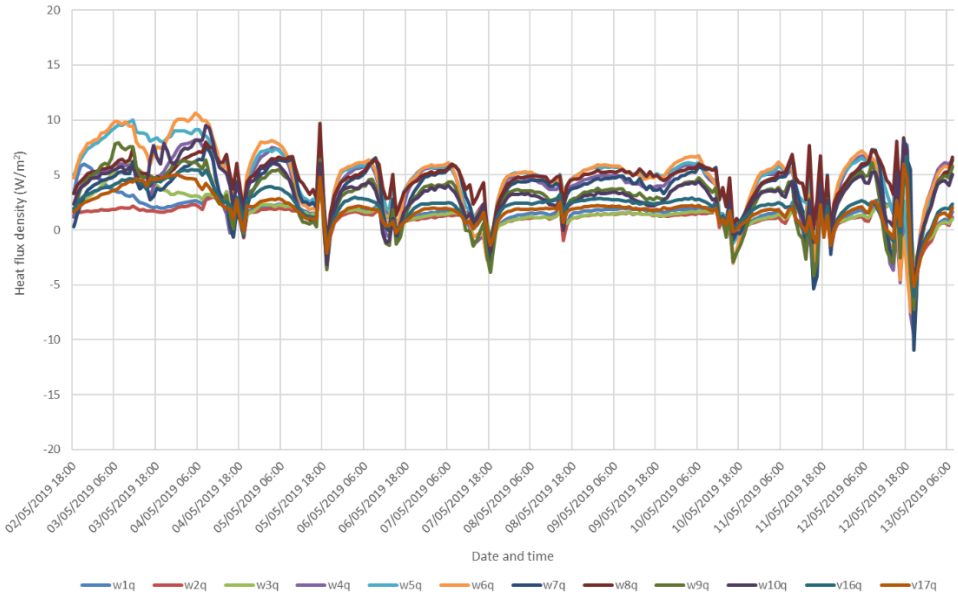

Figure 7-20 Heat flux density measured by each HFP on the conventional RiR post-retrofit

Figure 7-17, Figure 7-18, Figure 7-19, and Figure 7-20 show that heat flows from the external to internal environment through the RiR structure correspond with periods of high external temperature (low ΔT) and high solar irradiance. Conditions during such periods are unsuitable for *in situ* U-value measurement. To reduce the effect of solar radiation, *in situ* U-value measurements of lightweight roof structures undertaken in accordance with ISO 9869-1 were undertaken overnight, from one hour after sunset to one hour before sunrise.

Figure 7-21, Figure 7-22 and Figure 7-23 provide a more detailed illustration of the environmental conditions and heat flux densities measured during a 24-hour period which experience high external temperatures and high solar irradiance.

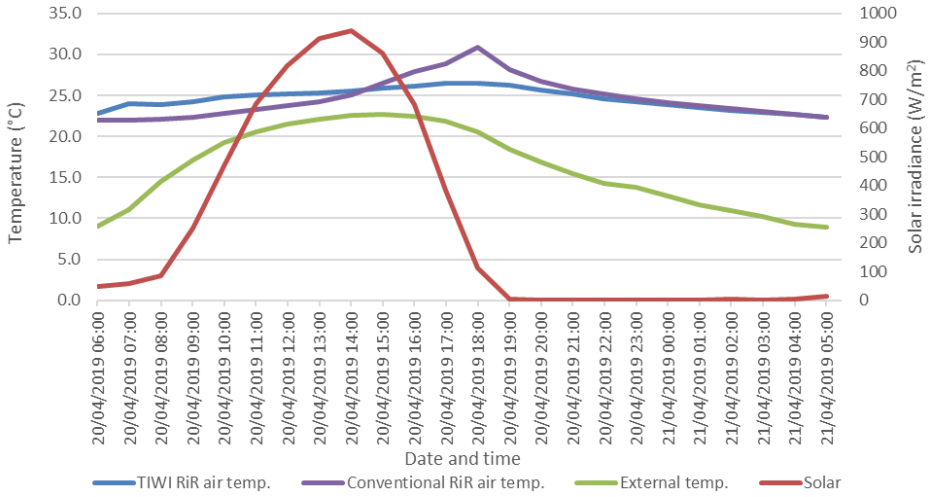

Figure 7-21 internal and external environmental conditions experienced during a warm and sunny 24-hour period during the baseline test

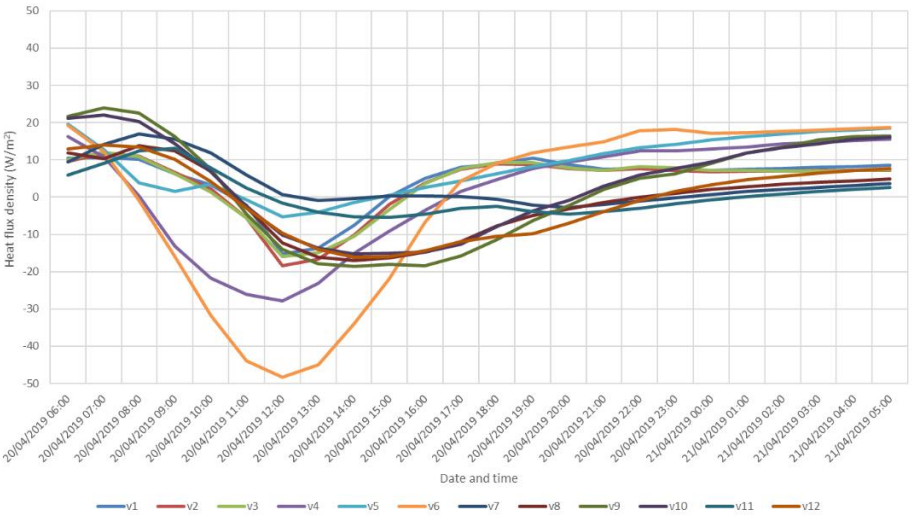

Figure 7-22 Heat flux density measured by each HFP on the TIWI over-boarded RiR at the baseline stage when uninsulated

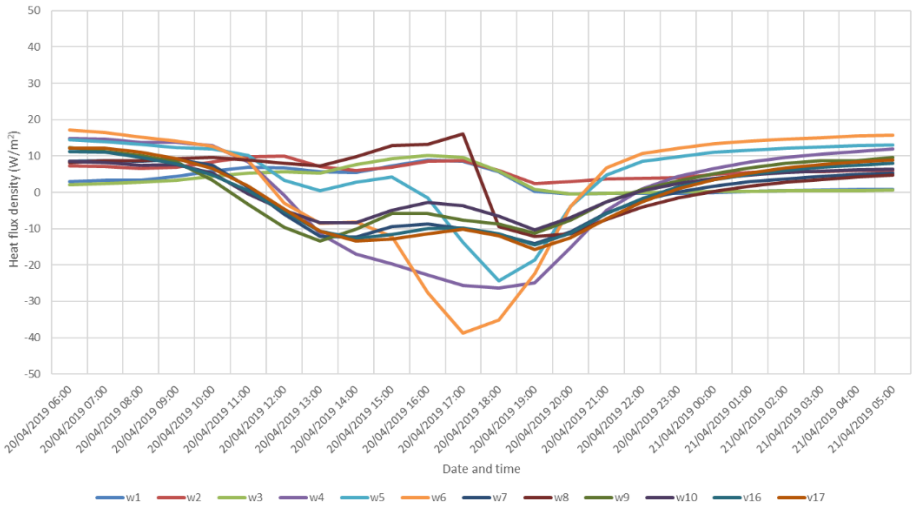

Figure 7-23 Heat flux density measured by each HFP on the conventional RiR at the baseline stage when the pre-existing insulation was in place

Figure 7-22 and Figure 7-23 show that although sunset occurred around 19:00, negative heat flux density was measured until 02:00 in some instances. To reduce the effect of high external temperatures and solar irradiance it was necessary to reduce the analysis period for each night to 00:00 – 04:00 and remove any days where the internal temperature had risen to over 25°C. The movement of the sun can also be observed in Figure 7-22 and Figure 7-23 as the TIWI RiR on the east elevation reacts to solar irradiance before conventional RiR on the west elevation. The measurements also suggest that the spike in overheating in the conventional RiR on the west elevation is caused by direct solar radiation through the glazing rather than through the opaque roof elements. Figure 7-24 compares the mean *in situ* U-value measurement for the RiR elements in each condition.

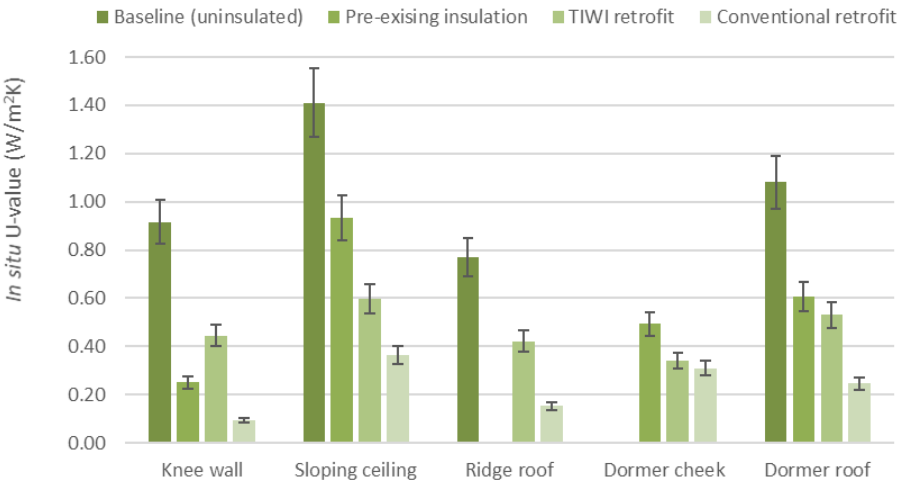

Figure 7-24 mean in situ U-value measurement for the RiR elements in each condition

The heat loss characteristics from each RiR element in each condition were generally as anticipated. The RiR with pre-existing insulation performed better than the uninsulated baseline RiR where applicable. The reason for the similar thermal performance of the dormer cheeks post-retrofit is due to the TIWI being over-boarded above the pre-existing insulation that was not removed prior to handover (see Section 7.3). Aside from the dormer cheeks, the conventional retrofit resulted in lower U-values than the TIWI retrofit, this was in line with expectation. Figure 7-25 shows the percentage U-value reduction achieved by each retrofit measure for each RiR element.

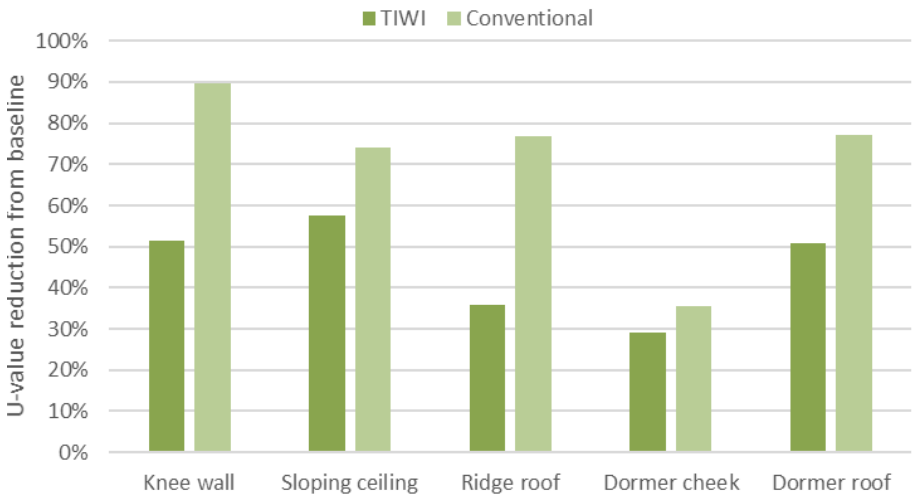

Figure 7-25 percentage U-value reduction achieved, values are based as reduction on uninsulated baseline measurements for each RiR element, apart from the dormer cheeks where the baseline value is the pre-existing

TIWI achieved at least a 50% U-value reduction for three of the RiR elements. Had the dormer cheek been uninsulated at the baseline stage, a greater percentage reduction would have been measured. Figure 7-26 compares the mean *in situ* U-value for each of the RiR elements retrofitted with TIWI with their retrofit target U-value. The retrofit target U-value was calculated using the method described in Section 3.2. Except for the dormer cheek, baseline values are taken from measurements of the uninsulated RiR elements.

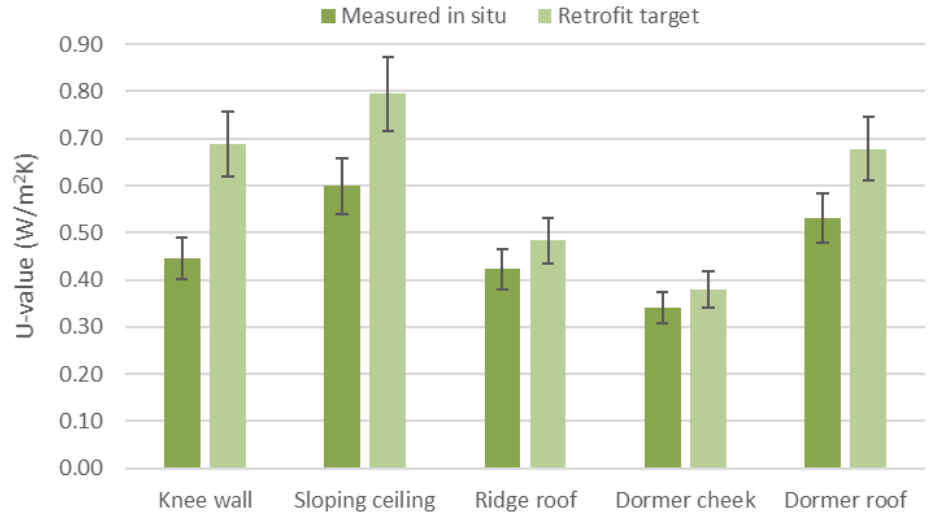

Figure 7-26 comparison of TIWI RiR retrofit in situ U-values with retrofit target U-values

The reason for most of the TIWI products performing better than their target U-values is uncertain. The wind direction during baseline measurements was from the east, which would have resulted in cooling of the east side of the roof structure by air infiltration. The wind direction during the retrofit measurements was from the west. This means that air movement across the roof structure would have been pre-heated by heat loss from the west side of the roof. This demonstrates that in dynamic thermal environments, there are multiple conditions that influence heat loss in homes of which some may not be able to be controlled by insulation alone. Figure 7-27 compares the mean *in situ* U-value for each of the conventionally retrofitted RiR elements with their retrofit target U-value.

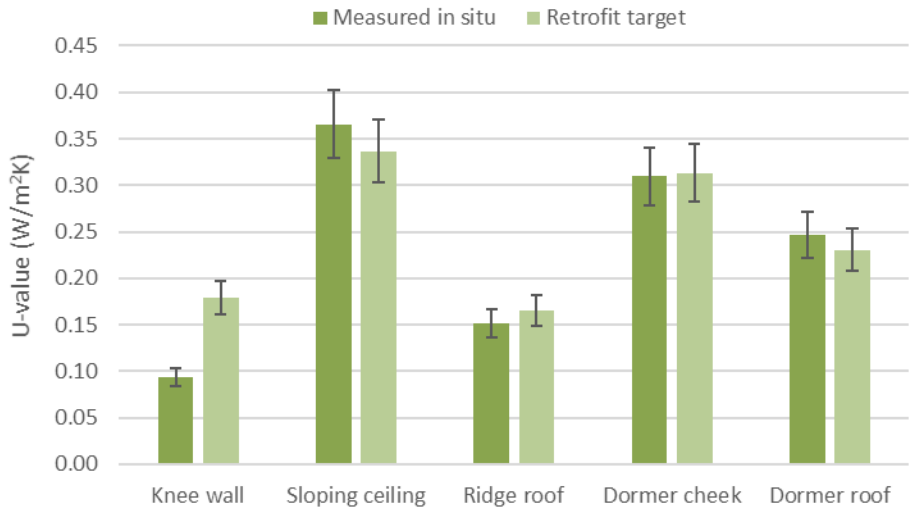

Figure 7-27 comparison of conventional RiR retrofit in situ U-values with retrofit target U-values

All the conventionally retrofitted RiR elements achieved their retrofit target U-value. The reasons for the better than predicted performance for the knee wall is not known. It was expected that this element may underperform as insulating the residual loft space reduces heat gains from the room below. The installers later mention that they had placed excess mineral wool into the residual loft space, if this abutted the knee wall it would provide additional thermal resistance. Figure 7-28 compares unbridged *in situ* U-value measurements undertaken between structural timbers (joists and studs) with bridged *in situ* U-value measurements for both methods.

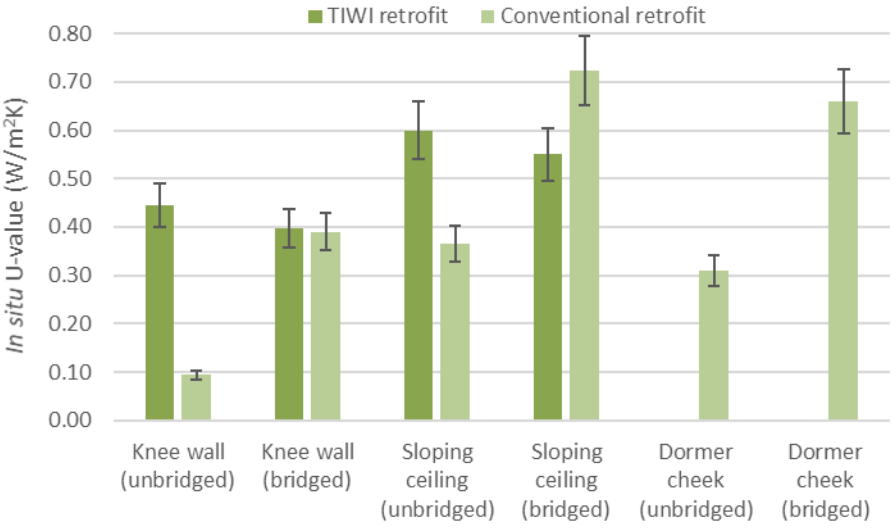

Figure 7-28 unbridged and bridged in situ U-value measurements for the TIWI and conventional retrofits

The measurements confirm the findings from thermography seen in Section 7.4. It shows locations of structural timber in the TIWI retrofit are associated with lower heat loss than unbridged areas, thus resulting in negative thermal bridging. The opposite is true for the conventional retrofit. Additional heat loss at structural timbers resulted in between 2-4 times the heat loss than surrounding areas.

7.7 RiR Retrofit HTC measurements

The coheating tests were less compromised than the *in situ* U-value measurements by external environmental conditions. The 6AM to 6AM aggregate period allows heat input from solar gains during the day to be released back into the building overnight. The multiple regression analysis also accounts for the reduction in power input caused by solar radiation, though vigilance is required to ensure the analysis is not compromised by collinearity between the independent variables (ΔT and solar irradiance). Figure 7-29 provides the coheating test measured baseline and retrofit HTCs for House D.

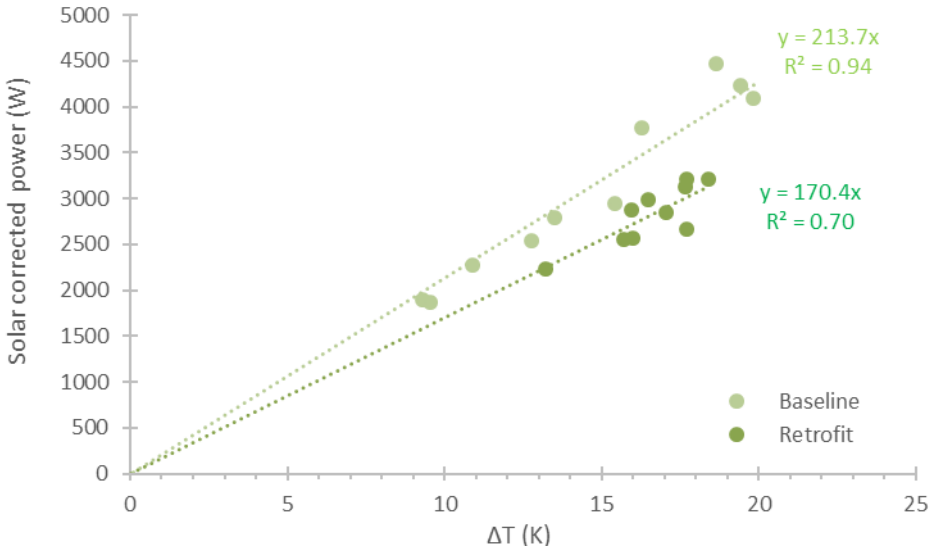

Figure 7-29 HTC of House D before and after the RiR retrofit

Table 7-2 provides a summary of the multiple linear regression analysis statistics for each of the coheating tests performed on House D.

Table 7-2 multiple linear regression analysis statistics for the coheating tests performed on House D

Test stage		Unstandardised Coefficients		Standardised Coefficients	t	Sig.	95.0% Confidence Interval for B		Collinearity Statistics	
		B	Std. Error	Beta			Lower Bound	Upper Bound	Tolerance	VIF
Baseline	ΔT	213.7	10.6	1.31	20.2	0.000	189.4	238.0	0.27	3.70
	Solar	-4.3	0.7	-0.39	-6.1	0.000	-5.9	-2.7	0.27	3.70
Retrofit	ΔT	170.4	7.4	1.18	23.1	0.000	153.4	187.4	0.23	4.39
	Solar	-4.8	1.1	-0.21	-4.2	0.003	-7.4	-2.2	0.23	4.39

The RiR retrofit resulted in a 20% HTC reduction, this is a substantial reduction in the same order of magnitude as insulating all the solid walls and therefore suggests RiR insulation could provide substantial fuel bill savings for solid wall homes which have a RIR. It also signifies that when installing IWI or SIWI including the RiR in the installation could double the likely savings for householders.

The coheating test results and *in situ* U-value measurements were used to calculate the HTC of House D under different scenarios:

- Had the RiR of House D been entirely uninsulated its baseline HTC would have been in the region of 221 W/K.
- Assuming an uninsulated baseline, a TIWI only RiR retrofit would have resulted in an HTC of approximately 176 W/K. This would represent a 20% HTC reduction.
- Assuming an uninsulated baseline, a conventional RiR retrofit would have resulted in an HTC of approximately 164 W/K. This would represent a 26% HTC reduction.
- The adjusted baseline of 221 W/K is close to the baseline HTC of 236.1W/K for House B located on a parallel street and is similar in age, form, and construction. It is highly likely that a TIWI retrofit of the RiR would have delivered a similar HTC reduction to the solid wall TIWI retrofit.

Figure 7-30 shows that 72% of the reduction can be attributed to an improvement in fabric thermal performance (e.g. reduction in conductive heat loss). Had both RiRs been uninsulated at the baseline stage then fabric heat loss would have comprised a greater proportion of the total heat loss reduction.

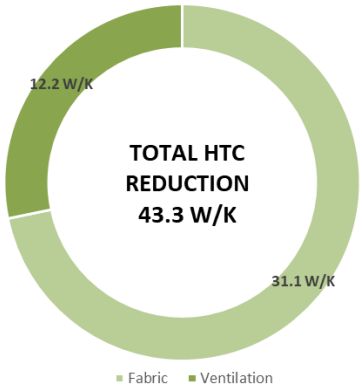

Figure 7-30 Disaggregation of fabric and ventilation heat loss reductions from the coheating test measured HTC reduction

7.8 RiR retrofit summary

Although the experimental work was compromised by a delay to handover and issues with the condition of the baseline dwelling, several conclusions can be made. Firstly, that TIWI reduced the U-value of roofs by half and delivered similar fabric heat loss reductions to those delivered by a TIWI retrofit addressing only the solid walls. RiR is arguably a less disruptive retrofit method than solid wall retrofit as it involves work in fewer rooms of a house and many of the obstacles to solid wall retrofit are not present in a RiR (e.g. fireplaces, boilers, coving, telephone sockets, etc.).

Additionally, although TIWI does not deliver the same reduction in fabric heat loss as a conventional retrofit, the cost savings attributable to specification, installation, and material make it a worthwhile option to consider, and may be particularly useful for improving the EPC for hard to treat archetypes such as converted flats in roofs of solid walled town houses. No performance gap was measured for any of the retrofit products. This can be partially attributable to the quality of the installation process. It is highly likely that a TIWI RiR retrofit is less susceptible to performance gap issues as the installation process is less complex. Finally, conventional RiR retrofits would benefit from a laminated insulation overboarding finish (instead of uninsulated plasterboard) as this would not only further reduce fabric heat loss, but also enable structural timbers to be treated and reduce thermal bridging. TIWI is also therefore a suitable retrofit option for RiR.

References

ATTMA 2010. Technical Standard L1A, Measuring Air Permeability of Building Envelopes (Dwellings) *In:* ASSOCIATION, A. T. T. A. M. (ed.). Air Tightness Testing and Measurement Association.

BAUWENS & ROELS 2014. Co-heating test: A state-of-the-art. *Energy and Buildings,* 82**,** 163-172.

BRE 2006. Conventions for U-valuecalculations 2006 edition, BR 443:2006. *Building Research Establiashment, Watford*.

BSI 2006. BS EN ISO 7730:2005 Ergonomics of the thermal environment. Analytical determination and interpretation of thermal comfort using calculation of the PMV and PPD indices and local thermal comfort criteria. London, UK: British Standards Institution.

BSI 2008. BS EN 15251:2007 Indoor environmental input parameters for design and assessment of energy performance of buildings addressing indoor air quality, thermal environment, lighting and acoustics. LONDON: British Standards Institution.

BSI 2014. BS ISO 9869-1:2014: Thermal insulation – Building elements - In situ measurement of thermal resistance and thermal transmittance. Part 1: Heat flow meter method. London: The British Standards Institution.

BSI 2017. Building components and building elements. Thermal resistance and thermal transmittance. Calculation methods BS EN ISO 6946:2017 *Bristish Standards Institute*.

BSI 2018. ISO 7345:2018 Thermal performance of buildings and building components — Physical quantities and definitions,. *Bristish Standards Institute, London*.

FANGER, P. O. 1970. *Thermal Comfort,* Copenhagen, Danish Technical Press.

FYLAN, F., GLEW, D., SMITH, M., JOHNSTON, D., BROOKE-PEAT, M., MILES-SHENTON, D., FLETCHER, M., ALOISE-YOUNG, P. & GORSE, C. 2016. Reflections on retrofits: Overcoming barriers to energy efficiency among the fuel poor in the United Kingdom. *Energy Research & Social Science,* 21**,** 190-198.

GORSE, C., GLEW, D., JOHNSTON, D., FYLAN, F., MILES-SHENTON, D., BROOKE-PEAT, M., FARMER, D., STAFFORD, A., PARKER, J., FLETCHER, M. & THOMAS, F. 2017. Core cities Green Deal monitoring project. *In:* BEIS (ed.). London.

INNOVATE UK 2016. Retrofit Revealed The Retrofit for the Future projects – data analysis report. *In:* UK, I. (ed.). Swindon: Innovate UK.

JACK, R., LOVEDAY, D., ALLINSON, D. & LOMAS, K. 2018. First evidence for the reliability of building co-heating tests. *Building Research & Information,* 46**,** 383-401.

JOHNSTON, MILES-SHENTON, FARMER, WINGFIELD & BELL 2013. Whole House Heat Loss Test Method (Coheating). *In:* ENVIRONMENT, C. F. T. B. (ed.). Leeds: Leeds Metropolitan University.

JOHNSTON, D. & FLETCHER, M. 2015. TSB BPE Project 450070 – Gentoo Racecourse, Sunderland. TSB BPE Phase 2 Final Report: In-use Performance and Post Occupancy Evaluation. *In:* BOARD, T. S. (ed.). Leeds Beckett University.

NBS 2010a. The Building Regulations 2010, Approved document L1B, Conservation of fuel and power in exisiting dwellings. London: NBS.

NBS 2010b. The Building Regulations 2010, Approved document Part F, Ventilation. London: NBS.

NBS 2010c. The Building Regulations, Approved document L1A, Conservation of fuel and power in new dwellings. London: NBS.

SHERMAN, M. H. 1987. Estimation of infiltration from leakage and climate indicators. *Energy and Buildings,* 10**,** 81-86.